TRANSITION FROM DEFLAGRATION TO DETONATION

by

Isaac Shanfield, B. Sc.

A thesis submitted to the Faculty of Graduate Studies and Research in partial fulfilment of the requirements for the degree of Master of Engineering

Dept. of Mech. Eng.
McGill University
Montreal

August 1964

SUMMARY

An investigation of combustion and transition phenomena in a cylindrical containing vessel has been carried out, using a streak camera to observe the processes.

The experiments have been conducted in an equimolar acetylene-oxygen mixture at an initial pressure of 100 mm Hg and an initial temperature of 300°K. Exploding copper wires of .003 and .006 inch diameters were used, with ignition energies from .6 to 9.23 joules per cm width of the cylindrical containing vessels. Vessels of both 1 and 2 inch widths were used.

A critical ignition energy exists above which a detonation is instantaneously formed at the ignition source, and below which normal burning is initiated. The critical energy is .9 joules per cm for the .003 inch diameter wire and 4.83 joules per cm for the .006 inch diameter wire. The critical energy per unit width is the same for both vessel widths investigated. The process of the cylindrical flame interaction with the precursor shock is observed, and the results compared to those predicted by a simplified theoretical model; qualitative agreement is indicated. True transition is not observed under these experimental conditions; pseudo-transition, due to shock heating of the unburned mixture close to the containing wall of the vessel by the multiple reflections of the pre-compression wave, occurs in some cases when most of the mixture has been consumed. Cylindrical transition is observed when turbulence is artificially generated by a spiral coil mounted on one of the sidewalls of the container. Cylindrical retonation waves are observed at the onset of detonation, and the detonation is initially overdriven.

ACKNOWLEDGEMENTS

The author wishes to thank his research director, Dr. J.H.T. Wu for his encouragement and support.

The author wishes to express his gratitude to Mr. J.H.S. Lee, who initiated the problem, and who was a source of guidance throughout this work. Thanks are due to Mr. B.H.K. Lee for his helpful suggestions, to Messrs. Donald A. Elliott and John Elliott for their assistance in the experimental work, and to Mr. L.J. Vroomen for his help in providing experimental instrumentation.

Thanks are due to Miss Joy Prazoff for her assistance in the final preparation and proofreading of the manuscript.

The financial support of the National Research Council of Canada under NRC Grant Number 1255 is acknowledged.

TABLE OF CONTENTS

NOMENCLATURE

Symbols

a	Speed of sound
A	Area
c_p	Specific heat at constant pressure
E	Energy
F_1	Parameter a/a_o
F_2	Parameter u/a_o
H	Enthalpy per unit mass
k	Proportionality constant for burning speed of mixture as a function of temperature
K	k/a_o
L	Vessel width
m	Mass
M	Molecular weight
M_s	Shock Mach number
p	Pressure
ΔQ	Chemical heat release
r	Radius
R	Universal gas constant
R_s	Shock front radius
S	Laminar flame burning velocity
t	Time
T	Temperature
u	Particle velocity
U	Wave front velocity
V	Volume
y_1	Shock pressure ratio p_s/p_o

Greek Letters

α	Proportionality constant
γ	Ratio of specific heats
Δ	Increment
∂	Partial differentiation
ρ	Density
ψ	Constant in Hugoniot Eq. 6.55
ξ	Similarity parameter $r/a_o t$

Subscripts

b	Burned gas
f	Flame
o	Undisturbed gas
p	Properties immediately ahead of piston
s	Shock, properties immediately behind shock
u	Unburned gas

CHAPTER I

INTRODUCTION

While studying the propagation of flames in tubes containing combustible mixtures, it was discovered by Berthelot and Vieille and independently by Mallard and Le Chatelier that under certain initial conditions, an accelerating flame propagates into the unburned mixture until, suddenly, a supersonic combustion wave is formed which travels at velocities of 1000 to 3500 metres per second, about 100 times the velocity of the flames which had previously been observed. This high speed combustion wave is now termed a detonation. The distance from the ignition source to the point at which the detonation forms is termed the induction distance, and the time required for the transition from the flame which is first formed to the detonation is the induction time.

In the eighty years or so since the initial observations of detonation, a formidable amount of experimental data, both of a qualitative and a quantitative nature, has been obtained in order to determine the exact nature of the transition process, and the variables which affect transition. The quantitative data obtained on induction distance is, for the most part, scattered. Comparison of data obtained by different researchers is extremely difficult, if not impossible, to correlate, since the process of transition is affected by numerous variables which are unlikely to have been identically the same in two independently performed experiments. All that one can hope to gain from this data is an insight into how changes in each of these variables affect qualitatively the process of transition.

A theoretical formulation of the problem is as yet impossible due to the complicated nature of the basic physical processes of conduction,

diffusion, pressure wave generation and turbulence generation which are all essential parts of the transition process in a tube. The complex coupling which exists among these phenomena involved in the transition process makes the problem even more unmanageable analytically.

It has been noted (Ref. 1) that the most destructive effects of detonation occur when transition takes place near the closed end of a tube. It would therefore be of great advantage in the design of vessels to contain detonable mixtures to be able to more reliably predict the transition phenomenon by a better understanding of the importance of each of the basic physical mechanisms individually, and of the coupling which exists among them.

It is with this in mind that the present research is undertaken. The presently existing experimental work will be reviewed and evaluated, the basic physical mechanisms influencing transition will be outlined, and the coupling of these processes will be described to form a model for the transition process. Existing theoretical analyses of the problem will be reviewed, and their severe limitations demonstrated. It is then proposed to decouple the basic mechanisms of transition by choosing containing vessels of suitable geometry, and to determine whether or not transition will occur in the absence of any of these processes.

CHAPTER II

EXISTING EXPERIMENTAL WORK

2.1 NATURE OF EXPERIMENTS

The experimental work on the transition process which has been carried out up to this time can be classified into two major categories. Many researchers, among them Dixon (Ref. 2), Payman and Titman (Ref. 3), Schmidt et al. (Ref. 4), Salamandra et al. (Ref. 5) and Oppenheim et al. (Ref. 6) have been concerned with the basic physical processes which contribute to the transition phonemenon, and by means of streak and streak schlieren photography, have succeeded in obtaining a detailed description of the acceleration of the initial laminar subsonic flame to a detonation.

Other experimenters have been concerned with the effect of changes in certain variables on the transition process, or on the initial flame acceleration process. Bollinger et al. (Ref. 7) have studied the effects on the induction distance of changes in such variables as fuel-oxidant system mixture ratio, initial pressure, and ignition method. Laderman et al. (Ref. 8) and Laderman and Oppenheim (Ref. 12) have studied the effects on the initial flame acceleration of changes in variables such as ignition method, ignition geometry and ignition energy. The influence of changes in tube geometry has been studied by Bollinger et al. (Ref. 9) , Shchelkin, Greifer and Shuey (as reported by Brinkley and Lewis in Ref. 1).

2.2 PHOTOGRAPHIC OBSERVATION OF THE TRANSITION PROCESS

Careful observation of the streak and streak schlieren photographs which have been obtained has led to a clear definition of the transition process. The essential features of this process in a tube are as follows: Upon ignition, a laminar flame begins to propagate into the unburned

mixture in the tube with a velocity of the order of 10 m/sec (in $C_2H_2 + O_2$ mixture) and a slow acceleration of the flame front is noted. During the acceleration process, comparatively weak pressure waves originate ahead of the flame front. The waves overtake one another until a weak shock is formed which travels into the unburned mixture ahead of the flame front. The acceleration of the flame is increased and a gradual transformation from a laminar to a highly turbulent flame is observed. Additional stronger shocks appear ahead of the flame front, and suddenly, a detonation is formed when the flame velocity is about 800 m/sec (in $C_2H_2 + O_2$ mixture). The detonation may be overdriven initially, but it rapidly decelerates to an equilibrium velocity. At the same instant that the detonation is formed, a strong shock (termed a retonation) is formed which propagates into the burned gas at a speed comparable to the detonation wave speed. In the region between the detonation and retonation waves, transverse oscillations, periodic in nature and of a frequency of about 65 kc/sec are observed.

2.3 VARIABLES AFFECTING THE TRANSITION PROCESS

Previous experimental investigations have indicated that the variables which significantly affect the transition process and consequently the induction distance are: i) fuel-oxidant mixture; ii) mixture ratio; iii) initial pressure of mixture; iv) ignition method; v) ignition energy input; vi) ignition geometry; vii) tube geometry. It is proposed here to indicate how each of these parameters affects the transition process, and to briefly outline the experimental work which has been done with regard to each of these parameters.

2.3.1 Fuel-Oxidant Mixture

Experimental evidence has shown that fuel-oxidant mixtures having high heats of combustion ($C_2H_2 + O_2$) and thereby producing high flame temperatures, will, in general, have relatively low detonation induction distances. The reaction rate is also a parameter of importance in determining whether or not a given fuel-oxidant system will detonate. It is found, for example, that for certain chemical systems which have a high flame temperature, the induction distance is large and the flame propagation speed low because the system has a low reaction rate ($H_2 + 2NO_2$).

Bollinger et al. (Ref. 7) have investigated the induction distances for mixtures of various fuels and oxidants such as hydrogen-oxygen and hydrogen-nitric oxide, using exploding wire ignition. The induction distance for stoichiometric hydrogen-oxygen mixture at 1 atm initial pressure and 40°C initial temperature was found to be about 75 cm in a tube of 15 mm ID and 115 inches in length. The corresponding induction distances for other fuel-oxidant systems obtained in the same investigation are tabulated below. Exploding wire ignition was used.

Fuel-Oxidant	Induction Distance
$2H_2 + O_2$	75 cm
$CH_4 + 2O_2$	75 cm
$C_2H_2 + 2.5\ O_2$	2 cm

The hydrogen-nitric oxide system did not detonate within a tube of length 12 feet and ID of 50 mm for initial pressures as high as 10 atm. An acceleration of the flame was observed, however, for a 50% mixture at an initial pressure of 10 atm.

2.3.2 Mixture Ratio

The mixture ratio is commonly defined as the per cent by volume of fuel in a given fuel-oxidant system. It has been experimentally determined that if all other variables are fixed, and the mixture ratio is varied over the range from a fuel-rich to a fuel-lean mixture, the induction distance is significantly altered. For many fuel-oxidizer mixtures, the minimum induction distance occurs at approximately stoichiometric composition, but this is not true for an acetylene-oxygen mixture, for example, in which the minimum induction distance occurs at a mixture ratio of 50% (the stoichiometric mixture ratio is 28.5%).

Bollinger et al. (Ref. 7) have obtained the following induction distances for a hydrogen-oxygen mixture of varying composition at an initial pressure of 1 atm and temperature of 100°F (the tube was 15 mm ID and 15 inches in length, and the mixture was ignited by exploding wire).

Composition	Induction Distance
30%	150 cm
60%	61 cm
80%	156 cm

2.3.3 Initial Pressure

A variation of induction distance with the initial pressure of an explosive mixture has been noted, and it is clearly indicated that the induction distance decreases as the initial pressure is increased. Again, the results of Bollinger et al. (Ref. 7) are quoted below for a tube of 15 mm ID and 115 inches in length. For a 60% hydrogen-oxygen mixture at an initial temperature of 100°F ignited by exploding wire, the induction distances are as follows:

Pressure	Induction Distance
1 atm	61 cm
5 atm	16 cm
10 atm	13 cm
25 atm	5 cm

In a later paper, Bollinger (Ref. 10) has found the induction distances for a 66.67% mixture at lower pressures in a tube of 74 mm ID, using exploding wire ignition.

Pressure	Induction Distance
.2 atm	500 cm
.5 atm	245 cm
1 atm	150 cm

2.3.4 Ignition Method

Appreciable changes in both the induction distance and in the flame acceleration process have been found by Bollinger et al. (Ref. 11) and by Laderman and Oppenheim (Ref. 12) as the ignition source was changed in a tube. Each investigator used three sources, electrical, thermal and chemical in nature, Bollinger et al. (Ref. 11) using an exploding wire, a glow wire and a chemical squib, and Laderman and Oppenheim (Ref. 12) using a spark, a glow coil and a pilot flame.

Bollinger et al. (Ref. 11) have investigated the detonation induction distances for mixtures of 45, 66.67 and 75 mole per cent hydrogen-oxygen at initial pressures of 1 and 5 atm and an initial temperature of 40°C. It was found that the chemical squib gave the shortest induction distances for both initial pressures; the glow wire produced the longest induction distances at 1 atm initial pressure; the exploding wire ignition

method resulted in the longest induction distances at an initial pressure of 5 atm.

Laderman and Oppenheim (Ref. 12) have studied the flame acceleration process in a tube filled with a stoichiometric hydrogen-oxygen mixture. The detailed flame front structure has been observed by streak schlieren, and pressure records in the vicinity of the ignition source have been obtained by use of transducers. It was found that radical differences in the flame acceleration process existed for the three different ignition methods investigated. For the spark-ignited mixture, it was found that no pressure discontinuity could be observed ahead of the flame during the early stages of propagation, but a pressure rise ahead of the flame was indicated by the transducer records. For ignition by pilot flame, an initially supersonic flame front emerged from the backwall, and rapidly decelerated to a speed of about 200 m/sec in several microseconds. The flame again accelerated to almost its initial velocity, and then slowed down slightly once more. The flame front became irregular in shape, and accelerated again. The pressures recorded ahead of the flame were considerably higher than those obtained for the spark-ignited mixture. The glow coil ignition produced the most rapid flame acceleration, and no deceleration was noted. The pressures recorded were slightly higher than the corresponding values for the pilot flame ignition.

2.3.5 Ignition Energy

The effect of ignition energy input on the initial flame acceleration has been investigated by Oppenheim et al. (Ref. 8) in a tube of 1 x 1.5 inches rectangular cross-section using a stoichiometric hydrogen-oxygen mixture at 1 atm initial pressure and at 25°C initial temperature.

Ignition was by spark discharge. It was found that for ignition energies over the range of 0.1 to 6 millijoules, no change in the flame acceleration process occurred.

2.3.6 Ignition Geometry

Oppenheim et al. (Ref. 8) and Laderman and Oppenheim (Ref. 13) have found that, as the ignition source to backwall distance was increased in a tube, an appreciable change in the flame acceleration process occurred. As this distance was increased from zero to about one tube radius, there was an increase in the acceleration rate of the flame. Small additional changes produced no noticeable effects on the process. As the ignition source was further advanced into the tube a distance greater than several tube diameters, an appreciable acceleration of the flame front took place at a later stage of its development. There was no significant change in the induction distance as the ignition source to backwall distance was varied.

2.3.7 Tube Geometry

Variations in detonation tube geometry such as changes in tube diameter, tube length, insertion of wire spirals, flow obstructions and bends have been found to considerably influence the process of transition.

i) Shuey (as reported by Brinkley and Lewis in Ref. 1) has studied the detonation of acetylene in long tubes from 1/4 to 4 1/2 inches in diameter. Ignition was accomplished by means of a squib. He found that the induction distance was about 60 tube diameters. Bollinger et al. (Ref. 7) have investigated the effect of tube diameter on the induction distance in hydrogen-oxygen mixture employing tubes of 15 and

50 mms ID. No correlation such as the one obtained by Shuey was apparent. In results more recently published, Bollinger (Ref. 10) has tabulated the induction distance to tube diameter ratio for tubes of 15, 50, 74 and 79 mm ID containing hydrogen-oxygen mixtures at various initial pressures and mixture ratios. Again, no correlation is apparent.

ii) Wire Spiral

Shchelkin (as reported by Brinkley and Lewis in Ref. 1) has placed a wire spiral in a tube near the ignition source, and found that the increased wall roughness resulted in a considerable decrease in the induction distance for a given mixture.

iii) Flow Obstructions

Shuey (reported in Ref. 1) has found that the placement of obstructions in the vicinity of the ignition source results in a decrease in the induction distance by a factor of 12. Bollinger and co-workers (Ref. 9) have placed cylindrical rods of diameters from .635 to 4.763 cm in a tube of 7.9 cm ID. Using a stoichiometric hydrogen-oxygen mixture, the induction distance was found to decrease with increasing rod diameter.

iv) Tube Configuration

Bollinger et al. (Ref. 9) have placed right-angle bends in a detonation tube at distances of 15 cm and 66 cm from the ignition end. A considerable decrease in induction distance (as compared to results in straight tube) was noted for every run.

2.4 SUMMARY

The bulk of the experimental work related to the transition process has been reviewed. A detailed description of the transition process can

be obtained from the photographic observation of the phenomenon. The quantitative data obtained, however, is impossible to correlate to any theoretical predictions of the process, due to the extremely complex nature of the physical mechanisms involved, and the great number of variables which affect the process. This data facilitates a physical explanation of the basic processes which contribute to the transition phenomenon.

CHAPTER III

PHYSICAL MODEL OF TRANSITION PROCESS

3.1 OBSERVED PHENOMENA OF THE PROPAGATION OF COMBUSTION WAVES IN TUBES

Examination of streak photographs of the propagation of combustion waves in a tube containing a fuel-oxidant mixture has indicated that there are three basic phenomena; i) immediate formation of a detonation upon ignition; ii) formation of a flame, with no transition to detonation; iii) formation of a flame with later transition to the detonation state. Each of these phenomena is characterized by certain features. The first, immediate detonation formation, often features a wave speed in the vicinity of the ignition source which is higher than the finally established detonation wave speed. The second is characterized by the initiation of a low-speed flame, and an acceleration of this flame near the ignition source. The flame speed then remains constant for some time until it is suddenly decelerated. The absolute flame speed may become negative after this interaction. Further accelerations and decelerations occur, and an intense explosion may occur in the unburned gas region as the flame approaches the closed end. The third possible phenomenon, that of transition, is the most interesting and complicated of the three. A low speed flame which accelerates rapidly is initiated near the ignition source. The flame travels at a relatively constant speed for some time, and a gradual widening of the luminous region occurs. An intensely luminous zone is formed, and two waves are initiated, one travelling into the unburned mixture, and the other into the burned gas region. The wave which propagates into the unburned mixture may initially have a velocity which is

greater than the final detonation wave speed.

3.2 BASIC PHYSICAL MECHANISMS OF COMBUSTION PROCESSES

In order to understand the mechanisms responsible for the phenomenon as observed, it is necessary to look into the basic physical processes which occur when a combustible mixture is ignited.

3.2.1 Laminar Flame Propagation

The process of laminar flame propagation into an undisturbed combustible medium is essentially a process dependent on transport phenomena such as diffusion and heat conduction. The ignition source is generally a source of heat or of a blast wave which heats the gas surrounding the source. The source may also produce chain carriers which help to propagate the reaction. The flow of heat and chain carriers from the region of the ignition source initiates chemical reaction in the surrounding gas. Heat is then transferred from this volume to the next layer. In this way, the combustion propagates through the medium.

The laminar propagation rate is strongly dependent on both the fuel-oxidant system considered, and the molar composition of the chemical species. It is also found, in general, that the laminar flame speed is essentially independent of the pressure of the reactants, though the flame speed varies with the temperature of the unburned mixture.

3.2.2 Generation of Pressure Waves by the Flame

Consider a small volume of reacting gas at one end of a tube, and an inert gas which fills the rest of the tube in contact with this volume. The combustible volume is ignited, and chemical reaction of

this gas takes place. The specific volume of the product gases is from 5 to 15 times that of the reactants (Ref. 14), and the expansion of the burned gas results in the generation of a compression wave (or waves) ahead of the interface between the burned and the inert gases. If the entire mixture in the tube were combustible, the flame propagation process could be considered as the reaction of successive layers of unburned mixture. The expansion of each of these elemental volumes results in the generation of compression waves ahead of the advancing flame front which propagate into the unburned reactants. The burning of a combustible mixture, therefore, results in a continuous generation of pressure waves ahead of the flame front.

3.2.3 Reaction Rate

It is well known that certain fuel-oxidant mixtures will not detonate even though they are capable of supporting combustion. Important in determining whether a given mixture will detonate is the chemical energy released during the reaction, and the rate at which this energy is released. The reaction rate is determined in general by the activation energy of the reacting molecules and by the temperature of the reacting gases. Reactions in which the product molecules or atoms have positive heats of formation, and the reactants have high activation energies and low heats of formation result in low final temperatures of the products. These reactions proceed with low reaction rates and low rates of heat release. A combustible mixture will detonate only if the reaction rate and the rate of heat release is sufficiently high - otherwise, only normal burning can occur.

3.2.4 Flame-Pressure Wave Interaction

One of the basic mechanisms influencing the combustion process in a tube or in vessels of other geometries is the interaction of the flame front with a compression or an expansion wave. The flame velocity relative to the stationary laboratory coordinates is the sum of the burning velocity and the particle velocity of the medium into which the combustion wave propagates. A disturbance in the unreacted gas which affects either the burning speed or the particle velocity in this region will influence the flame propagation speed. A compression wave in the unburned gas tends to raise the temperature of this gas and to accelerate the particles in the direction of wave travel, whereas an expansion wave tends to lower the temperature and to accelerate the gas particles in the direction opposite to the direction of wave travel. The burning speed of a mixture is dependent on the temperature of the mixture (Section 3.2.1) into which the flame propagates, so that these waves, whether they travel in the same direction as or in the direction opposite to the flame front, affect the absolute flame velocity by influencing both the temperature and the particle velocity in the region of the unburned gas.

3.2.5 Wall Effects

The generation of pressure waves ahead of the flame front has been outlined in Section 3.2.2. The propagation of these disturbances results in a downstream velocity of the unburned gas ahead of the flame. Due to wall friction which exists in a tube, a boundary layer is formed, and a non-uniform velocity profile of the unburned gas results. This non-uniformity results in a distortion of the flame front shape.

3.3 SHOCK PROPAGATION IN COMBUSTIBLE MEDIUM

In order to link the physical processes of combustion in a tube, the problem of shock propagation into a combustible mixture is considered. If the shock is of such strength that the temperature behind the shock front is greater than or equal to the ignition temperature of the mixture, burning is initiated. The advancing flame front generates pressure waves which propagate at a wave speed equal to the particle velocity plus the local sonic speed. The strength of the generated disturbances is dependent on the reaction rate and on the rate of heat release in the combustion zone. If the reaction rate is low, these disturbances are weak and the shock ahead of the flame is weak; if the reaction rate is high, the strength of the preceding shock is greater.

The shock in the reacting gas may be initiated and supported by a moving piston; corresponding to a given piston velocity, there is only one possible shock strength. The shock propagates into the reacting medium as it would into a non-reacting gas until the piston velocity is increased to a value large enough to support a shock of strength sufficient to heat the combustible gas to its ignition temperature. Once the reaction is initiated, a flame front begins to propagate behind the shock front. The particle velocity behind the flame must be the same as the piston velocity if the flame speed relative to the burned gas products is subsonic. The speed of propagation of small disturbances in the burned gas is equal to the sum of the local sound speed and the particle velocity. If the flame front velocity is the same as (or greater than) this velocity, the disturbances cannot overtake the flame front, and, consequently, cannot affect the flame propagation speed. Removal of the piston when this

critical flame velocity is exceeded will therefore not affect either the flame or the preceding shock; only the burned gas products will be affected.

3.4 THE TRANSITION PROCESS

Having examined the basic physical phenomena which contribute to the transition process, it is now possible to formulate the physical model for the transition process, based on work by Brinkley and Lewis (Ref. 1), Oppenheim et al. (Ref. 6) and Martin and White (Ref. 14).

Consider a combustible mixture in a closed end tube, using a glow wire as an ignition source. Heat conduction from the wire to the unburned gas results in a temperature rise, and slow burning begins. A series of pressure waves are generated ahead of the flame front by the mechanism which has already been discussed in Section 3.2.2. Each successive compression pulse raises the temperature of the unburned gas slightly, and imparts a velocity to the unburned gas particles. The burning velocity of the mixture is increased due to the rise in temperature, and this, coupled with the increase in particle velocity of the gas ahead of the flame front, results in an increase in the speed of the flame front. Since each compression pulse propagates into a gas of temperature slightly higher than that seen by the previous pulse, these compression waves coalesce after some time to form a weak shock which travels ahead of the flame front. This is termed the precursor shock. Each succeeding compression wave generated increases the temperature of the unburned mixture, accelerating the flame, and strengthening the precursor shock. A boundary layer is formed at the tube wall in the region between the precursor

shock and the flame front, and due to the change in velocity profile of the unburned mixture ahead of the flame, the flame area is increased. This increase in area results in an increased rate of heat release, and consequently, in acceleration of the flame, and, strengthening of the precursor shock. The boundary layer is transformed from laminar to turbulent, and there is further acceleration of the flame due to the increase in flame area. The turbulence level becomes so great and the flame front so distorted, that small pockets of unburned mixture are entrapped by the flame and burn almost instantaneously, generating intermittent pressure pulses to strengthen the shock. Secondary burning may occur in the hot boundary layer, and a large volume of unburned gas is entrapped between the original and secondary flame fronts. The burning of this gas by deflagrative implosion creates an arbitrarily high pressure, and the shock so formed coalesces with the precursor shock to form a detonation, and propagates back through the burned gas as a retonation.

CHAPTER IV

EXISTING THEORETICAL MODELS

Several highly idealized models for the mechanisms of transition from deflagration to detonation have been proposed. Adams and Pack (Ref. 15) and Jones (Ref. 16) have treated the accelerating flame front as a discontinuity preceded by a shock (a small amplitude wave in Jones' model), and have applied the basic conservation equations to determine the flow. Chu (Ref. 17) has demonstrated that heat release in a gaseous medium results in the generation of pressure waves ahead of the expanding hot mass of gas. This mechanism may greatly affect the process of transition from deflagration to detonation.

4.1 MODEL OF ADAMS AND PACK

Adams and Pack (Ref. 15) have proposed to clarify the process of transition by finding a theoretical solution of the gasdynamic state of flow set up by a combustion wave propagating with a given velocity into an explosive mixture contained in a semi-infinite tube. It is assumed that the flame is preceded by a shock which imparts a downstream velocity to the gas in the region between the shock and flame fronts. Several assumptions are made to simplify the problem:

i. The reactants and products are both perfect gases with constant specific heats.

ii. The flow is one-dimensional.

iii. The flame front is planar, with no wrinkles due to turbulence or boundary layer effects.

iv. a normal shock exists ahead of the flame for all flame velocities.

In order to obtain a solution, an additional condition is required which relates the flame speed to the particle velocity behind the flame front. It is assumed that until the flame has attained sonic velocity relative to the burned gas particles, these particles are at rest. Once this critical flame speed has been attained, and the flame is further accelerated, it is assumed that the burned gas accelerates in such a way that the Chapman-Jouguet condition is satisfied (i.e., the flame speed relative to the burned products remains sonic). The particles must then be decelerated through expansion waves to satisfy the boundary condition that the velocity of the particles be zero at the closed (ignition) end of the tube. The steady-state detonation velocity is said to be reached when the shock speed and the flame speed are identical.

4.2 MODEL OF JONES

Jones (Ref. 16) considers the dynamics of an accelerating flame in the process of transition from deflagration to detonation. The expansion of the gas behind the flame front leads to the development of compression waves ahead of the flame. The flame front is treated as a plane of discontinuity which moves with a prescribed acceleration. The disturbance preceding this plane is calculated by considering the flow ahead of the flame to be isentropic, and applying the equations of mass and momentum conservation to this region. The flame acceleration is assumed to be constant, and the particle velocity of the unburned gas just ahead of the flame is assumed to be directly proportional to the flame front speed.

The time τ_1 at which a shock wave first appears ahead of the flame is determined, and the distance between the flame and the shock is found. The density and pressure at the flame front are found for all times $0 < t < \tau_1$, and the properties immediately behind the flame can be found by applying the conservation equations across the flame discontinuity.

An analytical solution for the behaviour of the system after the formation of the shock is impossible, however, since the isentropic relationship is no longer valid, and a relationship independent of the shock speed cannot be found for the pressure and density across the shock. The detonation is formed after the shock has travelled some distance further down the tube, and has grown in strength. Further treatment of the problem requires that the flow across the shock front be assumed isentropic, and results have indicated that this is a poor assumption for time greater than $1.5\ \tau_1$.

The dynamics of the retonation wave are examined, and it is found that the predicted speed of the retonation is only about half of the value which is actually observed. It is suggested that this discrepancy is due to the fact that complete reaction does not occur at the flame front, and that further reaction takes place as the retonation propagates into the hot products.

4.3 MODEL OF CHU

In the study of transition from deflagration to detonation, it is necessary to study the dynamic effects of heat release in a gaseous medium, and to determine the strength of the pressure waves generated by the

expansion of the hot, reacted gas. Chu (Ref. 17) has treated the problem of heat release in a gaseous mixture, and has obtained a linearized solution for the pressure field generated by a moderate rate of heat release in a tube.

An exact solution is given to determine the strength of the shock generated by a uniform heat release at a plane at a constant rate per unit area per unit time in a tube of constant cross-section. The model consists of a heat source at the plane $x=0$, and a shock followed by a contact surface propagating in both the positive and negative x-directions away from the source. It is assumed that the pressure behind the shocks is uniform, and that a velocity discontinuity exists at $x=0$, the velocities being uniform for $x>0$ and $x<0$, assuming the values of the particle velocities immediately behind the shock fronts. The temperature behind the shocks is assumed to tend to infinity and the density to zero in such a way that their product remains constant. The shock strength is then related to the heat release through the energy equation.

The problem is extended to three dimensions, and it is found that for a moderate rate of heat release at the centre (the origin of the co-ordinate system), the strength of the generated pressure wave depends on the time rate of change of the rate of heat release, as opposed to the plane case, where the strength depends on the rate of heat release. To produce a shock whose strength is invarient with time, it is found that the rate of heat release must be proportional to t^2 (t is time). Taylor's (Ref. 33) solution of the uniformly expanding sphere is extended to determine the constant of proportionality for a number of shock strengths.

4.4 DISCUSSION OF LIMITATIONS OF THEORETICAL MODELS

Adams and Pack (Ref. 15), Jones (Ref. 16) and Chu (Ref. 17), in their theoretical models, have assumed the flow to be purely one-dimensional and the flame front to be planar without fluctuations in shape. It has been determined experimentally,however, that the generation of turbulence, and the resulting distortion of the flame front are important mechanisms in the transition phenomenon. These models, therefore, can at best predict only qualitatively the nature of the transition process.

Adams and Pack (Ref. 15), in their theoretical treatment, have assumed the existence of a shock ahead of the flame front for all flame velocities, but have not considered the mechanisms of formation or of strengthening of the shock. The transition from deflagration to detonation is considered a continuous process of flame acceleration which approaches assymptotically the final detonation velocity. Experimental results have shown, however, that the process of transition is not continuous. The flame acceleration is found to be discontinuous, and there is a sudden velocity change at the onset of detonation. The mechanism of formation of this discontinuity would have to be considered in any model which is to yield results of a quantitative nature.

Jones (Ref. 16), in his analysis, assumes a constant flame acceleration, an assumption which is not justified in view of experimental results which indicate that the rate of flame acceleration increases as the flame propagates down the tube, and that the acceleration process is in many cases discontinuous. In order to obtain an approximate solution for the flow ahead of the flame after the shock discontinuity has been formed, the entropy change across the shock is neglected. It is found, however,

that this assumption is invalid for time greater than 1.5 τ_1, where τ_1 is the time required for the formation of the shock. It seems, also, that the strength of the retonation is due, not to further reaction of the hot gas products, but to the process of formation of this discontinuity.

Chu's (Ref. 17) analysis of the one-dimensional case is based on the assumption that heat is released at a constant rate at a single plane in the tube. In the case of flame propagation, however, it is known that the rate of heat release varies during the flame acceleration process due to turbulence effects, changes in density of the unburned mixture ahead of the flame, and variations in the flame front area and velocity. No analytical formulation of the rate of heat release can be obtained. In addition, the position of the heat source changes with time.

In the case of spherical flame propagation, the heat source cannot be considered a point, since heat is released by chemical reaction in the combustion zone which is a spherical surface of finite thickness which advances radially away from the centre with increasing time.

All of the existing theoretical models related to the process of transition have been necessarily simplified to enable a mathematical solution to be obtained. The flame has been treated as a plane of discontinuity: the transport phenomena such as diffusion and conduction which considerably affect the low-speed burning process have been neglected. Boundary layer and turbulence effects, which may be the most important factors in the transition process have also been neglected. The one model in which the formation of the precursor shock is considered cannot be solved after the formation of this shock unless the flow is considered to

be isentropic across the discontinuity.

It is clear that the transition process is an extremely complex phenomenon involving heat transfer, diffusion and viscous effects, and pressure wave and turbulence generation. The present understanding of the problem is inadequate to enable one to establish a predictive theory. It is impossible, from a given set of initial conditions, to derive a quantitative description of the subsequent development of the process. The state of knowledge is such that most of the effort is presently being spent in the performance of critical experiments, and the rationalization of the results obtained by physical reasoning to qualitatively explain the nature of the basic phenomena involved.

CHAPTER V

UNCONFINED TRANSITION

5.1 REASONS FOR INVESTIGATION

As outlined in Chapter III, there are three basic mechanisms which are of influence in promoting transition from deflagration to detonation. They are: i) differential acceleration; ii) interaction of the flame front with reflected pressure pulses; iii) generation of turbulence. The coupling among these three physical phenomena has been described, and it is apparent that in a tube, neither the process of differential acceleration nor the turbulence generation process can be eliminated. Only the flame-pressure wave interaction mechanism can be minimized by employing a tube of sufficient length.

In the case of spherical unconfined combustion, however, where ignition occurs at a point, and the flame propagates radially outward into an infinite volume of combustible mixture, the mechanisms of pressure wave interaction and wall generation of turbulence are entirely absent. It would be of great advantage to be able to study the flame acceleration process under such experimental conditions, since it could then be determined whether or not the differential acceleration mechanism is sufficiently strong to promote transition in the absence of the other two. It would be difficult to carry out any such experimental program on spherical detonation. The observation of transition could be made only by photographic means or by use of ionization probe detectors. The first would be extremely difficult because of the geometry of the process, and the second impossible, since the introduction of any probes in the flow would greatly affect the phenomenon which is being observed.

The possibilities of using a cylindrical containing vessel have been considered. In a vessel of this type, ignition would be effected along the axis of the cylinder, and the combustion wave would propagate radially outward to the periphery of the cylinder. The mechanism of pressure wave interaction with the flame front could be minimized by utilizing a container of large diameter, and the turbulence generation mechanism would be minimal due to the geometry. Observation of the flame acceleration process could now be made along a diameter of the cylinder by use of the well-known technique of streak photography. The cylindrical vessel thus displays great experimental advantage over a spherical vessel, while still retaining the important characteristics of an unconfined geometry.

5.2 PREVIOUS RESULTS

The earliest observations of spherical detonation were made by Laffitte (Ref. 18) in mixtures of $CS_2 + 3O_2$ and $2H_2 + O_2$ in spherical glass containing flasks of 20 to 26 cm diameter and initiated at the centre by a strong ignition source. Since then, experimental investigation of spherical detonation has been carried out by Manson and Ferrie (Ref. 19), Zeldovich et al. (Ref. 20), Pliickebaum et al. (Ref. 21) and others. Experimental work to this point has indicated the following: i) spherical detonation is initiated if the energy supplied is greater than a critical value; this value for spherical detonation is greater than the critical value required to initiate instantaneous detonation in a tube; ii) the limits of detonability for the initiation of a spherical detonation are narrower than those for the initiation of a plane detonation in the same mixture.

Manson and Ferrie (Ref. 19) have studied the propagation of spherical detonation in latex flasks containing various combustible mixtures, and have

found that the wave speeds agree closely with the detonation wave speeds measured in a tube containing mixtures at corresponding conditions. When various mixtures of acetylene-oxygen were ignited by hot wire (15-20 mm length Ni-Cr, .18 mm diameter, 10-12 volts AC), deflagrations of non-uniform propagation velocities resulted. Alternate accelerations and decelerations of the wave were observed, but no transition to detonation was noted. When combustion in a 50% acetylene-oxygen mixture was initiated with an electrically-primed ignitor, a pre-detonation period was observed. It was noted, however, that retonation waves, which are known to form when transition from deflagration to detonation occurs (Chapter III), were not observed.

Pliickebaum et al. (Ref. 21) have also noted this predetonation period in oxy-acetylene mixtures ignited by spark and by exploding wire. Again, the final detonation velocities corresponded quite closely to the theoretical plane detonation velocities.

Zeldovich et al. (Ref. 20) have performed a number of experiments using a stoichiometric acetylene-oxygen mixture diluted with varying amounts of nitrogen. A detonation was initiated in the tube leading to a large chamber, and ignition in the large volume occurred when the detonation propagated out of the tube into this volume. For the undiluted C_2H_2-O_2 mixture, no visible collapse of the detonation occurred, and a spherical detonation was instantaneously formed. As the mixture was diluted, however, some delay was noted before a spherical detonation was formed. When the dilution was increased beyond a certain limit ($C_2H_2 + 2.5\ O_2 + 3.25\ N_2$), only deflagrative burning took place in the large volume. No transition from deflagration to detonation was observed in any of these cases.

An explanation for the contradictory observations is possible.

Both Manson and Ferrie (Fig. 19) and Pliickebaum et al. (Ref. 21) utilized ignitors which extended from the outside diameter of their spherical vessels to the centre. This obstruction might well be a disturbance to the flow large enough to generate considerable turbulence, and thus promote transition in this geometry where none would have occurred in the absence of this obstruction. The experiments of Zeldovich et al. (Ref. 20) which might more closely approximate the truly unconfined case, lead to the belief that transition in the spherical case is unlikely in the absence of any turbulence-producing mechanisms.

CHAPTER VI

THEORETICAL ANALYSIS

6.1 FLAME-PRESSURE WAVE INTERACTIONS

One of the mechanisms which promotes the transition process is the interaction of the advancing flame front with the precursor shock which is reflected from the closed end of the tube. It is known (Refs. 3 to 6) that soon after the initiation of slow burning in a tube, a large number of compression pulses are generated at the flame front, and these subsequently coalesce to form a shock. A detailed theoretical model of this wave generation process, and the coupled acceleration of the flame front is impossible to formulate, but the basic characteristics of the interaction of the flame front with the reflected shock can be obtained by the treatment of a simplified model. The main interest in this study is that of flame propagation and transition of cylindrical detonation. It is known that at small radius in the cylindrical geometry, the area divergence greatly affects the fluid properties, but as the flame-shock system propagates outward to a larger radius, the curvature effects become negligible. Preliminary investigation has shown that the first flame-pressure wave interaction occurs at about 3 cm from the containing wall of the cylindrical vessel (20 cm or more from the centre). Since the shock front is followed very closely by the flame front, a model which neglects the area divergence (at this large radius) can yield satisfactory results.

The model considered is shown in Fig. 1 and consists of a flame front (AC) preceded by a pressure wave (AB) which reflects from the wall of the containing vessel and interacts with the flame front at C. The following assumptions are made:

i. The flow can be treated as approximately one-dimensional, and isentropic except across the flame front.

ii. There are no friction or heat transfer losses.

iii. The normal burning velocity (the flame speed relative to the unburned gas particles just ahead of the flame front) is independent of the pressure and proportional to the temperature of the unburned mixture.

iv. There is no change in the gas constant or in the specific heat of the mixture as it is burned.

v. The pressure across the flame is constant.

6.1.1 Relations Across Flame Front

According to assumption (iii) of the previous paragraph, the normal burning velocity may be written as

$$S = k T_u \qquad \ldots\ldots (6.1)$$

where k is a constant of proportionality.

The flame speed relative to a stationary co-ordinate system may therefore be written as

$$U_f = u_u + k T_u \qquad \ldots\ldots (6.2.)$$

By transforming the moving flame to a stationary co-ordinate system (Fig. 2) the equation of continuity across the flame front is written as

$$\rho_b (u_b - U_f) = \rho_u (u_u - U_f) \qquad \ldots\ldots (6.3)$$

Combining Eqs. 6.2 and 6.3,

$$\rho_u / \rho_b = 1 + (u_u - u_b)/S \qquad \ldots\ldots (6.4)$$

In a tube which is closed at both ends, the boundary condition which must be satisfied is that

$$u_b = 0 \qquad \ldots\ldots (6.5)$$

The equation of state may be written as

$$p = \rho \frac{R}{M} T \qquad \ldots\ldots (6.6.)$$

Since it has been assumed that there is no change in pressure or in the value of the gas constant across the flame, Eq. 6.6 takes the form

$$\rho_u / \rho_b = T_b / T_u \qquad \ldots\ldots (6.7)$$

If $\Delta T = T_b - T_u$, Eq. 6.7 becomes

$$\rho_u / \rho_b = 1 + \Delta T / T_u \qquad \ldots\ldots (6.8)$$

Combining Eqs. 6.4 and 6.8

$$(u_u - u_b) / S = \Delta T / T_u \qquad \ldots\ldots (6.9)$$

Eqs. 6.1 and 6.9 may now be combined to yield

$$u_u - u_b = k \Delta T \qquad \ldots\ldots (6.10)$$

From assumption (iv),

$$\Delta T = \Delta Q / c_p \qquad \ldots\ldots (6.11)$$

where ΔQ is the heat release per mole of reactants and C_p is the specific heat per mole ^{o}K.

Since the speed of sound $a = \sqrt{\gamma \frac{R}{M} T}$

$$a_b / a_u = \sqrt{T_b / T_u} = \sqrt{1 + \Delta T / T_u} \qquad \ldots\ldots (6.12)$$

6.1.2. Relations Across Pressure Wave

If it is assumed that the change of state across the pressure wave is isentropic,

$$\Delta u = \frac{2}{\gamma - 1} \Delta a \qquad \ldots\ldots (6.13)$$

Referring to Fig. 1,

$$u_2 - u_o = \frac{2}{\gamma - 1} (a_2 - a_o)$$

Since $u_o = 0$,

$$u_2 = \frac{2}{\gamma - 1} (a_2 - a_o) \qquad \ldots\ldots (6.14)$$

Also,

$$a_2 / a_o = \sqrt{T_2 / T_o} \qquad \ldots\ldots (6.15)$$

6.1.3. Flame-Pressure Wave Interaction

In order that the following analysis applies to the interaction whether the pressure wave propagates through burned or unburned mixture, the flow regions are numbered as in Fig. 3 (a) and Fig. 3 (b).

Since it is assumed that the only change in entropy occurs across the flame front

$$p_2/p_4 = (a_2/a_4)^{\frac{2\gamma}{\gamma-1}} \quad \ldots\ldots \quad (6.16)$$

$$p_1/p_5 = (a_1/a_5)^{\frac{2\gamma}{\gamma-1}} \quad \ldots\ldots \quad (6.17)$$

Since it is also assumed that there is no pressure change across the flame ,

$$p_1 = p_2 \quad \text{and} \quad p_4 = p_5$$

From Eqs. 6.16 and 6.17

$$a_2/a_4 = a_1/a_5 \quad \ldots\ldots \quad (6.18)$$

$$a_2/a_1 = a_4/a_5 = (a_2 + \Delta a + \Delta a')/(a_1 + \Delta a'') \quad \ldots\ldots \quad (6.19)$$

From Eq. 6.10

$$u_1 - u_2 = k\Delta T = u_5 - u_4 \quad \ldots\ldots \quad (6.20)$$

From the isentropic relation across pressure waves

$$u_4 = u_2 + \frac{2}{\gamma-1}(\Delta a - \Delta a') \quad \ldots\ldots \quad (6.21)$$

$$u_5 = u_1 + \frac{2}{\gamma-1}\Delta a'' \quad \ldots\ldots \quad (6.22)$$

Combining Eqs. 6.20, 6.21 and 6.22 yields

$$\Delta a - \Delta a' - \Delta a'' = 0 \quad \ldots\ldots \quad (6.23)$$

Combining Eqs. 6.19 and 6.23 yields

$$\Delta a' = \left(\frac{a_2 - a_1}{a_1 + a_2}\right)\Delta a \quad \ldots\ldots \quad (6.24)$$

$$\Delta a'' = \left(\frac{2a_1}{a_1 + a_2}\right)\Delta a \quad \ldots\ldots \quad (6.25)$$

In examining Eqs. 6.24 and 6.25, there is an interesting point to be noted. If the pressure wave propagates through the burned medium ($a_2 > a_1$), both the reflected and transmitted pressure waves $\Delta a'$ and $\Delta a''$ are of the same sense (compression or rarefaction) as the incident wave. If the incident wave propagates through the unburned medium, the reflected wave $\Delta a'$ is of opposite sense.

6.1.4 Results

The limitations of this model in quantitatively predicting the acceleration of a flame in a cylindrical geometry is apparent. The process of formation of the pressure wave ahead of the flame front is not considered, and the gradual strengthening of the wave into a shock is disregarded. Once the pressure wave becomes strong enough, the assumption of isentropic flow across this wave is no longer valid, and the conservation equations must be applied to both the shock and flame fronts. The dependence of the normal burning velocity of a mixture on its temperature and pressure has been oversimplified, and may not be valid for many mixtures. The assumption of constant pressure across the flame front is only valid for flame velocities of the order of one-tenth of the speed of sound in the unburned medium. In the chemically-reacting flow which is considered, the assumption of constant values of the specific heat ratio and constant molecular weight may be very poor due to large temperature and composition changes. The validity of neglecting the curvature effect in the cylindrical geometry is open to question, though this may be a justifiable assumption at large radius.

It is expected, however, that this analysis leads to a qualitative prediction as to how the burning process may occur. Two sample calculations of non-dimensionalized space-time diagrams have been obtained, and

are shown in Figs. 4 and 5. The first was calculated on the basis of the values used by Rudinger and Rinaldi (Ref. 22) for a general fuel-oxidant system:

$$\Delta T = 2220^{\circ}K.$$

$$S/a_o = KT \quad ; \quad K = 1.8 \times 10^{-3} \ {}^{\circ}K^{-1}$$

Several steps in this calculation are given in Appendix I. The second was calculated on the basis of data for C_2H_2-O_2 mixture obtained from Lewis and von Elbe (Ref. 23).

$$\Delta T = 2700^{\circ}K.$$

$$S/a_o = KT \quad ; \quad K = 5.67 \times 10^{-4} \ {}^{\circ}K^{-1}$$

The flame interacts with the reflected compression wave, the transmitted wave is a compression, and the reflected wave is an expansion wave. Since the boundary condition that the particle velocity in Region 3 (Fig. 4) is zero must be satisfied, and the velocity imparted to the gas particles by an expansion wave is in the direction opposite to the direction of wave propagation, the particle velocity in Region 4 (Fig. 4) is toward the ignition end of the tube. The normal burning speed of the mixture in Region 4 (Fig. 4) is less than the particle velocity, and so the absolute flame speed, which is the algebraic sum of these two velocities, is also toward the ignition source at this instant. The character of a flame-pressure wave interaction is apparent from Fig. 4. It is seen that if the disturbance propagates in the burned gas, a compression wave accelerates the flame front, and an expansion wave decelerates it. For a disturbance which propagates in the unburned gas, a compression wave decelerates the flame, and an expansion wave accelerates it.

This model, which neglects both the differential acceleration and turbulence generation mechanisms of flame acceleration, provides no process by which transition to detonation might occur: it is thought that in the absence of the other two mechanisms, no such transition can take place.

6.2 PISTON-DRIVEN SHOCK

It is well known that in the case of piston-supported spherical and cylindrical shocks, the divergence of flow area gives rise to a non-uniform distribution of fluid properties behind the shock. Unlike the plane case, therefore, where the fluid properties are constant behind the driven shock, this variation must be considered in any attempt to theoretically formulate a flame-shock model for either the cylindrical or the spherical case.

The first step in the formulation of such a model would be to consider a uniformly-expanding piston (either cylindrical or spherical) which drives a shock front ahead of it. It would be of interest also to evaluate the energy stored in the compressed slug of gas between the shock and piston faces in order to see whether or not the heat released by a flame propagating behind the shock is sufficient to support the shock.

In order to obtain an idea as to the amount of energy required to support a shock of given strength in a cylindrical or spherical geometry, it is necessary to obtain the distribution of fluid properties behind the advancing wave front. Consider a spherical or a cylindrical piston expanding in a perfect gas. It is assumed that the piston begins to move at zero time, and continues to propagate radially outward at a constant rate, driving a shock ahead of it. The flow behind the shock and ahead of the piston is considered to be isentropic and self-similar.

6.2.1 Basic Equations

The basic equations for the unsteady flow behind the shock front may be written as

Momentum: $$\frac{\partial u}{\partial t} + u\frac{\partial u}{\partial r} + \frac{1}{\rho}\frac{\partial p}{\partial r} = 0 \quad \ldots\ldots \quad (6.26)$$

Continuity: $$\frac{\partial \rho}{\partial t} + \rho\frac{\partial u}{\partial r} + u\frac{\partial \rho}{\partial r} + j\frac{\rho u}{r} = 0 \quad \ldots\ldots \quad (6.27)$$

where $j = 0$ for the plane case

1 for the cylindrical case

2 for the spherical case

Assuming that the isentropic relation is valid behind the shock front, Eqs. 6.26 and 6.27 may be rewritten as

$$\frac{\partial u}{\partial t} + u\frac{\partial u}{\partial r} + \frac{2}{\gamma-1}\,a\frac{\partial a}{\partial r} = 0 \quad \ldots\ldots \quad (6.26a)$$

$$\frac{2}{\gamma-1}\frac{\partial a}{\partial t} + a\frac{\partial u}{\partial r} + \frac{2}{\gamma-1}u\frac{\partial a}{\partial r} + j\frac{au}{r} = 0 \quad \ldots\ldots \quad (6.27a)$$

6.2.2 Similarity Parameter

The similarity transformation made is

$$\xi = r/a_0 t \quad \ldots\ldots \quad (6.28)$$

$$F_1(\xi) = a/a_0 \quad \ldots\ldots \quad (6.29)$$

$$F_2(\xi) = u/a_0 \quad \ldots\ldots \quad (6.30)$$

Putting Eqs. 6.28, 6.29 and 6.30 into Eqs. 6.26a and 6.27a, one obtains

$$F_2'(F_2 - \xi) + \frac{2}{\gamma-1}F_1F_1' = 0 \quad \ldots\ldots \quad (6.31)$$

and $$\frac{2}{\gamma-1}F_1'(F_2 - \xi) + F_1F_2' + j\frac{F_1F_2}{\xi} = 0 \quad \ldots\ldots \quad (6.32)$$

where $'$ denotes differentiation with respect to ξ.

Eqs. 6.31 and 6.32 can be combined to yield

$$F_2' = -j\frac{F_2}{\xi}\,\frac{F_1^2}{\left[F_1^2 - (F_2 - \xi)^2\right]} \quad \ldots\ldots \quad (6.33)$$

$$F_1' = j\frac{F_1F_2}{\xi}\left(\frac{\gamma-1}{2}\right)\frac{[F_2 - \xi]}{\left[F_1^2 - (F_2 - \xi)^2\right]} \quad \ldots\ldots \quad (6.34)$$

6.2.3 Boundary Conditions

The relations derived above are valid in the region of isentropic flow bounded by the shock front and the piston face. In order to find the starting values for F_1 and F_2, the Rankine-Hugoniot relations are applied across the shock.

The pressure ratio across the shock may be written as

$$P_s/P_o = y_1 = \frac{2\gamma M_s^2}{\gamma+1} - \frac{\gamma-1}{\gamma+1} \quad \ldots\ldots (6.35)$$

Also,

$$a_s/a_o = \left\{ \frac{y_1[y_1(\gamma-1)+\gamma+1]}{y_1(\gamma+1)+\gamma-1} \right\}^{\frac{1}{2}} \quad \ldots\ldots (6.36)$$

$$\mu_s/U_s = 2(y_1-1)/[y_1(\gamma+1)+\gamma-1] \quad \ldots\ldots (6.37)$$

$$\xi_s = \tau_s/a_o t = U_s/a_o = M_s \quad \ldots\ldots (6.38)$$

The starting values of F_1 and F_2 may now be written as

$$F_1(\xi_s) = a_s/a_o \quad \ldots\ldots (6.39)$$

$$F_2(\xi_s) = \mu_s/a_o = M_s\, \mu_s/U_s \quad \ldots\ldots (6.40)$$

One additional boundary condition which must be satisfied is that the particle velocity just at the piston face must be equal to the piston velocity. This condition may be expressed as

$$\xi_p = \tau_p/a_o t = U_p/a_o = (\mu/a_o)_{\xi=\xi_p} = F_2(\xi_p) \ldots\ldots (6.41)$$

6.2.4. Fluid Properties Behind Shock Front

Two fluid properties have already been expressed as

$$\mu/a_o = F_2(\xi) \quad ; \quad a/a_o = F_1(\xi)$$

The pressure ratio can be written as

$$\frac{p}{p_s} = \left(\frac{a}{a_s}\right)^{\frac{2\gamma}{\gamma-1}} = \left[\frac{F_1(\xi)}{F_1(\xi_s)}\right]^{\frac{2\gamma}{\gamma-1}}$$

Then

$$\frac{p}{p_0} = \frac{p_s}{p_0}\,\frac{p}{p_s} = y_1\left[\frac{F_1(\xi)}{F_1(\xi_s)}\right]^{\frac{2\gamma}{\gamma-1}} \qquad \ldots\ldots \quad (6.42)$$

The density ratio is expressed as

$$\frac{\rho}{\rho_s} = \left(\frac{a}{a_s}\right)^{\frac{2}{\gamma-1}} = \left[\frac{F_1(\xi)}{F_1(\xi_s)}\right]^{\frac{2}{\gamma-1}}$$

or

$$\frac{\rho}{\rho_0} = \frac{\rho_s}{\rho_0}\left[\frac{F_1(\xi)}{F_1(\xi_s)}\right]^{\frac{2}{\gamma-1}} \qquad \ldots\ldots \quad (6.43)$$

The temperature ratio is

$$\frac{T}{T_s} = \left(\frac{a}{a_s}\right)^2 = \left[\frac{F_1(\xi)}{F_1(\xi_s)}\right]^2$$

or

$$\frac{T}{T_0} = \frac{T_s}{T_0}\left[\frac{F_1(\xi)}{F_1(\xi_s)}\right]^2 \qquad \ldots\ldots \quad (6.44)$$

6.2.5 Energy Integral

The total energy of the shocked gas can be expressed as

$$E = \int\left[\frac{p - p_0}{\gamma - 1} + \frac{1}{2}\rho u^2\right] dV \qquad \ldots\ldots \quad (6.45)$$

The term within the brackets can be written in terms of F_1, F_2, and known conditions as

$$C = \frac{p_0}{\gamma-1}\left[\frac{p_s}{p_0}\left[\frac{F_1(\xi)}{F_1(\xi_s)}\right]^{\frac{2\gamma}{\gamma-1}} - 1\right] + \frac{1}{2}\rho_0\left(\frac{\rho_s}{\rho_0}\right)a_0^2\left[F_2(\xi)\right]^2\left[\frac{F_1(\xi)}{F_1(\xi_s)}\right]^{\frac{2}{\gamma-1}} \quad \ldots\ldots \quad (6.46)$$

The energy integral becomes

$$E = A a_o t \int_{\xi_p}^{\xi_s} C \, d\xi \qquad \text{for the plane case}$$

$$E = 2\pi a_o^2 t^2 L \int_{\xi_p}^{\xi_s} C \xi \, d\xi \qquad \text{for the cylindrical case}$$

$$E = 4\pi a_o^3 t^3 \int_{\xi_p}^{\xi_s} C \xi^2 \, d\xi \qquad \text{for the spherical case} \quad \ldots\ldots \quad (6.47)$$

6.2.6. Numerical Solution of Problem

A numerical solution of Eqs. 6.33 and 6.34 has been obtained on an IBM 7040 digital computer using the Runge-Kutta Method (Ref. 24). An interval of $\Delta\xi$ of .001 was used. The starting values for F_1 and F_2 were obtained using Eqs. 6.39 and 6.40, and the numerical procedure was followed until the boundary condition expressed by Eq. 6.41 was satisfied. The energy integral (Eq. 6.47) was obtained by numerical integration using Simpson's Rule (Ref. 24). Results were obtained for shock Mach numbers ranging from 1.25 to 10.0, the distribution of fluid properties and the energy integral being evaluated for the plane, cylindrical and spherical cases for each shock strength, assuming an initial pressure of 100 mm Hg for the undisturbed mixture.

6.2.7. Results and Discussion

A plot of F_2 as a function of ξ for both the cylindrical and the spherical expanding pistons driving shocks of various strengths is shown in Fig. 6 and it is immediately noted that for both the cylindrical and spherical cases, F_2 increases as ξ decreases. It is also seen that the rate of increase is greater for the spherical case than it is for the cylindrical case. An examination of the derivatives F_1' and F_2' in Eqs. 6.33 and 6.34 yields a mathematical explanation for

this behaviour. The denominator $\left[F_1^2-(F_2-\xi)^2\right]$ can be expressed in the form $\left[F_1+(F_2-\xi)\right]\left[F_1-(F_2-\xi)\right]$. The starting values for a shock Mach number of 2 are: $F_1 = 1.299$; $F_2 = 1.250$; $\xi = 2.00$. It is seen that $\left[F_2-\xi\right]$ is negative, and that $F_1 > |F_2-\xi|$. Both factors of the denominator, $\left[F_1+(F_2-\xi)\right]$ and $\left[F_1-(F_2-\xi)\right]$ are therefore positive. Inspection of Eqs. 6.33 and 6.34 now shows that

$$F_1' < 0$$
$$F_2' < 0$$

As ξ decreases, therefore, it is expected that F_1 and F_2 increase, a trend which is noted in the results obtained.

It is seen also from the results that the zone of shocked gas (between the shock front and the piston face) is greater for the cylindrical than the spherical case. The gradients of F_1 and F_2 are both greater for the spherical case $(j=2)$ than for the cylindrical case $(j=1)$, and so the boundary condition $u_p/a_0 = \xi_p$ is reached at a value of ξ closer to the shock front in the spherical case. The piston velocity u_p/a_0 is therefore higher for the spherical case. A plot of p/p_0 as a function of ξ for various shock strengths is shown in Fig. 7.

Plots of F_2 and p/p_0 as functions of ξ for plane, cylindrical and spherical shocks of Mach number of 8.25 are seen in Figs. 8 and 9. Again, it is apparent that the pressure gradient is steepest for the spherical case. By physical reasoning, it seems that this should be so since the flow area diverges more rapidly for the spherical geometry than for the cylindrical case. The gas nearest the piston face $(\xi = \xi_p)$ must be more highly compressed in order that the equation of continuity be satisfied at every ξ.

Several points are to be noted in the evaluation of the energy integral of Eq. 6.47. The total energy required to support a shock of given strength is, in the plane case, dependent on the cross-sectional area of the tube considered, and in the cylindrical case, dependent on the width of the cylindrical vessel. In the spherical case, the energy does not depend on any characteristic dimension since the expansion is uniform in all directions. It is also seen that in the plane case, energy must be released at a constant rate in order to maintain a shock of given strength; in the cylindrical case, the rate of energy release must vary as t; in the spherical case, the rate of energy release must vary as t^2. The result obtained for the spherical shock is in agreement with that obtained by Chu (Ref. 17), who by dimensional analysis found that the rate of energy supply required to sustain a shock of given strength varies as t^2.

The time dependence of the energy required to produce a shock of given strength is due to the effect of area divergence in both the cylindrical and spherical cases. The energy release required to support cylindrical and spherical shock of Mach numbers from 7.25 to 8.75 is shown in Figs. 10 and 11. A complete tabulation of this required energy for shock Mach numbers from 1.25 to 10 is given in Table 1.

It is interesting to note at what rate heat is released by a flame which follows the shock front in each of these geometries. The rate of heat release by burning can be written as

$$Q_t = \rho_u S A \Delta Q$$

where Q_t is rate of heat release
S is burning speed of mixture
ρ_u is unburned gas density
ΔQ is heat release per unit mass of mixture
A is area of flame front.

For the plane case, A is simply the cross-sectional area of the tube, and the rate of heat release by the flame varies as this area A and is independent of time. In a cylindrical geometry, the flame area can be expressed as

$$A = 2\pi L r_f$$

Since $r_f = \xi_f a_o t$, the area can be written as

$$A = 2\pi \xi_f a_o t L$$

The rate of energy release Q_t now becomes

$$Q_t = 2\pi \rho_u S \xi_f a_o t L \Delta Q$$

In the cylindrical case, therefore, the rate of energy release by the flame is proportional to the rig width L and varies as t. For the spherical case, the flame area becomes

$$A = 4\pi r_f^2$$

or

$$A = 4\pi \xi_f^2 a_o^2 t^2$$

The rate of energy release becomes

$$Q_t = 4\pi \rho_u S \xi_f^2 a_o^2 t^2 \Delta Q$$

The rate of energy release by burning varies as t^2. In each case therefore, the rate of energy release by the flame varies in identically the manner required to sustain a constant-strength shock.

6.3 FLAME-DRIVEN CYLINDRICAL SHOCK

In the previous section, the distribution of fluid properties behind a piston-driven shock has been calculated. It is well known that a flame propagating in a combustible medium is preceded by a shock which is generated as the hot products of combustion expand. In this respect, therefore, the flame front can be thought of as a piston-gas interface. However, a very basic difference between the flame front and a piston face does exist: in the case of the piston, there is no mass flux across the

face, whereas in the case of a flame, there is a mass flux from the unburned (but shocked) mixture to the burned gas. It would therefore be expected that a flame would be less effective in driving a shock than a piston face propagating at the same velocity.

In order to obtain a quantitative idea of the differences in the property distributions behind piston-driven and flame-driven shocks, the following model will be considered:

i. The cylindrical shock of known strength propagates radially outward into unburned gas at known initial conditions.

ii. The shock is followed by a flame front.

iii. The flow is isentropic between the shock and the flame fronts.

iv. There is no change in the specific heat ratio or in the gas constant across the shock.

v. A similarity solution exists for which both the shock front and flame front propagate at constant speeds.

vi. The burned gas products behind the flame front are at rest.

6.3.1. Analysis

The following analysis is based on the shock-flame system shown in Fig. 12.

Following the procedure outlined in Section 7.2, the distribution of fluid properties behind the cylindrical shock (of given strength) can be found as a function of the similarity parameter ξ.

Since $$\xi = r/a_o t \quad \ldots\ldots \quad (6.28)$$

and $$\xi_s = R_s/a_o t \quad \ldots\ldots \quad (6.48)$$

Then $$r/R_s = \xi/\xi_s \quad \ldots\ldots \quad (6.49)$$

The fluid properties at each radius r behind the shock front is determined, and a flame front is assumed at each successive radius until the

boundary condition that the burned products behind the flame are at rest is satisfied.

Denoting the fluid properties ahead of the flame by the subscript μ, Eq. 6.30 may be written as

$$u_\mu / a_o = F_2(\xi_f) \quad \ldots\ldots (6.50)$$

Since the flame speed U_f is the sum of the laminar burning speed S and the particle velocity u_μ ahead of the flame front,

$$U_f / a_o = S/a_o + u_\mu / a_o \quad \ldots\ldots (6.51)$$

Since $$r_f = U_f t \quad \ldots\ldots (6.52)$$

Eq. 6.51 becomes

$$S/a_o = r_f / a_o t - u_\mu / a_o \quad \ldots\ldots (6.53)$$

Also,

$$T_\mu / T_o = (a_\mu / a_o)^2 = [F_1(\xi_f)]^2 \quad \ldots\ldots (6.54)$$

An approximation for the Hugoniot equation across the flame front in 50% acetylene-oxygen mixture at a pressure of 1 atm is obtained from Emmons (Ref. 25) based on the results of Manson (Ref. 26).

$$(x - .08)(y + .08) = .474 + 22.326\left(\frac{T_o}{T_\mu}\right) = \psi \quad \ldots\ldots (6.55)$$

Where $$x = \rho_\mu / \rho_b \quad \ldots\ldots (6.56)$$

$$y = \rho_b / \rho_\mu \quad \ldots\ldots (6.57)$$

The value of T_o in Eq. 6.55 is 288°K. The continuity and momentum equations across the flame front are written as:

$$\text{Continuity:} \quad \rho_u S = \rho_b \left(S + u_u - u_b\right) \quad \ldots\ldots \quad (6.58)$$

$$\text{Momentum:} \quad p_u + \rho_u S^2 = p_b + \rho_b \left(S + u_u - u_b\right)^2 \quad \ldots\ldots \quad (6.59)$$

Eliminating $\left(u_u - u_b\right)$, Eqs. 6.58 and 6.59 combine to yield

$$\frac{(1-y)}{(x-\psi)} = S^2 \frac{\rho_u}{p_u} = \frac{S^2}{a_o^2} \gamma_o \frac{T_o}{T_u} = B \quad \ldots\ldots \quad (6.60)$$

Since S/a_o and all the fluid properties ahead of the flame front can be calculated for any flame radius r_f, a quadratic equation for x can be obtained by eliminating y between Eqs. 6.55 and 6.60.

$$-Bx^2 + x(1.08 + 1.08B) - .08B - \psi - .0864 = 0 \quad \ldots\ldots \quad (6.61)$$

One additional equation is required to obtain a solution. A physically possible state behind the flame front is that the burned gas is at rest.

Putting $u_b = 0$ in Eq. 6.58, one obtains

$$\frac{u}{a_o} + (1-x)\frac{S}{a_o} = 0 \quad \ldots\ldots \quad (6.62)$$

At the flame radius for which this condition is satisfied, a physically possible flame-shock system is found.

6.3.2 Numerical Solution

At each assumed flame radius, all the gas properties ahead of the flame can be evaluated by Eqs. 6.50, 6.53 and 6.54. The co-

efficients Ψ and B in Eq. 6.61 can be evaluated from Eqs. 6.55 and 6.60 respectively. The roots of Eqs. 6.61 can now be obtained. These roots are imaginary above a certain flame radius, and no solution can be obtained. Below this flame radius, however, these roots are real, and are denoted by x_1 and x_2. The terms $\frac{S}{a_0}(x_1-1)$ and $\frac{S}{a_0}(x_2-1)$ are evaluated at each radius. The critical radius is attained when Eq. 6.62 is satisfied.

Results are obtained on an IBM 7040 digital computer for six shock strengths with pressure ratios varying from 2 to 70. A plot of $\frac{S}{a_0}(x-1)$ and u/a_0 vs. r/R_s is shown in Fig. 13 for a shock pressure ratio of 10. The critical flame radius is seen to be $r_f/R_s = 0.8966$. The corresponding critical values of S/a_0, u_f/a_0 and U_f/a_0 are respectively 0.2334, 2.4125 and 2.6459. The shock Mach number U_s/a_0 is 2.952.

6.3.3 Results and Discussion

A plot of r_f/R_s (flame radius) vs. p_s/p_0 (shock strength) is shown in Fig. 14. It is noted that the flame front is closer to the shock front in the spherical case than it is in the cylindrical case. This result is qualitatively the same as for a piston-driven shock, where the shocked gas region is thinner for the spherical case. The ratio r_p/R_s (piston radius) is also plotted in Fig. 14. For both the cylindrical and spherical geometries considered, it is seen that the flame front is much closer to the shock front than is the piston face for a driven shock of the same strength. It is noted also that as the initial shock strength increases, the critical flame radius for the cylindrical case approaches closer to the value for the spherical case.

In Fig. 15, both the flame velocity U_f/a_o $\left(= S/a_o + u_f/a_o\right)$ and the piston velocity u_p/a_o are plotted as functions of shock strength p_s/p_o for the cylindrical and the spherical cases. It is seen that to produce a shock of given strength (in the cylindrical geometry), the flame velocity required is greater than the piston velocity required to produce the same shock. This result can be explained by a physical argument. For an expanding cylindrical flame, unlike the corresponding piston, there is mass flux across the flame front. Even though the flame front may act as a pseudo-piston due to the expansion of the hot gas products behind it, this flow of mass across the front decreases the effectiveness of the flame in compressing the gas ahead of the front, and the shock wave generated by the moving flame is consequently weaker than the shock generated by a solid-face piston moving at the same velocity. A similar trend is noted in the spherical case, where the results are shown in Fig. 15 by the broken line.

The burning speed S/a_o is plotted against the shock strength p_s/p_o for the cylindrical and spherical cases (Fig. 16). It is noted that for low pressure ratios (up to 10.0), the burning speed for the spherical case is greater than that for the cylindrical case. Above pressure ratios of 10.0, there is negligible difference in burning speed between the two cases. The burning speed S/a_o is dependent on the gas properties, especially the temperature, immediately ahead of the flame front. For $p_s/p_o > 10$, it is seen from Fig. 14 that $T_f/R_s > .9$ for both the cylindrical and spherical cases. Though the temperature gradient is steeper for the spherical than for the cylindrical case, the temperature ratio is rather insensitive to changes in T_f/R_s in this small range, and there is little difference in burning speed behind

cylindrical and spherical shocks of high strength. For weak shocks, however, where the flame front follows the shock at a greater distance, a significant difference in the temperature ahead of the flame exists between the cylindrical and spherical cases: the burning speed in the spherical case is higher due to the higher temperature ahead of the flame front.

The shock speed U_s/a_o and the absolute flame speed U_f/a_o $(= S/a_o + u_f/a_o)$ are plotted as functions of the shock strength p_s/p_o (Fig. 17). It is seen that for the critical flame speed at which the products of combustion are at rest, the shock speed is greater than the flame speed for all shock strengths and for both the cylindrical and the spherical cases. The flame propagation speed is slightly higher for the spherical case, since both the burning speed S/a_o and the particle speed u_f/a_o are greater for the spherical case. At high pressure ratios, however, where the burning speed S/a_o is almost the same for both cases, the cylindrical flame speed is closer to the corresponding spherical value.

In order to obtain an idea as to the order of magnitude of the rates of energy release involved in the shock propagation and flame propagation, some calculations have been done. From the energy integral evaluated in Section 6.2.5, it is found that to support a spherical shock of Mach number of 4.0, the rate of energy release required is

$$Q_t = 2 \times 10^8 \, a_o^3 t^2 \quad \text{joules/sec}$$

Chu's (Ref. 17) analysis of a spherically-expanding shock has indicated that to support a shock of Mach number of 3.95, the heat release parameter $\frac{\alpha}{a_o^3 p_o}$ is 4×10^4. The rate of energy release at the centre re-

quired to support the shock is therefore $Q_t = \alpha t^2$

$$Q_t = 5.33 \times 10^8 \; a_o^3 \; t^2 \qquad \text{joules/sec}$$

It would be of interest to note the rate at which heat would be released by a flame front following a shock of Mach 3.95 in an acetylene-oxygen mixture at 100 mm Hg initial pressure. The rate of heat release can be expressed as

$$Q_t = \rho_u \, S \, A \, \Delta Q$$

For the cylindrical case considered,

$$\rho_u / \rho_o = 4.26$$
$$S / a_o = 0.39$$
$$r_f / a_o t = 3.75$$

The density of the undisturbed mixture (100 mm Hg initial pressure) is 0.155 kg/m^3. Since the flame area $A = 4\pi r_f^2$, the rate of heat release becomes

$$Q_t = 1.13 \times 10^8 \; a_o^3 \; t^2 \qquad \text{joules/sec}$$

It would also be of interest to obtain an idea of the rate at which energy is supplied to the expanding hot gas products behind the flame front. The temperature of the stationary products of combustion is about 3000°K (Ref. 23). The enthalpy of the burned gas ($2CO + H_2$) is found from thermodynamic tables (Ref. 27) to be

$$H = 4.77 \times 10^6 \quad \text{joules/kg}$$

Since the unburned gas is at the reference state (T = 298°K), the change in enthalpy of the gas in burning is

$$\Delta H = 4.77 \times 10^6 \quad \text{joules/kg}$$

The rate of energy supply to the expanding "fireball" is

$$Q_t = \frac{dm}{dt} \Delta H = \frac{dV}{dt} \rho_b \Delta H$$

Since $$V = \frac{4}{3}\pi r_f^3$$

$$\frac{dV}{dt} = 4\pi r_f^2 \frac{dr_f}{dt}$$

Now, $$r_f / a_o t = 3.75$$

$$\frac{dr_f}{dt} = 3.75\, a_o$$

$$\rho_u / \rho_b = x \cong 10$$

$$\rho_u = 4.26\, \rho_o$$

$$\rho_b = 0.426\, \rho_o$$

Since $\rho_o = .155$ kg/m^3, the rate of energy supply can now be written as

$$Q_t = 1.89 \times 10^8\, a_o^3\, t^2$$

The rate of energy release at the flame front is not high enough to suggest that such a shock-flame system can "burn to detonation". Martin (Ref. 28) states, in fact, in discussing his results, that "the rate of formation of hot products on passage through the flame front is just sufficient to maintain a constant piston velocity and hence constant shock and flame velocities. It would then appear that if the flow remained laminar, in the absence of reflected shocks, the flame would propagate indefinitely at this constant rate.". It is stated by Taylor (Ref. 25) that "it seems that there is evidence that spherical detonation waves can be produced but there is no evidence that a spherical deflagration flame can increase in speed until detonation occurs at or near the flame.". In addition, experimental observation (Ref. 6) of the transition process by streak and streak schlieren photography has shown it to be a discontinuous process, so that a continuous flame acceleration

to detonation through a high rate of heat release could hardly constitute the entire process of transition.

It would be of great interest and advantage to experimentally investigate the flame acceleration process in an unconfined geometry, where other effects can be minimized or eliminated, in order to determine whether or not transition due to the self-acceleration of the flame (heat release) is possible.

CHAPTER VII

EXPERIMENTAL APPARATUS AND PROCEDURES

7.1 APPARATUS

7.1.1. Cylindrical Detonation Vessel

A schematic drawing of the cylindrical containing vessel is shown in Fig. 18. The end plate and the inner rings are fabricated of mild steel, and the transparent front face is of 1 inch thick acrylic plate. The vessel OD is 24 inches and the ID is 20 inches.

The 1 inch mild steel end plate contains a small hole and a 1/4 inch valve through which the rig is evacuated and the mixture filled. In addition, there is a threaded hole at the centre of the plate into which the ignitor is placed.

The inner rings, which can be removed singly to vary the thickness of the vessel, are located concentrically on the end plate by four dowel pins. These rings are vacuum-sealed by means of O-rings fabricated of 3/8 inch OD soft polyvinylchloride tubing, and Dow-Corning vacuum grease.

The acrylic front plate is entirely masked with black tape except for a horizontal slit along the diameter. The slit width is 2 mm, and allows observation of the combustion phenomenon by streak photography. The rig is easily assembled and disassembled, since it is held together by eight C-clamps evenly spaced around the circumference. A spiral coil made of 1/4 inch copper wire can be affixed to the sidewall of the vessel as shown in Fig. 18a.

7.1.2. Ignition Sources

An ignitor fabricated for use with the 2 inch width cylindrical vessel is shown in Fig. 19. The body of the ignitor is made of polyethylene, and the threaded portion is placed into the hole on the steel back plate.

Two brass rods are placed and cemented into the ignitor body as shown. An exploding wire (copper) or a Ni-Cr glow wire can then be soldered onto the terminals. The ignitors for other rig widths are essentially the same, except for the length of the terminal labelled A in Fig. 19.

7.1.3 Detonation Tube

A short detonation tube (Fig. 20) is constructed of extruded acrylic tubing of 1 inch ID and 1 1/4 inch OD. The ends are closed with plugs machined of polyethylene, and one of these ends contains a hole of 1/4 inch diameter for evacuating and filling of the tube. Ignition is accomplished by either an exploding wire or a glow wire soldered onto the two brass electrodes which are mounted at the tube centre.

7.1.4 Flow System

A schematic diagram of the flow control system is shown in Fig. 21. Commercial tanks of oxygen and acetylene are used to prepare the mixtures. A pressure regulator is mounted in each tank to control the filling operation. The valves used are Swagelock Whitey valves (1VM4) which have been slightly modified for vacuum service by inserting O-rings over the stem between the packing gland and nut. Five high-pressure tanks capable of withstanding a static pressure of 4000 psi are used as mixing tanks, and are never filled to pressures exceeding 2 atmospheres. A manometer and a McLeod gauge are used to measure the pressure in the vessel. Two high-capacity Balzers Type Duo 5 vacuum pumps are used to evacuate the system.

7.1.5 Streak Camera

A rotating drum streak camera with a writing speed of about 65 metres/sec and a drum circumference of 1 foot is used in the photographic study of the combustion phenomena. A schematic diagram of the camera is

shown in Fig. 22. It consists basically of a lens and a 45° prism which projects the image on the periphery of the rotating drum on which the film strip (35 mm Tri-X) is placed. The drum-shaft assembly is mounted on two ball-bearings, and is driven by an air jet which is directed on a series of buckets milled onto the outside circumference of the drum. The entire camera assembly can be easily removed from its supporting stand to facilitate loading and unloading of the film strips. A coil and permanent magnet are employed as a speed-measuring system, the output signal from the coil being displayed on a Tektronix Dual Beam 555 oscilloscope screen with a time-calibrated sweep.

7.1.6 Energy Sources

i. Exploding Wire Ignition

For exploding wire ignition, the procedure is to charge a bank of capacitors to a voltage in excess of 1 KV. The exact value of the voltage and capacitance used is determined by the energy desired. The voltage supply is continuously variable from 0 to 14 KV. The wire used is copper, either .003 inch or .006 inch in diameter.

ii. Hot Wire Ignition

For hot wire ignition, the glow wire used is Ni-Cr. The voltage applied to the wire is varied by using a variac to step down the normal 110 volts AC power supplied to the laboratory.

7.2 PROCEDURES

7.2.1 Preparation of Mixtures

The partial pressure technique is used to prepare acetylene-oxygen mixtures of the desired composition. The mixture tanks are first evacuated to a few microns, and acetylene is run into the tanks to the desired pressure. The lines are again evacuated, and the required amount of oxygen

is then added. The mixture is allowed to stand for 24 hours before any firing is done in order to ensure that the explosive gas is homogeneously mixed.

7.2.2 Procedure

A uniform procedure is followed for every experimental run. After the desired ignition source has been placed in the rig, the system is evacuated to several microns. While the mixture is bled into the system, the streak camera is brought up to speed. The system is filled to double the desired firing pressure, and the excess mixture is evacuated to the required pressure. If an exploding wire ignition source is used, the capacitor bank is now charged. The shot is fired, and the streak photograph is immediately developed.

7.2.3 Interpretation of Results

For each experimental run, a streak photograph is taken, utilizing the self-light of the combustion phenomenon. Tape markers are placed on the tube a known distance apart, and these appear as unexposed strips on the streak photographs. From these markers, the magnification factor can be determined in each streak picture. For the cylindrical vessel, no markers are placed, but the wave reflections from the periphery of the cylinder can be observed, so that the magnification factor may be obtained from the known inside diameter of the vessel.

The streak photograph is used for both qualitative and quantitative observation of the phenomenon. The speed of any wave in the streak picture may be determined (Fig. 23) from the relationship

$$W = \frac{V}{\mu \tan \theta} \qquad \ldots\ldots (7.1)$$

where W is the wave speed

V is the film writing speed

μ is the magnification factor

θ is the angle between the wave trace and a horizontal reference line.

CHAPTER VIII

RESULTS AND DISCUSSION

8.1 INITIATION OF COMBUSTION

It has been stated in Section 3.1 that there are three possible combustion phenomena which can occur when burning is initiated in a chemically-reactive fuel-oxidant system. They are: i) instantaneous formation of a detonation wave; ii) formation of a flame which subsequently interacts with the pressure waves which are generated ahead of it, and reflected from the constraining boundary; iii) formation of a flame which subsequently undergoes transition to detonation. At initiation, therefore, either a detonation or a flame may be formed, depending upon the method of ignition or the energy of the ignition source.

It has been found (Ref. 29) that for a fuel-oxidant system, at each mixture ratio and initial pressure, there exists a critical ignition energy above which instantaneous detonation is formed at the source, and below which a flame is initiated in the mixture. A series of experiments was performed in the cylindrical rig of 1 inch width, using various ignition energies to initiate combustion in an equimolar acetylene-oxygen mixture at an initial pressure of 100 mm Hg and an initial temperature of 300°K. It was found that for an exploding copper wire of .006 diameter, the critical energy is 4.83 joules/cm (8 μf capacitor charged to 1.74 KV; 2.54 cm rig width). For mixture at the same initial conditions in a 2 inch wide cylindrical vessel, the critical energy (using the same diameter exploding wire) is also 4.83 joules/cm (8 μf, 2.4 KV). It was found, as well, that if an exploding wire of .003 inch diameter is used, the critical energy becomes 0.9 joules/cm for both the

1 inch and 2 inch vessel widths.

Zeldovich (Ref. 20) has outlined the criterion for the instantaneous formation of a detonation at the ignition source. The instantaneous vapourization of the exploding wire (or spark discharge in the case of spark ignition) results in the formation of a blast wave which propagates radially away from the source. The pressure decays rapidly behind the wave front, but if the pressure-time profile is such that chemical reaction in the compressed reactants can go to completion before the pressure just ahead of the reacted zone has dropped below the Chapman-Jouguet pressure, a detonation can be formed instantaneously. In a mixture at given initial conditions, therefore, a blast wave of a certain strength is required to produce instantaneous detonation.

On this basis, the results obtained above can be qualitatively explained. It has been seen in Section 6.2.5 that the energy required to sustain a cylindrical shock of given strength is directly proportional to the width of the cylindrical containing vessel. To produce a blast wave of given strength, therefore, the instantaneous energy release must be proportional to the cylinder width. It would thus be expected that the critical energy per unit width of the containing vessel is the same for vessels of any width, since the same energy input per unit width would produce blast waves of the same strength.

The difference in critical energy for the .003 inch and .006 inch diameter wires can be qualitatively explained as follows: A greater amount of energy input is absorbed in the vapourization of the larger diameter wire. The energy input required to produce a blast wave of a strength sufficient to initiate instantaneous detonation is the same in both cases, but due to

the increased energy required to vapourize the wire, the critical energy for the .006 inch diameter wire is greater than that for the .003 inch diameter wire. The critical energy increase is approximately proportional to the increase in mass of the copper wire.

Combustion has also been initiated at the centre of a detonation tube of 1 inch inside diameter by exploding copper wire of .003 inch diameter. The critical energy for an equimolar acetylene-oxygen mixture at an initial pressure of 100 mm Hg and an initial temperature of $300^{\circ}K$ is found to be 4.38 joules (4 μf 1.48 KV).

Referring to the energy integral of Section 7.2.5, the energy required to sustain a shock of given strength in a tube is seen to be directly proportional to the cross-sectional area of the tube. In order to obtain some correlation between the critical energies for the cylindrical and the plane cases, the critical energy per unit area of the tube should be evaluated. This is found to be 0.88 joules/cm^2, as compared to 0.9 joules/cm for the cylindrical case. This agreement must be looked upon as only qualitative since no further experimental data was taken for tubes of different cross-sectional area. In addition, the energy in the tube is supplied along a line rather than in a cross-sectional plane.

8.2 PROPAGATION OF CYLINDRICAL DETONATION

If a sufficiently high quantity of energy is instantaneously released at ignition (energy greater than the critical energy of 4.83 joules/cm), a detonation is immediately formed which propagates radially outward toward the periphery of the cylindrical containing vessel. All instantaneously formed detonations are overdriven to a certain extent, the degree being determined

by the ignition energy input. A streak photograph of a cylindrical detonation (1 inch rig width) in equimolar acetylene-oxygen mixture at an initial pressure of 100 mm Hg and an initial temperature of 300°K is shown in Fig. 24. The ignition energy was 5.5 joules/cm (4 μf 1.87 KV), using an exploding wire of .006 inch diameter.

Over the small range of ignition energies used (9.23 to 0.6 joules/cm), no initial overdriving of the detonation can be detected by streak photography. The measured detonation wave speed is 2910 m/sec, as compared to the theoretically calculated value of 2805 m/sec (Ref. 30). The cylindrical detonation wave speed is thus extremely close to the plane wave speed in the corresponding mixture, as it is in the case of spherical detonation (Ref. 19 and 21).

After the reflection of the detonation front from the rim of the cylindrical vessel, the particle paths of the burned gas products can be seen in Fig. 24. The reflected wave speed is initially 1790 m/sec, and is accelerated to 2390 m/sec as it propagates radially inward. This acceleration can be qualitatively explained by examining the distribution of fluid properties behind the detonation wave, as tabulated by Lee et al. (Ref. 29). It is seen that F_2 (u/D) decreases from .4528 to 0.0 as ξ (r/Dt) decreases from 1.0 to 0.0. Since the left-running wave propagates at a velocity of (u - c), the wave speed becomes increasingly negative as the particle velocity u decreases toward the centre of the cylindrical vessel. In addition, the shock convergeance toward the centre of the vessel results in compression heating of the mass of gas at the centre, and, consequently, an increase in the local speed of sound.

8.3 CYLINDRICAL FLAME PROPAGATION

If the ignition energy supplied at the initiation of combustion is below the critical energy, a cylindrical flame is formed which propagates radially outward from the centre of the containing vessel. Streak photographs of such flames in an equimolar acetylene-oxygen mixture at 100 mm Hg initial pressure and an initial temperature of 300°K are shown in Figs. 25 and 26. Both flames were initiated in a vessel of 1 inch width, the first using an exploding wire of .006 inch diameter and an ignition energy of 4.83 joules/cm (8 μf 1.74 KV), and the second using an exploding wire of .003 inch diameter and an ignition energy of .9 joules/cm (2 μf 1.5 KV).

The flame speed at combustion initiation is 425 m/sec, and there is a slight deceleration of the flame to 405 m/sec after it has propagated to a radial distance of about 8 cm from the ignition source. The flame speed remains constant at 405 m/sec for most of the flame travel through the combustible medium, until the flame front is approximately 2.5 cm from the vessel periphery. At this point, the absolute flame velocity suddenly changes from a positive 405 m/sec to a negative value of 133 m/sec, and a compression wave is seen which is transmitted through the burned products at a speed of 1930 m/sec (toward the centre). A number of additional flame accelerations occur, and the absolute flame speed successively becomes 95 and 200 m/sec. The flame front comes to a distance of 2 mm from the cylinder wall at about 200 μsec after the initial flame interaction, and an instantaneous explosion occurs at the vessel wall at about 350 μsec after this first interaction. This explosion appears to occur slightly after the arrival of a compression wave from the burned gas products to the wall of the vessel. This explosion is not always a feature of cylindrical flame propagation and does not occur

in Fig. 26. For low initiation energies, and low initial pressures, the initial flame speed and the rate of heat release are low, making pseudo-transition less likely to occur.

The flame speed in the region of ignition is initially higher than the flame speed through most of the mixture due to the effect of the blast wave generated by the exploding copper wire. The flame initially propagates into an unburned mixture at a higher temperature, resulting in a higher propagation speed. Since the blast wave front velocity is much greater than the flame velocity, and the temperature decays rapidly behind the blast wave, the flame decelerates slightly as it propagates away from the region of ignition.

The subsequent accelerations and decelerations of the flame front in the vicinity of the cylinder walls can be qualitatively explained on the basis of the model proposed in Section 6.1. Due to the expansion of the hot gas products behind the flame, a shock is formed which precedes the flame front into the unburned mixture. From the flame front trace, and the trace of the compression wave transmitted through the burned gas products after the interaction with the flame, the speed (U_s/a_o) of this shock can be found to be 1.24. A shock of this strength cannot be considered a pressure pulse, but it would be instructive to continue the calculation on the basis of this model to obtain a qualitative description of the subsequent events. Following the calculation procedure of Appendix I (and using the constant established in Section 6.1.4 for the laminar burning speed of equimolar acetylene-oxygen mixture at various temperatures), the calculated flame velocities are (Fig. 27):

$$U_{f_{AB}} = 386 \text{ m/sec}$$

$$U_{f_{BC}} = - 171 \text{ m/sec}$$

$$U_{f_{CD}} = 78 \text{ m/sec}$$

The measured velocities of the corresponding cycles in the flame acceleration process of Fig. 25 are 405.0, - 133.0 and 95 m/sec respectively. This does not constitute a quantitative agreement of the theoretical predictions with the experimental results. Considering, however, the neglect of the entropy change across the shock preceding the flame, neglect of the area divergeance effect in the cylindrical geometry, and the approximation made for the burning speed of the unreacted mixture, these results do provide at least a qualitative understanding of the physical phenomena involved in the flame propagation process in the cylindrical vessel.

The sudden explosion which occurs near the vessel wall after a number of flame-pressure wave interactions is likely due to multiple reflections of the shock wave from the wall and the flame front which raises the temperature of the small volume of unburned mixture to the ignition temperature. This type of pseudo-transition has been reported in the work of Cassutt (Ref. 31) and Litchfield (Ref. 32) in spherical detonation. A similar effect has been noted in plane detonation propagation in closed end tubes, where transition to detonation occurs at a distance close to the end. Such phenomena have been reported by Brinkley and Lewis (Ref. 1), where it is stated that the most destructive effects of detonation are observed when such a transition occurs. A streak photograph illustrating this phenomenon in a 2 foot-long closed end tube filled with equimolar acetylene-oxygen mixture at 100 mm Hg

and 300°K initial pressure and temperature respectively ignited by exploding wire at the centre is shown in Fig. 28.

It would be of interest to compare the flame-shock system of Fig. 25 to the cylindrical model developed in Section 6.3. The shock Mach number has been calculated earlier to be 1.24, corresponding to a pressure ratio of 1.633. The corresponding values for r_f/R_s and U_f/a_o can be found from Figs. 14 and 15 to be about 0.725 and 0.8 respectively. The values measured for r_f/R_s and U_f/a_o are 0.865 and 1.23 respectively. The large discrepancy observed in the velocity of flame propagation may be due to the effect of turbulence generated at the side walls of the container to increase the flame front velocity.

One of the most important features of the flame propagation process in this cylindrical geometry is that transition from deflagration to detonation was not observed for any vessel width, ignition energy, or mixture used in the course of the experiments. A turbulent flame is noted in Fig. 25, possibly due to boundary layer effects on the side walls of the container, and a gradual increase in the degree of turbulence behind the flame is noted in Fig. 26. There is, however, no indication of the high degree of turbulence and the accompanying rapid flame acceleration which characterizes the final deflagration run before transition to detonation in a tube. It is quite clear that (Ref. 1) wall-induced turbulence is an important factor in the transition process in a tube, but that the level of turbulence generated due to sidewall effects in the cylindrical geometry investigated is insufficient to cause transition. The rate of burning in this geometry, therefore, becomes a function solely of the temperature and the other fluid property changes due to the shock preceding the flame front. If the burning rate remains constant,

the whole system expands uniformly.

It now seems unlikely that transition due solely to pressure wave-flame interactions or self-acceleration of the flame can occur in an unconfined geometry.

8.4 TRANSITION FROM CYLINDRICAL DEFLAGRATION TO DETONATION

It has been shown conclusively (Ref. 6, 14 and 28) that one of the dominant mechanisms in the transition from deflagration to detonation in tubes is the generation of turbulence due to the presence of the boundary layer in the unburned gas region between the advancing flame front and the precursor shock. It is generally agreed, that the formation of the boundary layer has a great effect on the process of flame acceleration. Brinkley (Ref. 1), in interpreting the results obtained by Shuey, states that the turbulence generated throughout the tube cross-section by an obstruction placed at the ignition end, and by wall friction in the case of a smooth-walled pipe, result in rapid flame accelerations, and emphasizes the fundamental role played by turbulence in the mechanisms of flame acceleration. The work of Shchelkin (reported by Brinkley in Ref. 1), in which wire spirals were placed near the ignition source to roughen the tube walls, also indicates the importance of turbulence in the process of transition. Martin (Ref. 28) expresses also the view that the final flame acceleration depends upon the development of turbulent regions in the boundary layer.

In the experimental work presented in the previous section (Section 8.3), it is seen that the weak turbulence generation mechanism which does exist due to sidewall effects is not sufficient to produce transition. It was considered of great importance to determine whether or not the arti-

ficial generation of turbulence in the cylindrical vessel would produce conditions under which transition to detonation could occur. A spiral coil, analogous to that used by Shchelkin (reported by Brinkley in Ref. 1) in a tube, made of 1/4 inch OD copper wire, was placed on one sidewall of the cylindrical vessel, as outlined in Section 7.1.1.

A streak photograph of the combustion process in an equimolar acetylene-oxygen mixture at an initial pressure of 100 mm Hg and an initial temperature of 300° K in the cylindrical vessel of 1 inch thickness is shown in Fig. 29. An exploding wire of .003 inch dia. was used, and the ignition energy supplied was 0.9 joules/cm (4 μf 1.06 KV). A flame is initiated at the ignition source which propagates radially outward. No deceleration of the flame is observed in the vicinity of the ignition source as is seen in cylindrical flame propagation without the spiral coil (Fig. 25). The initial flame speed is approximately 180 m/sec. A number of discontinuous "kicks" are imparted to the flame in its acceleration process, and very intense, turbulent burning is noted behind the flame during the later stages of the acceleration process. The flame speed just before transition is in this case about 450 m/sec. Transition occurs at about 260 μsec after ignition, at a radius of 9 cm from the centre of the vessel. The detonation formed is initially overdriven, but the wave speed decays to the Chapman-Jouguet detonation speed within 2 or 3 cm of propagation. The formation of a cylindrical retonation wave is a characteristic of the transition process in the cylindrical geometry as it is in the plane case.

The initial deceleration of the flame where no spiral is placed on the sidewall has been attributed to the decay of the blast wave which initiated the combustion process (Section 8.3). In this case, where the spiral is present, it is thought that the flame acceleration due to turbulence

effects compensates for the deceleration due to the blast decay, and no such deceleration is observed.

The discontinuous acceleration of the flame front is likely due to a mechanism which has been proposed by Brinkley (Ref. 1) who suggests that intermittent pressure pulses are generated due to the almost instantaneous reaction of small "pockets" of unburned mixture which are trapped by the turbulent flame. The actual transition to detonation, and the formation of the retonation occurs when a sufficiently large pocket of unburned mixture is left behind the flame front, and this entrapped gas is consumed by a deflagrative implosion, creating an extremely high pressure at the centre. The resulting spherical shock initiates a detonation which is initially overdriven due to the high driving force of the shock, and a retonation which propagates into the burned gas products.

A streak photograph of the combustion process in a mixture at the same conditions as above is shown in Fig. 30. The ignition energy in this case was .5 joules/cm (2 μf 1.12 KV). The flame acceleration and transition process appears qualitatively the same as in Fig. 29, but the initial flame velocity is 130 m/sec, as compared to 180 m/sec in Fig. 29. This decrease in flame velocity is apparently due to the lower energy input in this case, resulting in a weaker blast wave in the vicinity of the ignition source, a lower temperature, and consequently a lower flame velocity. The flame velocity before transition is also lower, being about 320 m/sec. Transition occurs at the same distance from the centre, 9 cm, but the time from initiation to transition increases to 370 μsec. Differences in the initial flame acceleration process have been noted by Laderman (Ref. 8) due to variation in ignition source-to-backwall distance, but the results of Baumann et al. (as reported by Laderman and Oppenheim in Ref. 13) have indi-

cated that the induction distance is relatively insensitive to these changes in the flame acceleration process. Similarly here, the induction distance is relatively insensitive to the energy input, though changes in the flame acceleration process do occur.

Similar runs have been taken in the 2 inch width cylindrical vessel, using ignition energies of both .9 and .5 joules/cm, and the resulting streak photographs are shown in Figs. 31 and 32. The initial flame velocity is comparable to the corresponding flame velocity in the 1 inch vessel, but the flame accelerates more slowly since the spiral coil has less effect in the 2 inch width. The induction distance in this vessel is about 17 cm. The time from flame initiation to transition is 400 μsec for .9 joules/cm energy input, and 540 μsec for .5 joules/cm energy input.

A streak photograph of the transition process in the same mixture in the 1 inch width vessel using a nichrome glow wire as the ignition source is shown in Fig. 33. Here, at initiation, the flame speed is much lower than in the exploding wire-ignited mixtures, 98 m/sec, and the flame propagates to a radius of about 3 cm before any significant acceleration of the flame occurs. At this radius, however, a gradual transformation to turbulent burning is observed, and the discontinuous accelerations previously observed for exploding wire-ignited mixtures are again observed. Extremely turbulent burning is noted before transition occurs, and, the features of the transition process, the initially overdriven detonation and the retonation are seen. Transition takes place at a radius of 14 cm about 650 μsec after ignition. The low initial flame propagation velocity in the region of the ignition source is due to the manner in which the mixture is ignited. The energy released by slow ohmic heating of the nichrome wire does not provide a mechanism by which a strong shock (or blast) can form in the vicin-

ity of this ignitor, and the initial flame speed is consequently lower than it is for the same mixture ignited by exploding wire, where a blast wave is produced by the instantaneous energy release.

Three additional experiments were performed in the 1 inch cylindrical vessel in equimolar acetylene-oxygen mixture at 100 mm. Hg initial pressure and 300° K initial temperature. For each run, a single circular ring made of 1/4 inch OD copper wire was placed concentric with the ignitor. The ring diameters used were 6, 15 and 26 cm respectively. For each run, an exploding wire of .003 inch dia. and an ignition energy of .9 joules/cm was used. The streak photographs obtained are shown in Figs. 34, 35 and 36. In Fig. 34 where the 6 cm ID coil is used, an increase in the degree of turbulence is noted as the flame front reaches the coil radius. The flame is slightly accelerated after this interaction with the coil. The turbulence is seen to subside, and the flame decelerates again soon after the coil is passed, and the burning then develops as in Fig. 26, where no coil was present. Flame interactions with reflected pressure waves are observed. For both the 15 cm and 26 cm ID coils (Figs. 35 and 36) the initial burning process is identically the same as that observed with no coil (Fig. 26). A slight deceleration of the flame front is noted at 2 or 3 cm from the ignition source as the generated blast wave decays. As the flame front reaches the coil radius, intensely turbulent burning begins, the flame is accelerated, and transition occurs within 5 cm from the coil. Again, the detonation formed is initially overdriven.

It would seem that the level of turbulence introduced by the single coil during the very early stages of flame propagation is insufficient to cause an appreciable flame acceleration or transition; during the later stages of flame propagation, however, when some turbulence has been intro-

duced due to sidewall boundary layer effects, the turbulence generated by a single coil provides a sufficiently strong mechanism to produce transition to detonation.

The fundamental importance of the turbulence generation mechanism in the transition process is stressed by this series of experiments. It is thought that in the absence of this mechanism in unconfined combustion, transition from deflagration to detonation cannot occur.

8.5 SYMMETRY OF CYLINDRICAL COMBUSTION WAVES

The streak photographs of Figs. 24 to 36 indicate that there is always a lack of symmetry in the combustion process, slight in some cases, and very pronounced in others.

In Fig. 24, where a detonation is instantaneously formed, the very slight asymmetry is probably due to the geometry of the ignitor (Fig. 19). The exploding wire is not located at the true centre of the cylindrical vessel, since it is the threaded portion of the ignitor assembly which is concentric with the vessel rim. In addition, the current loop which is set up when the capacitor bank is discharged causes the two conductors, the exploding wire and the return rod, to repel one another. This results in an acceleration of the copper particles in a preferred direction, and may contribute to the asymmetry of the detonation. In Figs. 25 and 26, where a flame is formed, this same slight asymmetry is noted. Six-slit streak photographs (1/8-inch wide slits placed on plexiglass face of cylindrical vessel along the horizontal diameter, and on two diameters inclined at 45^{o} to the horizontal) were obtained of both the detonation and flame propagations, and are shown in Figs. 37 and 38. These photographs demonstrate clearly that both the detonation and the flame are very nearly symmetrical along all the radii observed.

Streak photographs of the transition process (Figs. 29 to 36) have indicated that there is a decided lack of radial symmetry in most of the shots. In addition to the effects of the ignitor geometry, this asymmetry can be attributed to the geometry of the coil, since the coil turns are not symmetrical about the centre of the vessel. Turbulence would therefore be generated more quickly along a radius where the coil turns are closer to the centre. The random nature of the turbulence generation process may also contribute to the lack of symmetry. In Figs. 34 to 36, where the single turn coil was used, a faint outline of the coil can be seen, and the lack of symmetry can be attributed to the non-concentric placement of the coil. The six-slit photograph of the transition process (Fig. 39) demonstrates clearly the lack of radial symmetry when the spiral coil is used.

CHAPTER IX

CONCLUSIONS

The following conclusions may be drawn from this investigation of cylindrical combustion and transition phenomena:

i. equi-molar acetylene-oxygen mixture at an initial pressure of 100 mm Hg and an initial temperature of 300° K is investigated in cylindrical vessels of 1 and 2 inch widths, using exploding wires of .003 and .006 inches in diameter. The critical energy per unit width of the vessel is the same for both vessel widths for a given wire diameter, and increases as the wire diameter is increased. The values determined are: 4.83 joules/cm for a wire diameter of .006 inches; 0.9 joules/cm for a wire diameter of .003 inches.

ii. the observed cylindrical flame accelerations and decelerations are due to interactions of the flame front with the multiple reflections of the original precursor shock; qualitative agreement of the experimental results with those predicted by a simplified theoretical model is indicated.

iii. true transition from cylindrical deflagration to detonation is not observed in any of the performed experiments, and is not likely to occur. Pseudo-transition, due to the shock-heating of the unburned mixture near the containing wall of the vessel by the multiple reflections of pressure waves, is observed in some cases when most of the unburned mixture has been consumed.

iv. transition from cylindrical deflagration to detonation is observed in the mixtures investigated when a spiral coil is placed on one of the sidewalls of the container to generate turbulence. A cylindrical re-

tonation is observed at the onset of detonation. Boundary layer and turbulence effects are the predominant mechanisms in the transition process, and are thought to be essential to the occurrence of transition.

REFERENCES

1.	Brinkley, S. R., and Lewis, B.	Seventh Symposium (International) on Combustion, p. 807, Butterworths, 1959.
2.	Dixon, H.B.	Phil. Trans. Roy. Soc. A200, 315 (1903).
3.	Payman, W. and Titman, H.	Proc. Roy. Soc. (London) A 152, 418(1935).
4.	Schmidt, E.H.W., Steinicke, H. and Neubert, U.	Fourth Symposium (International) on Combustion, p. 658, Williams and Wilkins, 1953.
5.	Salamandra, G.D., Bazhenova, T.V. and Naboko, I.M.	Seventh Symposium (International) on Combustion, p. 851, Butterworths, 1959.
6.	Oppenheim, A.K., Laderman, A.J. and Urtiew, P.A.	Combustion and Flame Vol. 6, 193 (1962).
7.	Bollinger, L.E., Fong, M.C. and Edse, R.	ARS Journal Vol. 31 No. 5, 588 (1961).
8.	Laderman, A.J., Urtiew, P.A. and Oppenheim, A.K.	Combustion and Flame Vol. 6, 325 (1962).
9.	Bollinger, L.E., Fong, M.C., Laughrey, J.A. and Edse, R.	NASA TN D-1983 June 1963.
10.	Bollinger, L.E.	NASA TN D-2256 April 1964.

11. Bollinger, L.E., Laughrey, J.A. and Edse, R. — ARS Journal Vol. 32 No. 3, 428 (1962).

12. Laderman, A.J. and Oppenheim, A.K. — Proc. Roy. Soc. A 268, 153 (1961).

13. Laderman, A.J. and Oppenheim, A.K. — Physics of Fluids Vol. 4 No. 6, 778 (1961).

14. Martin, F.J. and White, D.R. — Seventh Symposium (International) on Combustion, p. 856, Butterworths, 1959.

15. Adams, G.K. and Pack, D.C. — Seventh Symposium (International) on Combustion, p. 812, Butterworths, 1959.

16. Jones, H. — Proc. Roy. Soc. A 248, 333 (1958).

17. Chu, B.T. — NACA TN 3411 June 1955.

18. Laffitte, P. — Ann. de Phys. 10e ser. 4, 587 (1925).

19. Manson, N. and Ferrie, F. — Fourth Symposium (International) on Combustion, p. 486, Williams and Wilkins, 1953.

20. Zeldovich, Ia. B., Kogarko, S.M. and Simonov, N.N. — Soviet Phys. Tech. Phys. Vol. 1 No. 8, 1689 (1957).

21. Pliickebaum, J.W., Strauss, W.A. and Edse, R. — ARL 63-101, June 1963.

22. Rudinger, G. and Rinaldi, L.D. — Squid Tech. Memo. No. CAL-23, November 1948.

23. Lewis, B. and von Elbe, G. — Combustion, Flames and Explosions of Gases, p. 267,766, Academic Press, 1951.

24. Hildebrand, F.B. — Advanced Calculus for Engineers, p. 103, 118.

25. Emmons, H.W. — Fundamentals of Gas Dynamics, Section G Ch. 3, Princeton University Press, 1958.

26. Manson, N. — Compt. rend. 222, 46 (1946).

27. Janaf Thermochemical Data — Dow Chemical Co. Thermal Laboratory

28. Martin, F.J. — Physics of Fluids Vol. 1 No. 5, 399 (1958).

29. Lee, J.H., Lee, B.H.K. and Shanfield, I. — Two Dimensional Unconfined Gaseous Detonation Waves (to be published in Tenth International Symposium on Combustion).

30. Shanfield, I., Lee, J.H. and Lee, B.H.K. — Theoretical Calculation of Gaseous Detonation, McGill Univ. Publication MERL TN 64-10 GD22 (1964).

31. Cassutt, L.H. — ARS Journal Vol. 31 No. 8, 1122 (1961).

32. Litchfield, E.L. — Physics of Fluids Vol. 5 No. 1, 114 (1962).

33. Taylor, G.I. — Proc. Roy. Soc. A 186, (1946).

APPENDIX I

SAMPLE CALCULATION OF FLAME-PRESSURE WAVE INTERACTION

The initial conditions of the assumed mixture are:

$$\gamma = 1.4$$

$$T_0 = 300^\circ K$$

$$u_0/a_0 = 0$$

$$K = 1.8 \times 10^{-4}\ {}^\circ K^{-1}$$

$$\Delta T = 2220^\circ K$$

The subscripts refer to the regions in the x-t diagram as they are numbered in Fig. 4.

From Eq. 6.10,

$$\frac{u_2}{a_0} = \frac{k}{a_0}\Delta T = K\Delta T = 0.400$$

From Eq. 6.13,

$$\frac{a_2 - a_0}{a_0} = \frac{\gamma - 1}{2}\left(u_2 - u_0\right) = 0.080$$

$$a_2/a_0 = 1.080$$

From Eq. 6.15,

$$T_2/T_0 = \left(a_2/a_0\right)^2 = 1.1662$$

$$T_2 = 349.8\ {}^\circ K$$

From Eq. 6.2,

$$\frac{U_f}{a_0} = \frac{u_2}{a_0} + KT_2 = 0.463$$

From Eq. 6.12,

$$\frac{a_1}{a_2} = \sqrt{1 + \frac{2220}{349.8}} = 2.709$$

$$a_1/a_0 = 2.925$$

From Eq. 6.24 and 6.25,

$$\Delta a'/a_0 = -0.0368$$

$$\Delta a''/a_0 = 0.117$$

Now, $$\frac{a_3}{a_0} = \frac{a_2}{a_0} + \frac{\Delta a}{a_0} = 1.160$$

$$\frac{a_4}{a_0} = \frac{a_3}{a_0} + \frac{\Delta a'}{a_0} = 1.123$$

$$\frac{a_5}{a_0} = \frac{a_1}{a_0} + \frac{\Delta a''}{a_0} = 3.042$$

From Eq. 6.13,

$$\frac{u_4}{a_0} = \frac{u_3}{a_0} + \frac{2}{\gamma - 1}\left(\frac{a_4}{a_0} - \frac{a_3}{a_0}\right) = -0.184$$

$$\frac{u_5}{a_0} = \frac{u_1}{a_0} - \frac{2}{\gamma - 1}\left(\frac{a_5}{a_0} - \frac{a_1}{a_0}\right) = -0.585$$

From Eq. 6.15,

$$T_4/T_0 = (a_4/a_0)^2 = 1.263$$

$$T_4 = 379^{\circ}K$$

From Eq. 6.2,

$$U_f/a_0 = u_4/a_0 + KT_4 = -0.117$$

No further complications are encountered in extending the wave diagram.

TABLE I

Shock Mach No.	Cylindrical Energy Factor	Spherical Energy Factor
1.25	1.6897×10^4	1.5565×10^4
1.50	4.0387×10^4	4.3047×10^4
2.00	1.3353×10^5	1.8045×10^5
2.50	3.2143×10^5	5.4176×10^5
3.00	6.2998×10^5	1.3639×10^6
3.50	1.1384×10^6	2.7432×10^6
4.00	1.9635×10^6	5.2854×10^6
4.50	3.0353×10^6	9.9299×10^6
5.00	4.6378×10^6	1.6473×10^7
5.50	6.7883×10^6	2.5986×10^7
6.00	9.5954×10^6	3.9350×10^7
6.50	1.3177×10^7	6.0245×10^7
7.00	1.7661×10^7	8.5533×10^7
7.50	2.3185×10^7	1.2331×10^8
8.00	2.9894×10^7	1.6705×10^8
8.50	3.8877×10^8	2.3023×10^8
9.00	4.8617×10^8	3.0096×10^8
9.50	6.0061×10^8	4.0050×10^8
10.00	7.3395×10^8	5.0906×10^8

Energy required to support cylindrical shock is

$$E = 2\pi a_o^2 t^2 L \times \text{Cylindrical Energy Factor}$$

Energy required to support spherical shock is

$$E = 4\pi a_o^3 t^3 \times \text{Spherical Energy Factor}$$

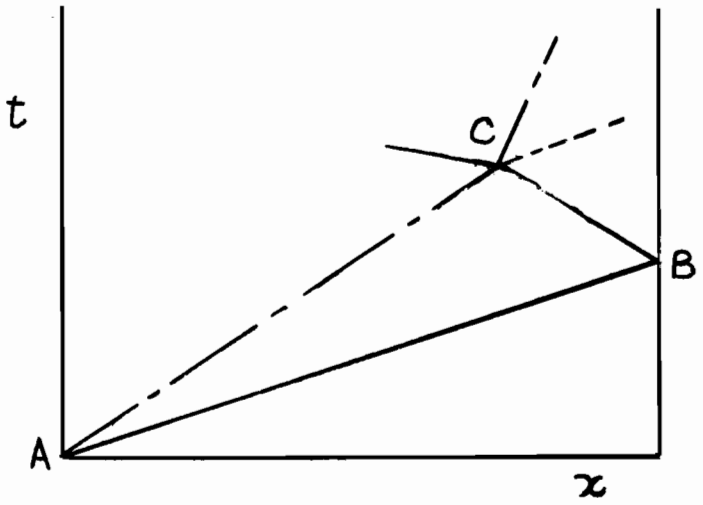

Fig. 1 Flame Preceded by Pressure Wave

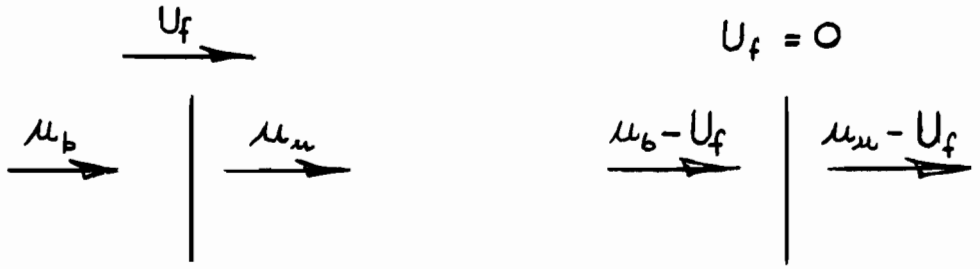

Fig. 2 Transformation of Flame to Stationary Co-ordinates

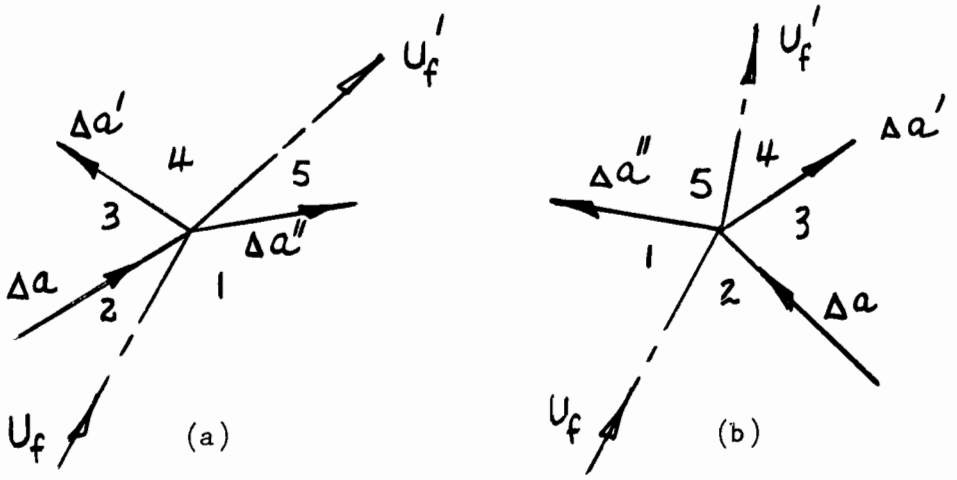

Fig. 3 Flame - Pressure Wave Interaction

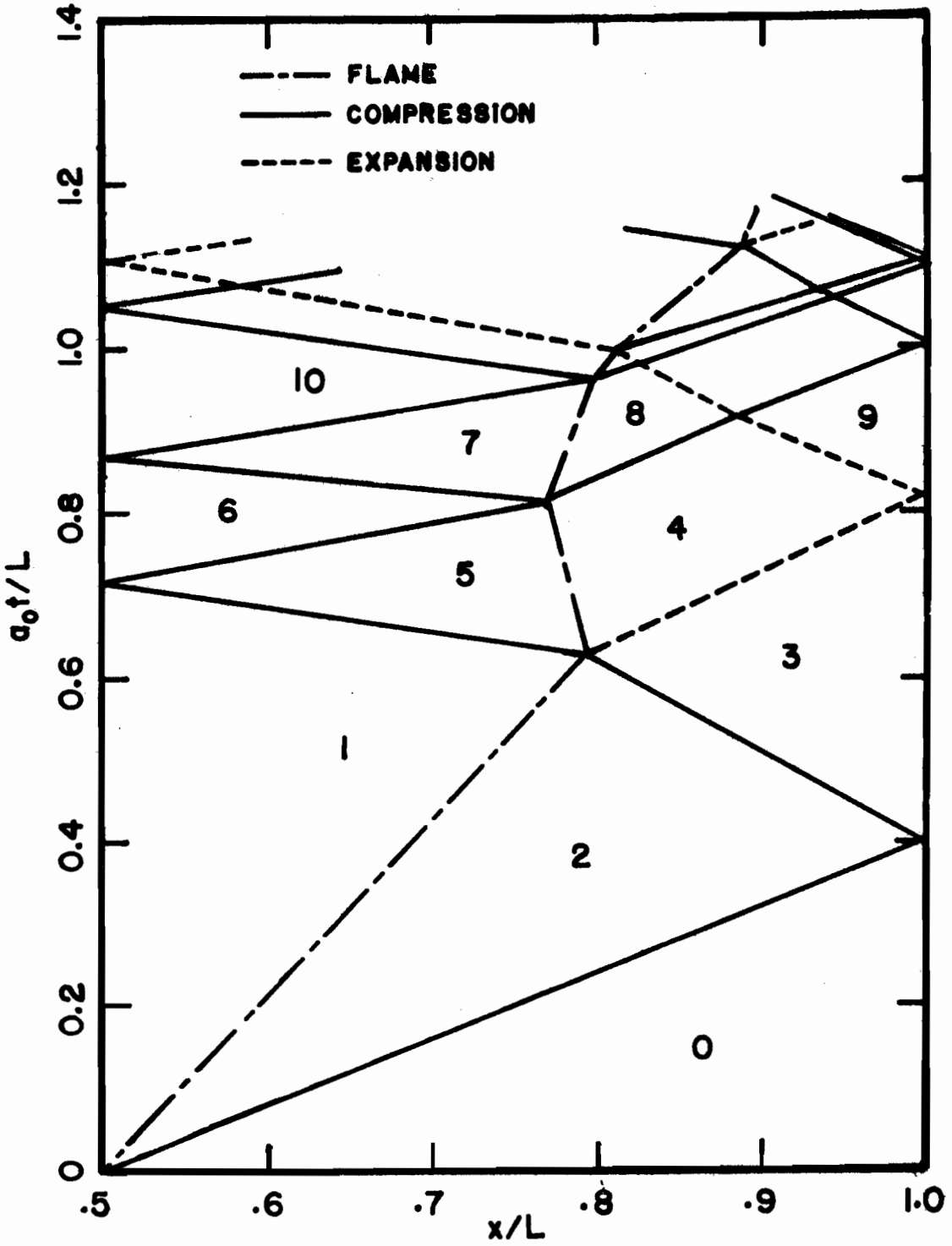

Fig. 4 Calculated flame-pressure wave interaction in fuel-oxidant mixture. $\Delta T = 2220^{\circ}K$; $K = 1.8 \times 10^{-3}\ ^{\circ}K^{-1}$.

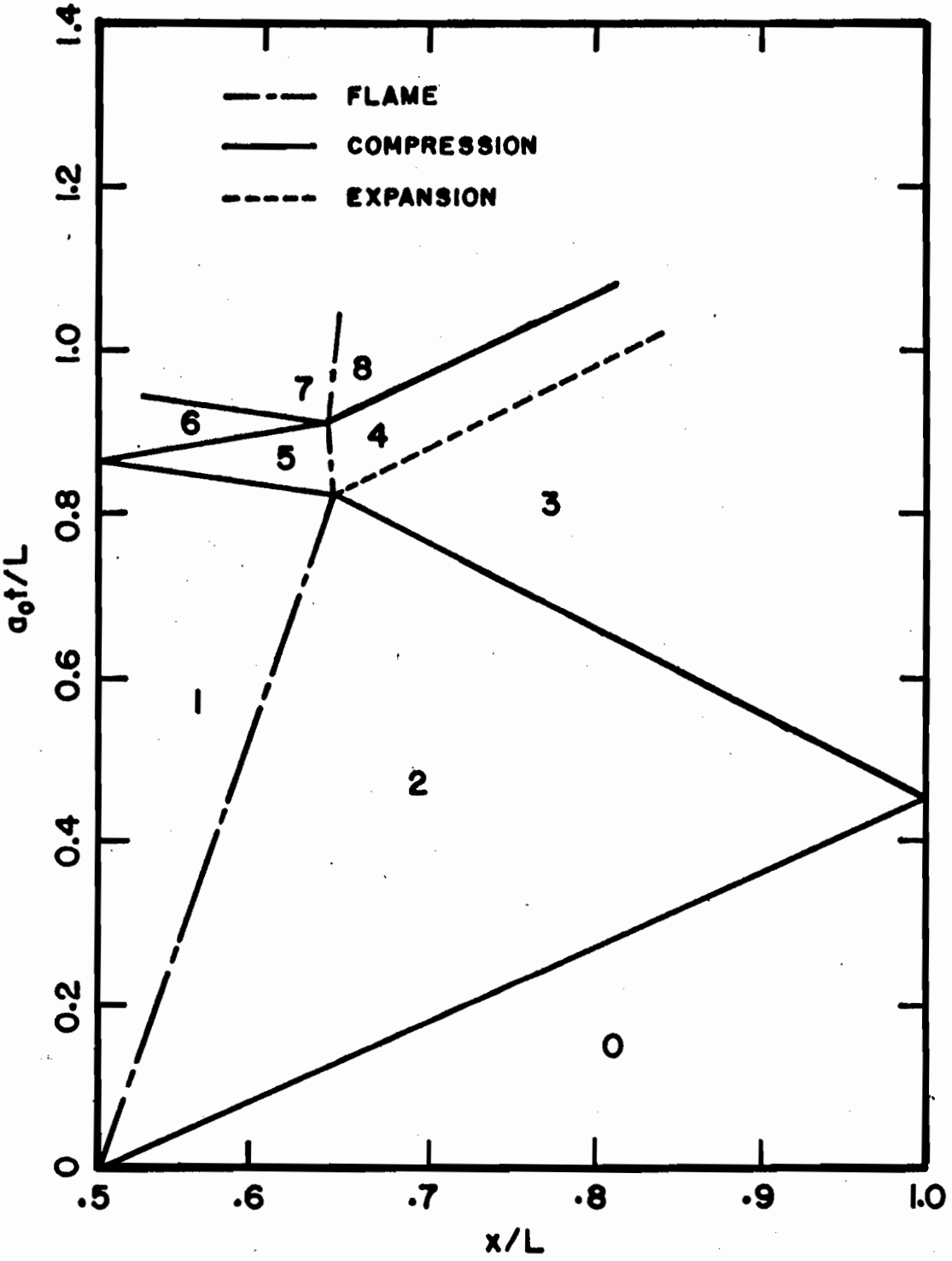

Fig. 5 Calculated flame-pressure wave interaction in equimolar acetylene-oxygen mixture. $\Delta T = 2700^{\circ}K$; $K = 5.67 \times 10^{-4}\ {}^{\circ}K^{-1}$.

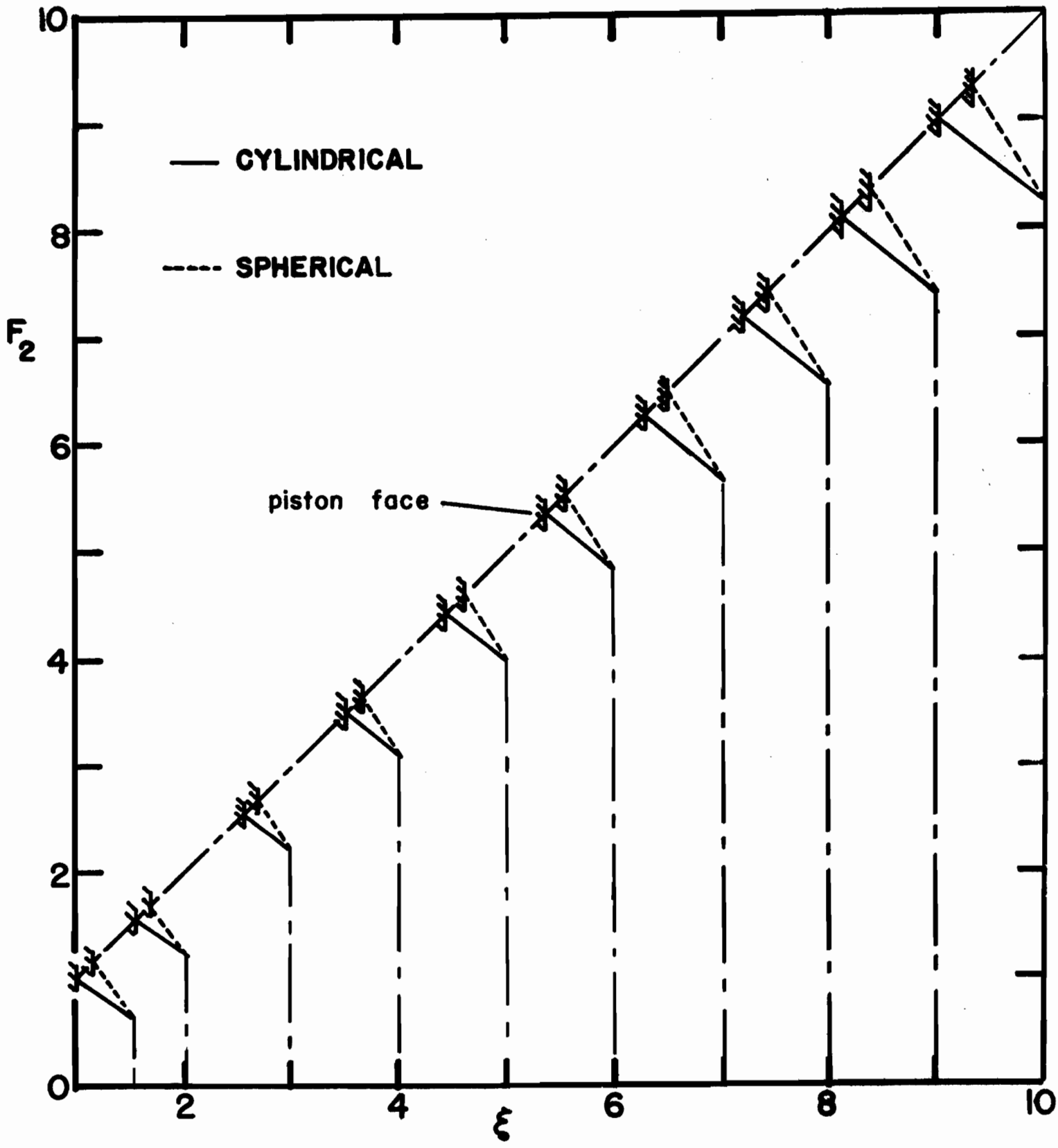

Fig. 6 F_2 vs. ξ for shocks of Mach numbers from 1.25 to 10.0.

Fig. 7 p/p_0 vs. ξ for shock Mach numbers from 1.25 to 10.0.

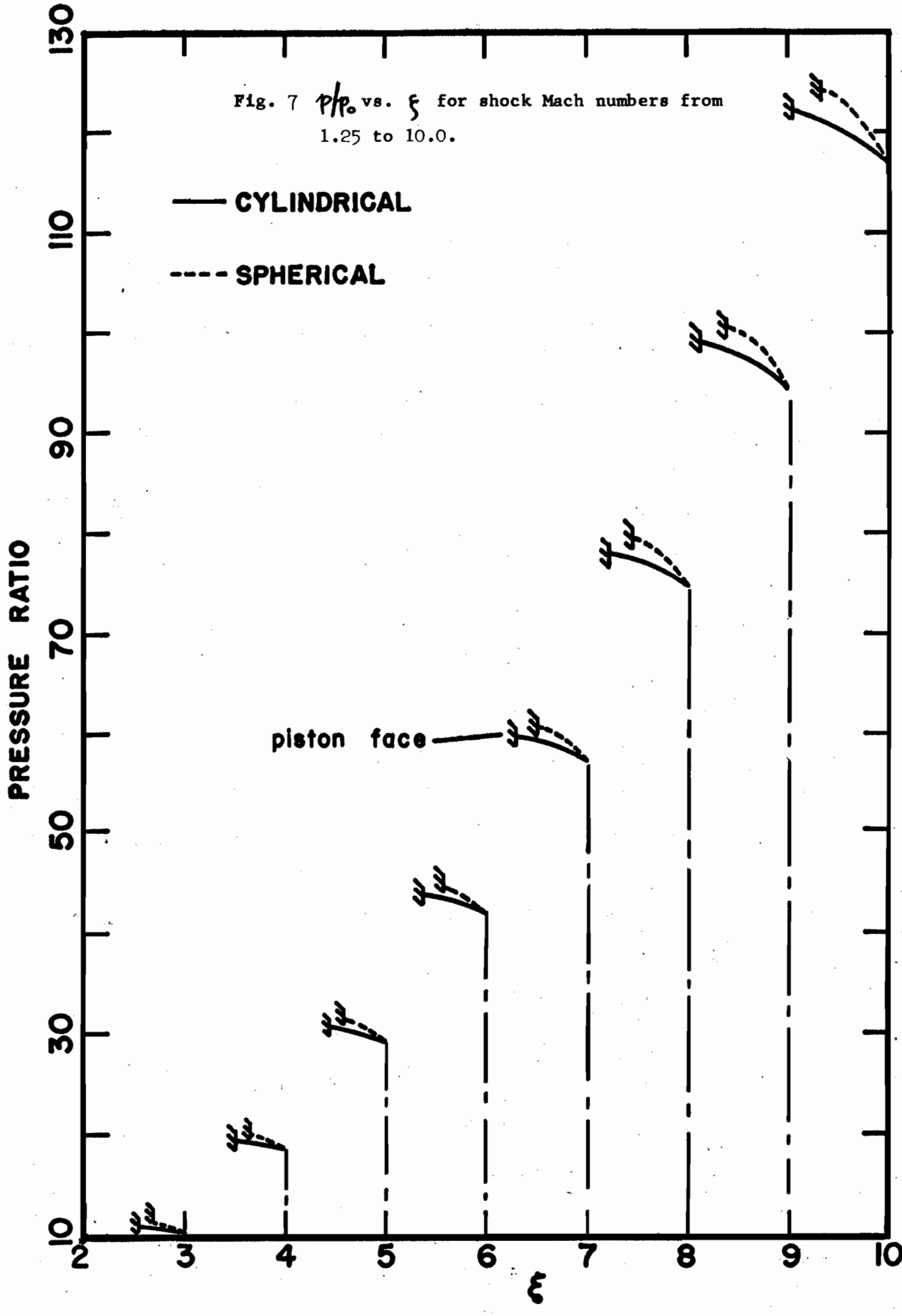

Fig. 8 F_2 vs. ξ for a shock Mach number of 8.25.

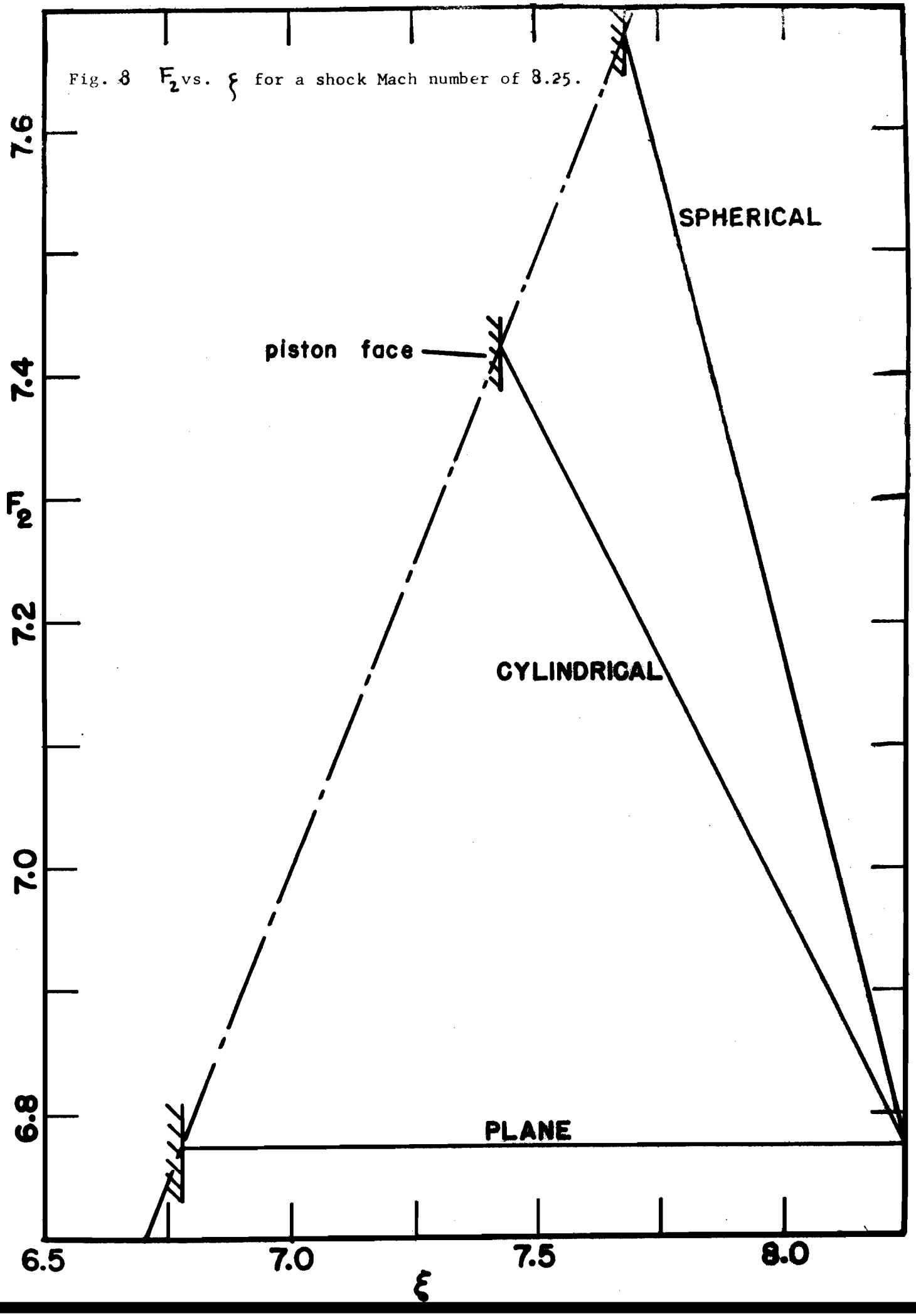

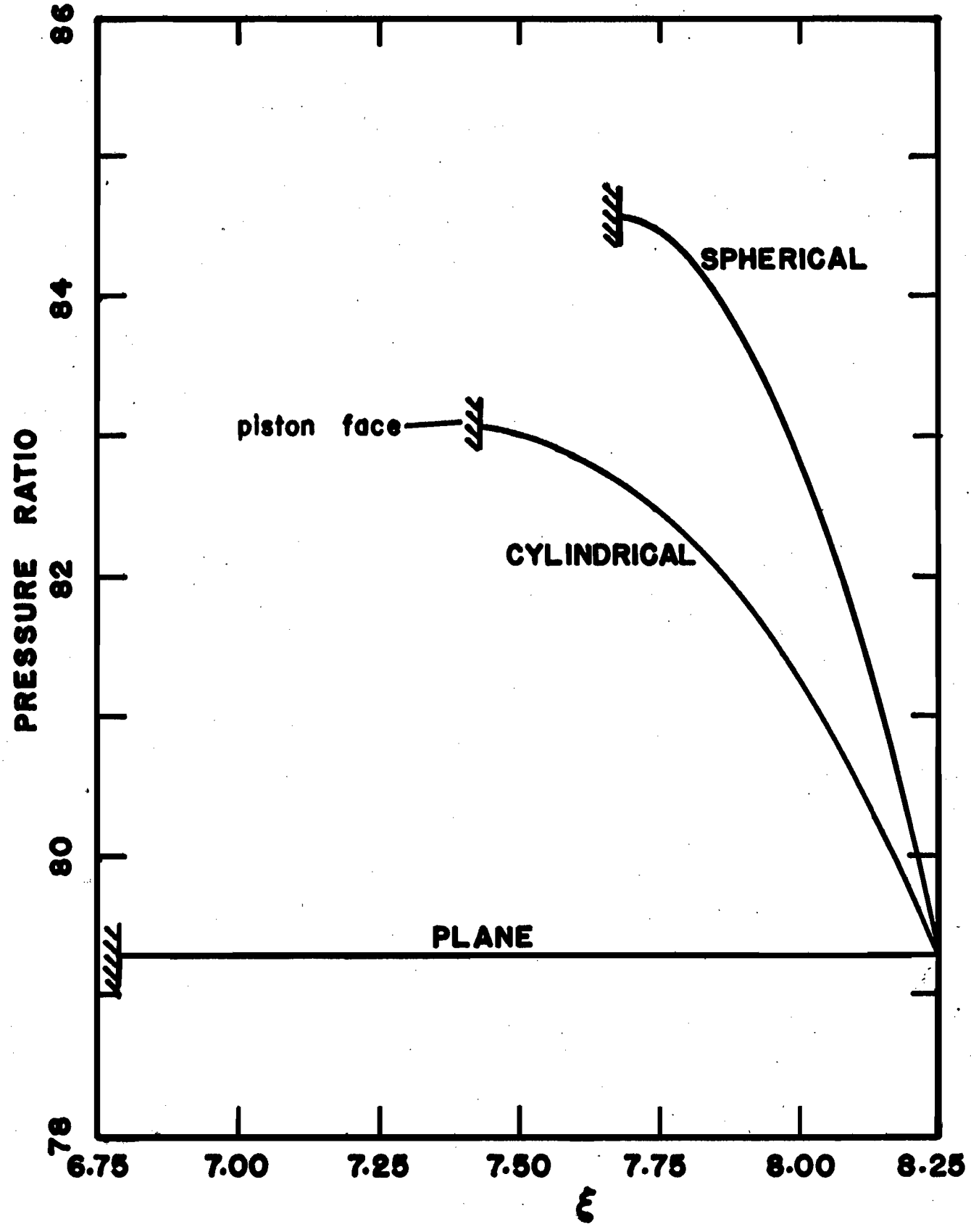

Fig. 9 p/p_0 vs. ξ for a shock Mach number of 8.25.

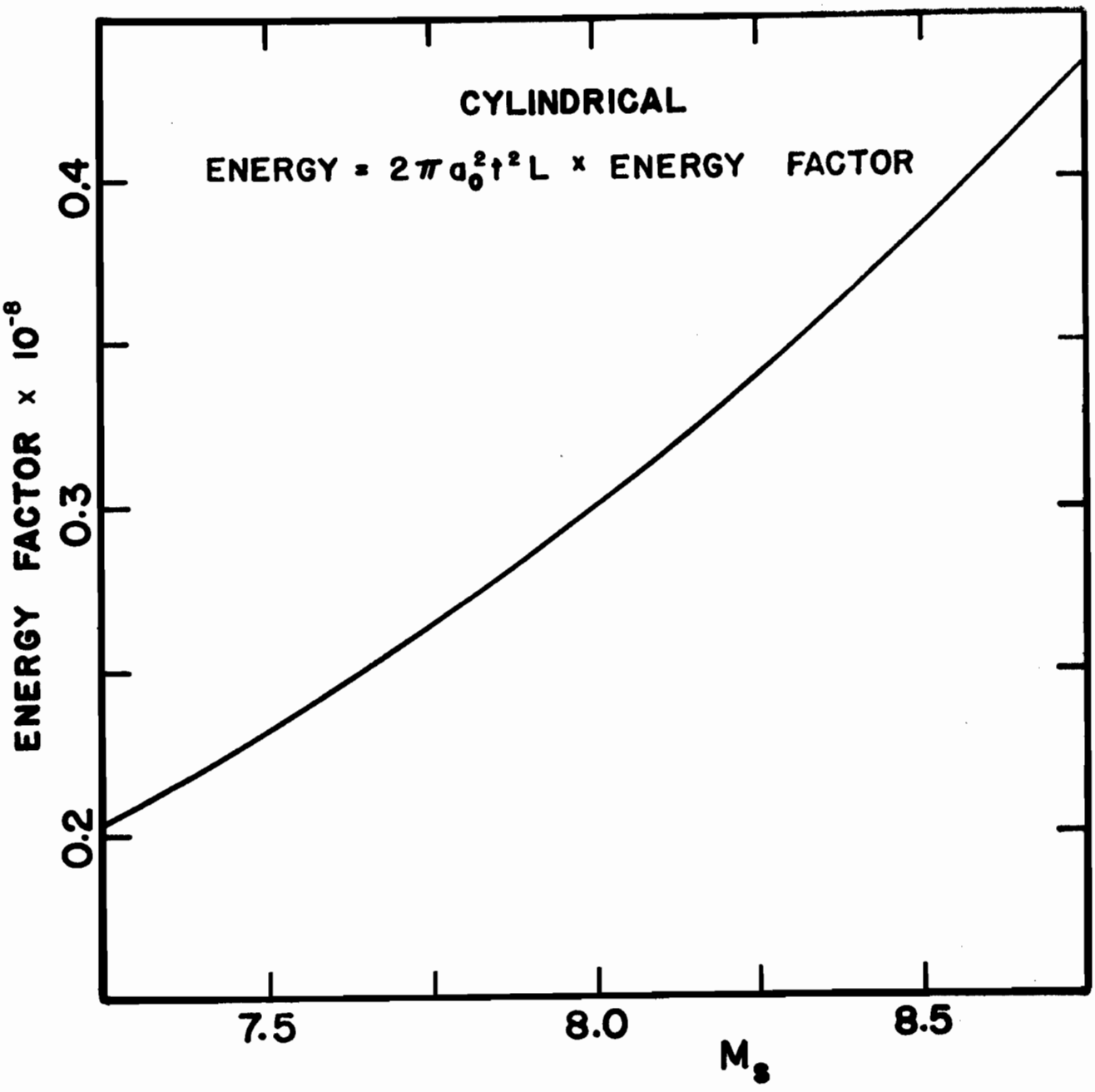

Fig. 10 Energy release required to support cylindrical shocks of Mach numbers from 7.25 to 8.75 in a perfect gas at an initial pressure of 100 mm Hg.

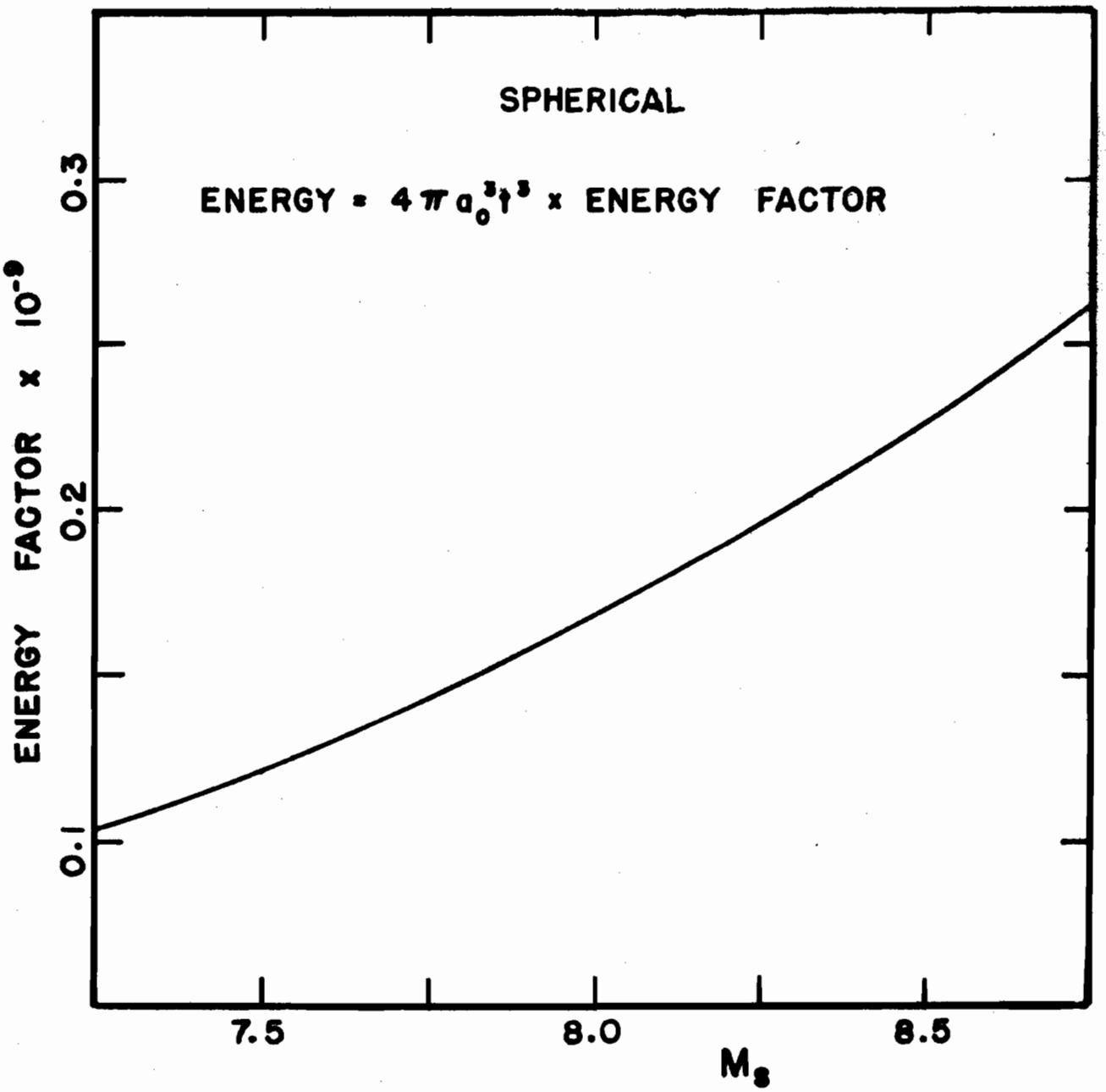

Fig. 11 Energy release required to support spherical shocks of Mach numbers from 7.25 to 8.75 in a perfect gas at an initial pressure of 100 mm Hg.

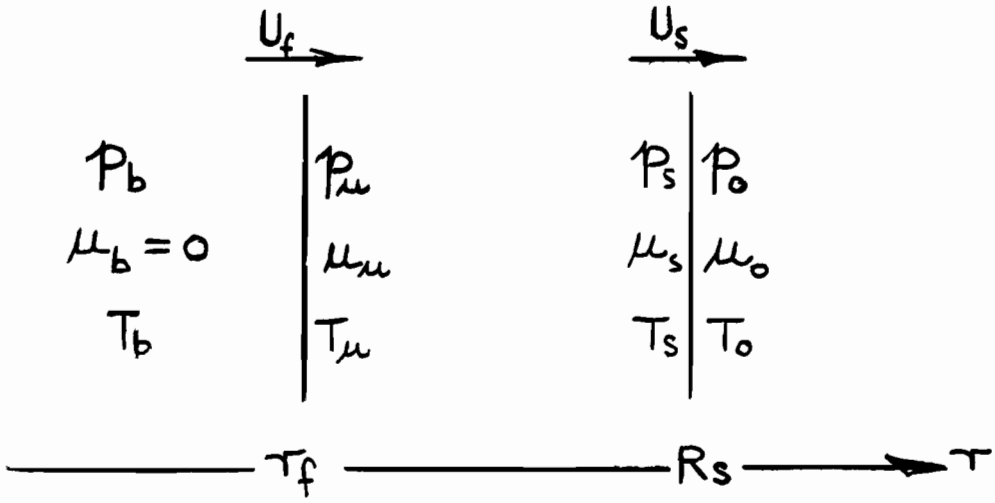

Fig. 12 Flame Preceded by Shock

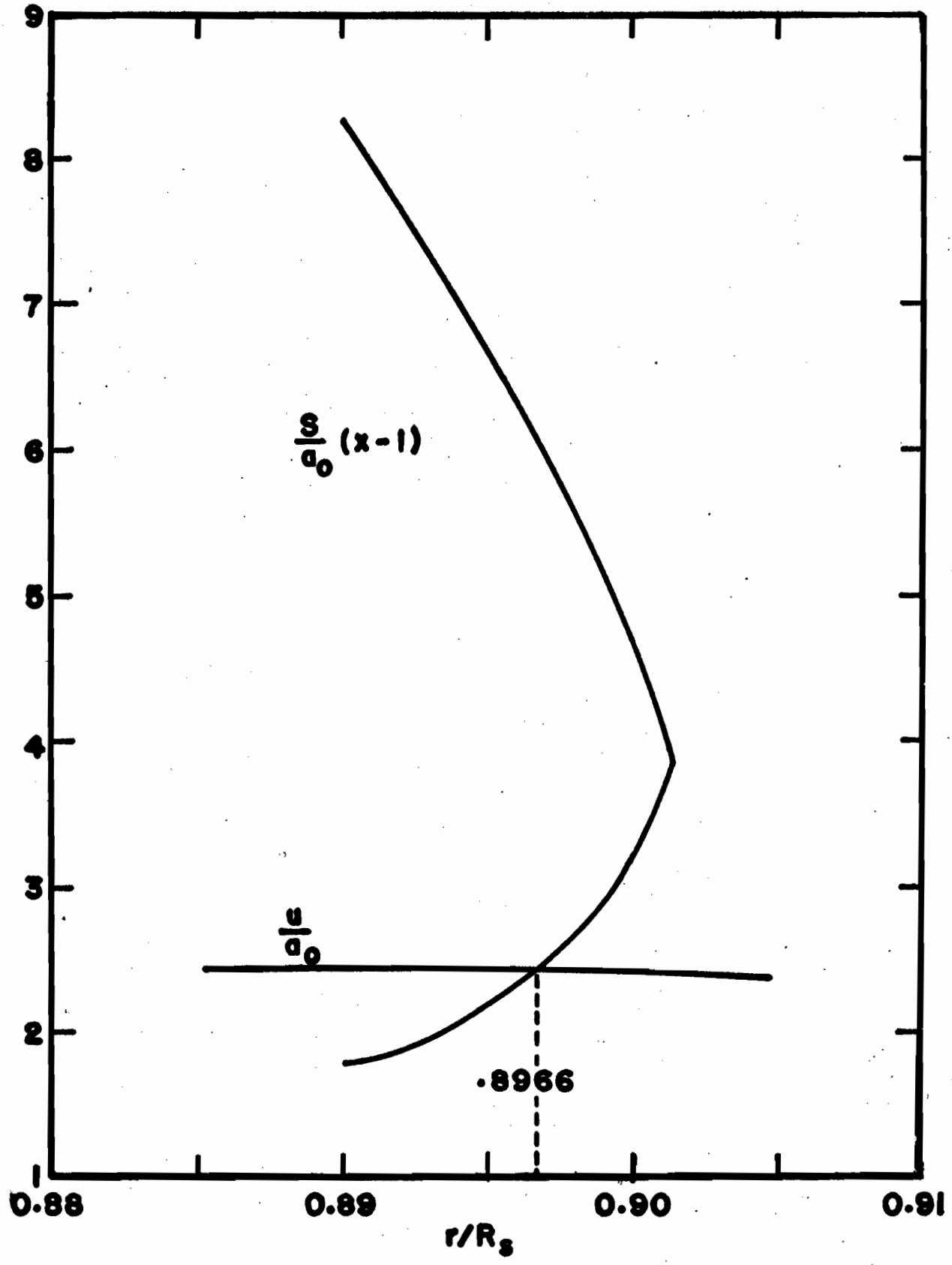

Fig. 13 $\frac{S}{a_0}(x-1)$ and u/a_0 vs. r/R_s for a flame-driven cylindrical shock of pressure ratio 10.0. The critical flame radius is 0.8966.

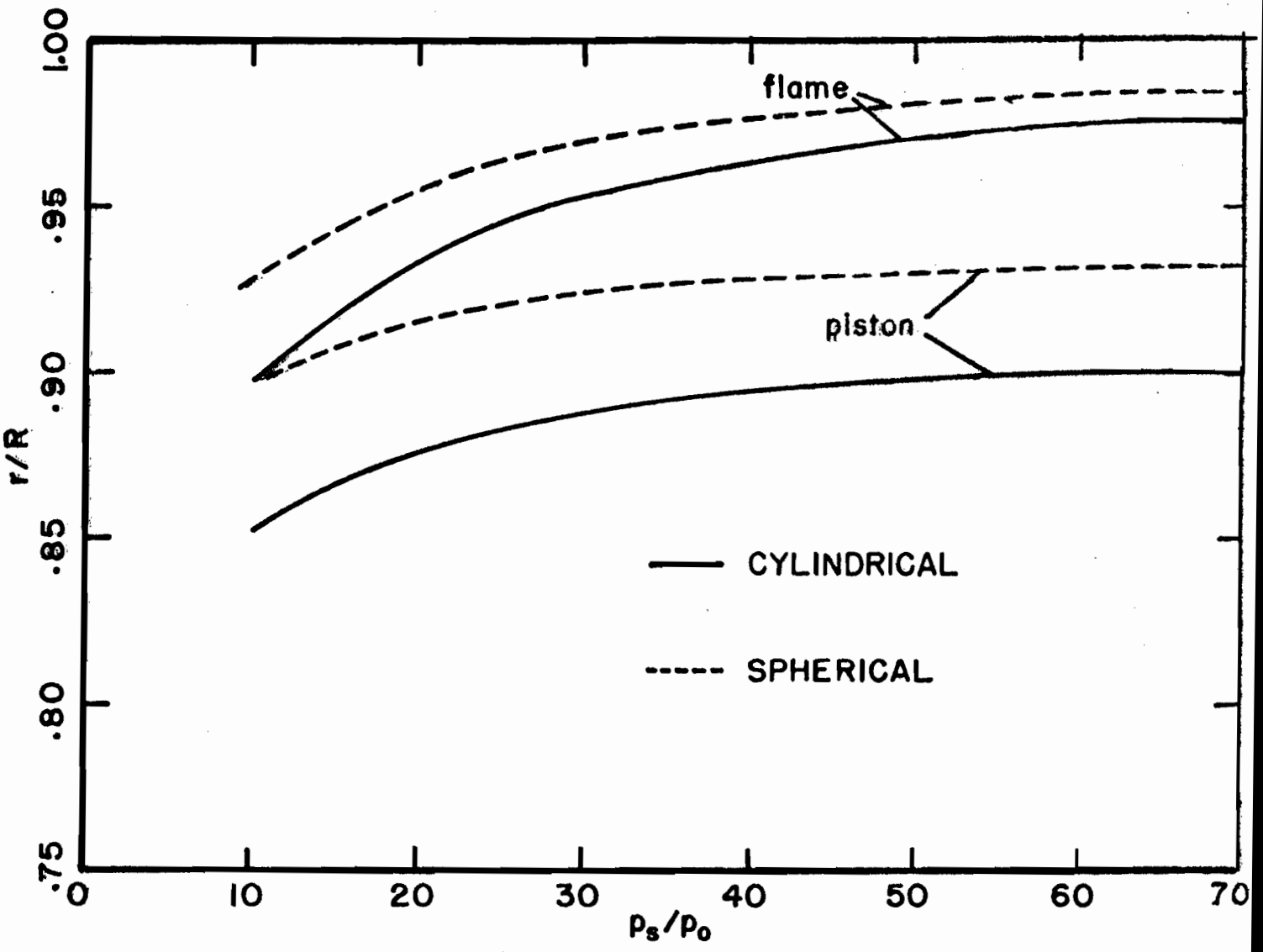

Fig. 14 r_f/R_s and r_p/R_s for cylindrical shocks of various strengths.

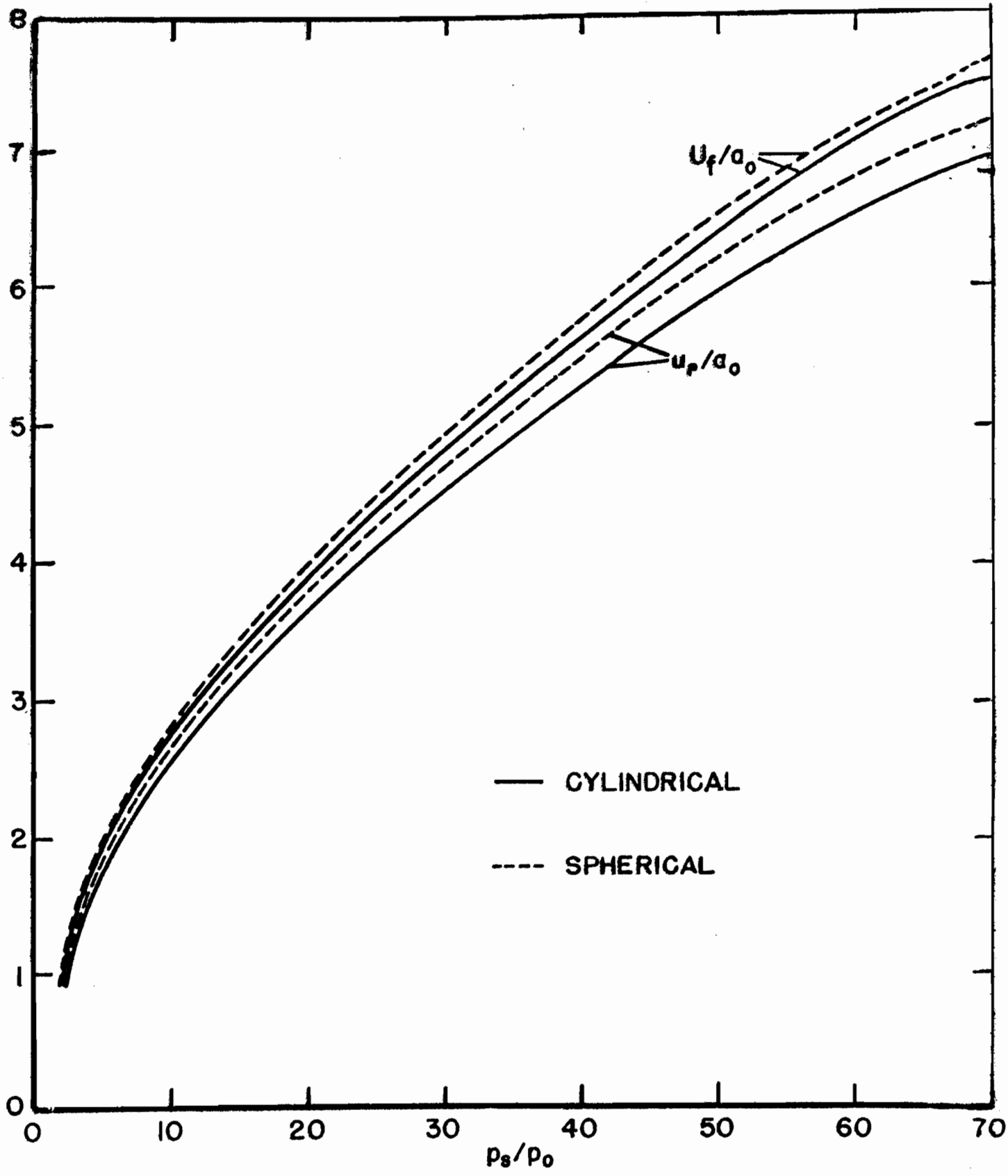

Fig: 15 U_f/a_0 and u_p/a_0 for cylindrical and spherical shocks of various strengths.

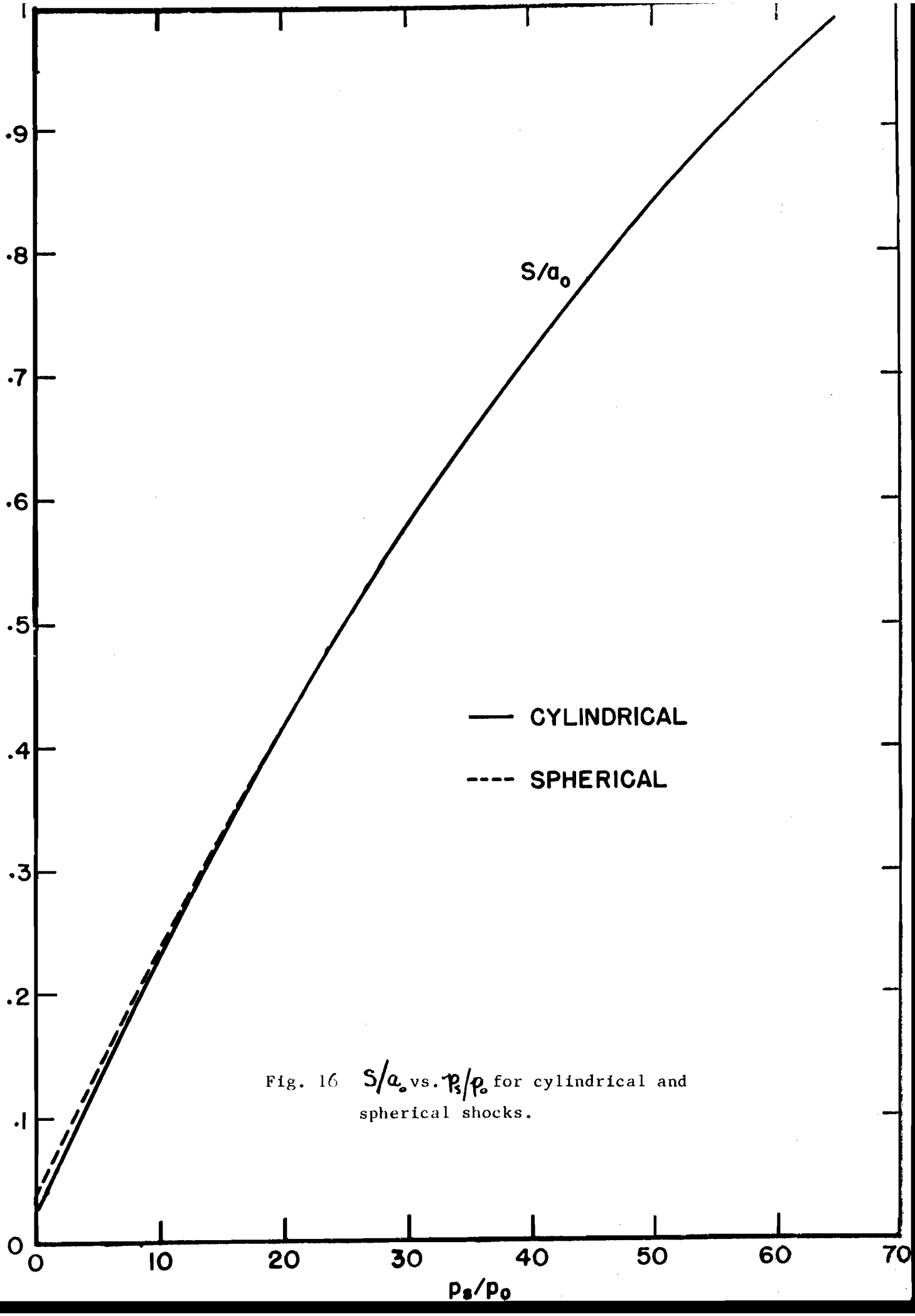

Fig. 16 S/a_0 vs. p_s/p_0 for cylindrical and spherical shocks.

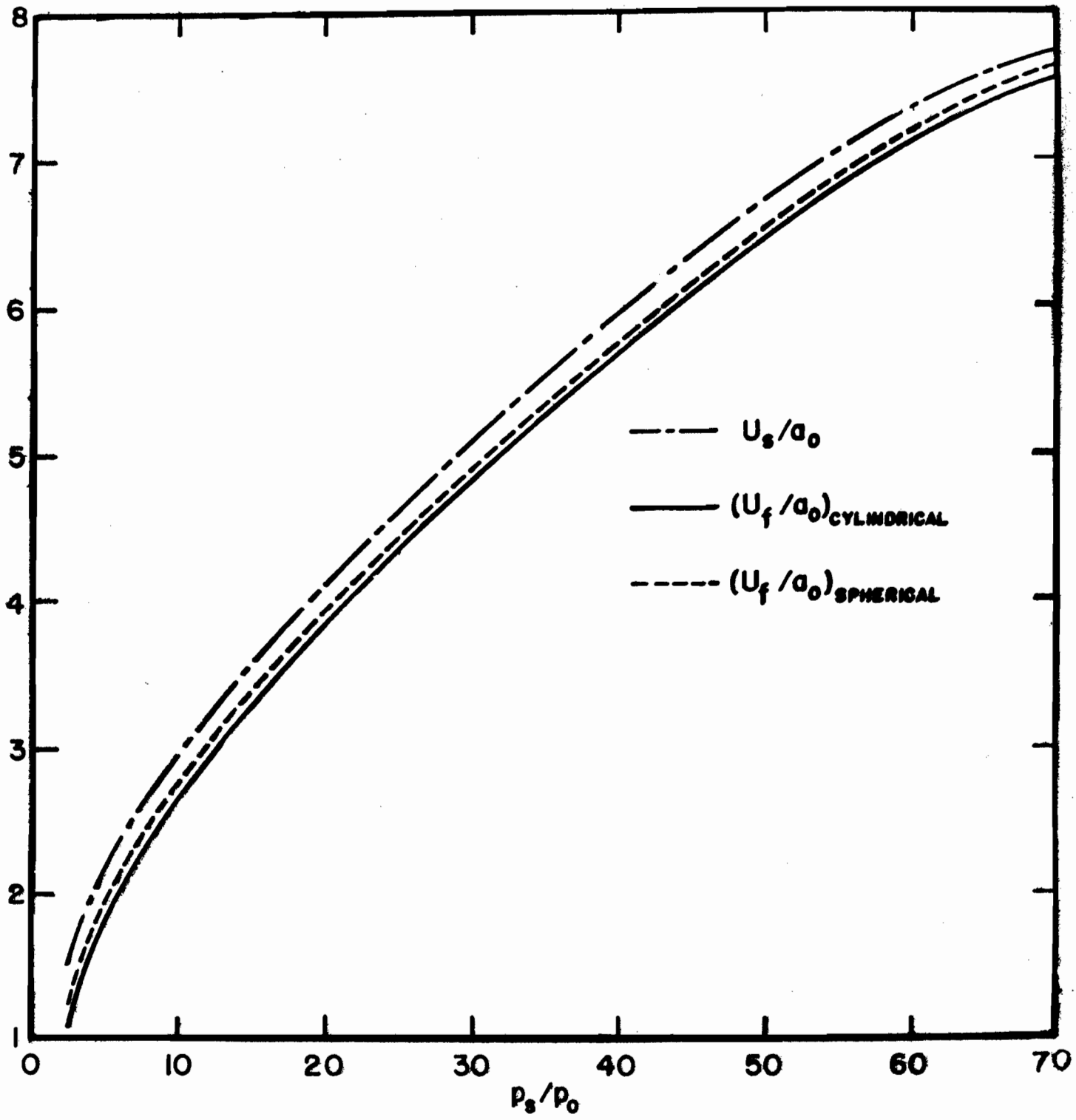

Fig. 17 U_s/a_0 and U_f/a_0 as functions of shock strength p_s/p_0.

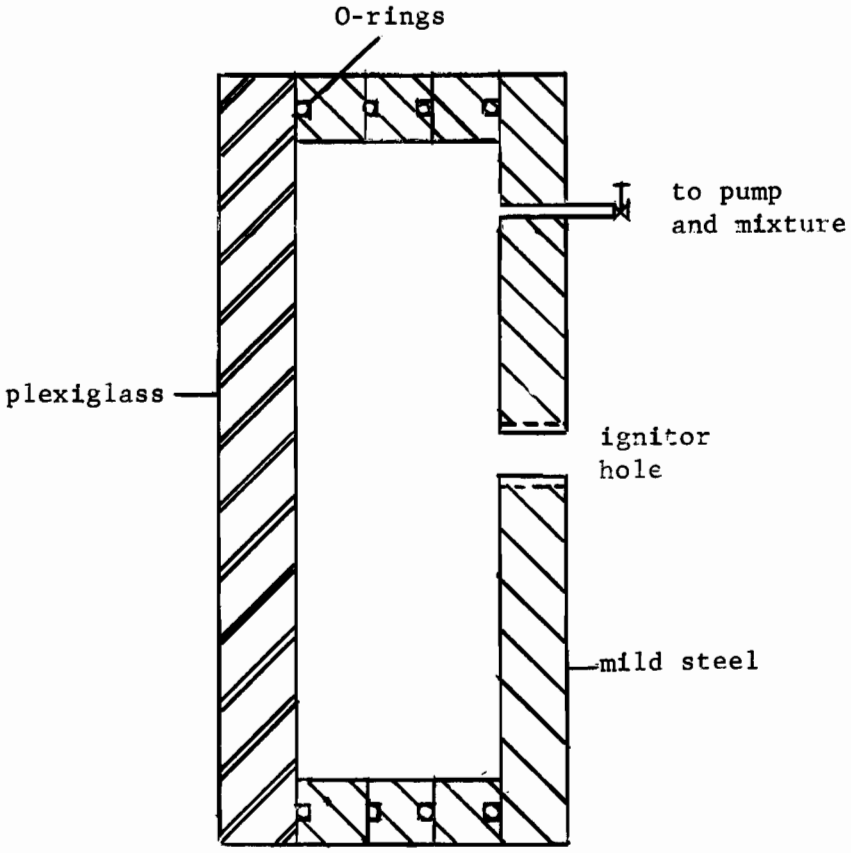

Fig. 18 Cylindrical Vessel

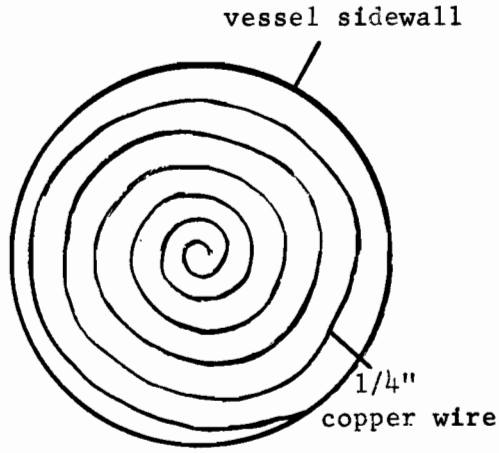

Fig. 18a Spiral Coil

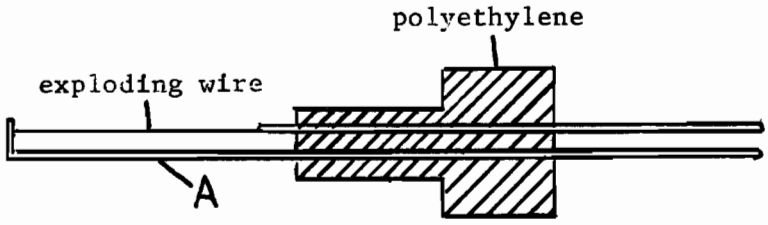

Fig. 19 Ignitor

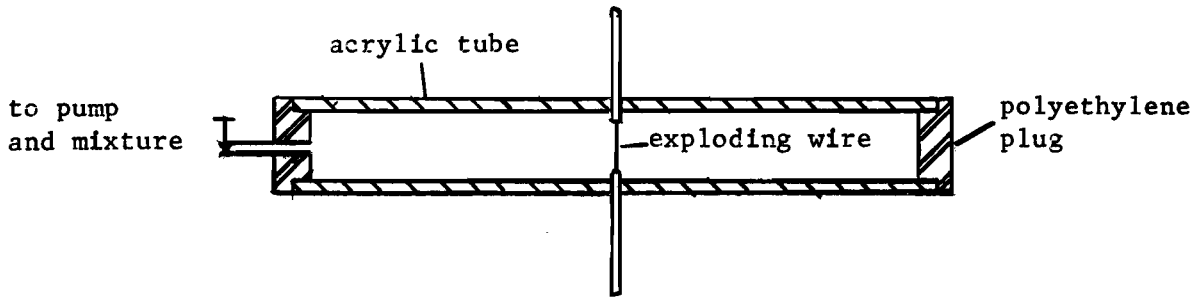

Fig. 20 Detonation Tube

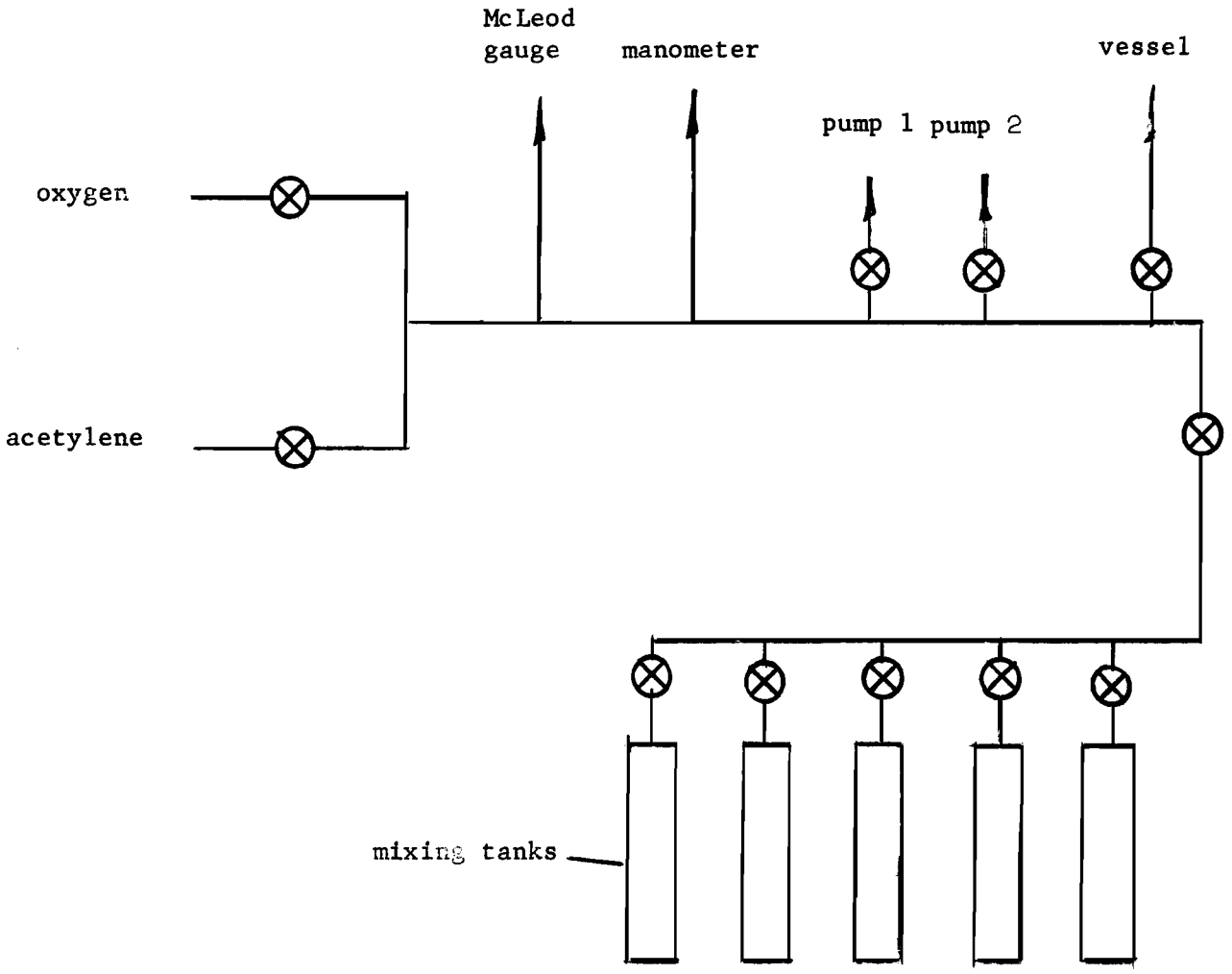

Fig. 21 Flow System Schematic

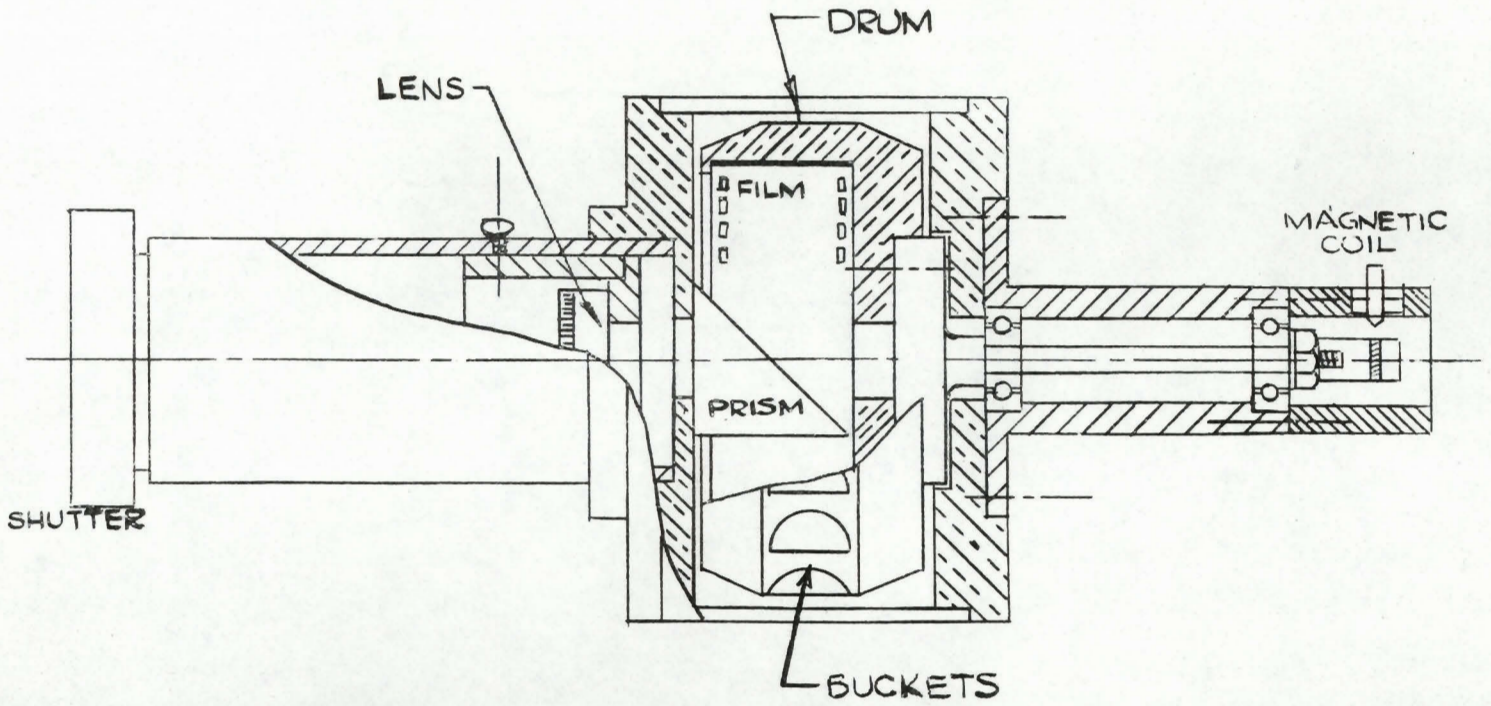

Fig. 22 Streak Camera Schematic

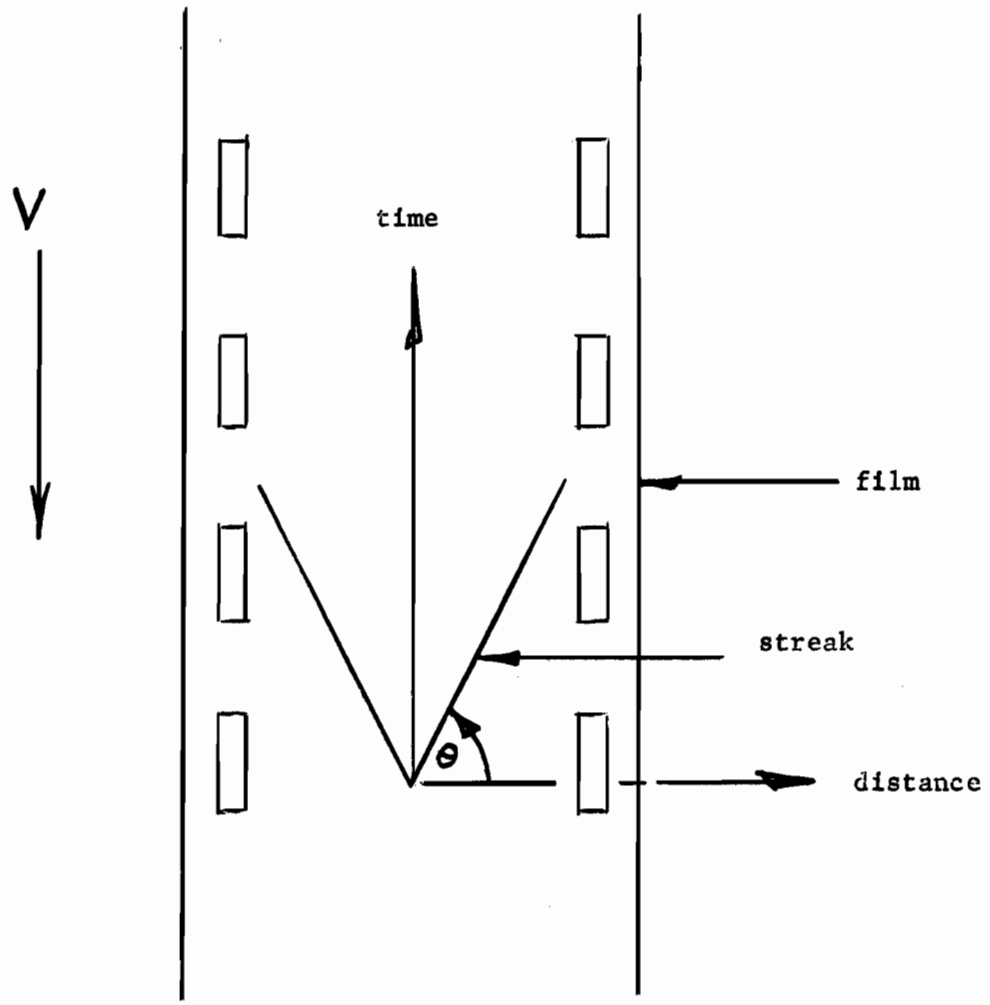

Fig. 23 Streak Photograph Schematic

Fig. 24 Streak photograph of a cylindrical detonation wave in equimolar acetylene-oxygen mixture at an initial pressure of 100 mm Hg and an initial temperature of 298°K. Ignition by exploding wire in vessel of 1 inch width, using ignition energy of 5.5 joules/cm.

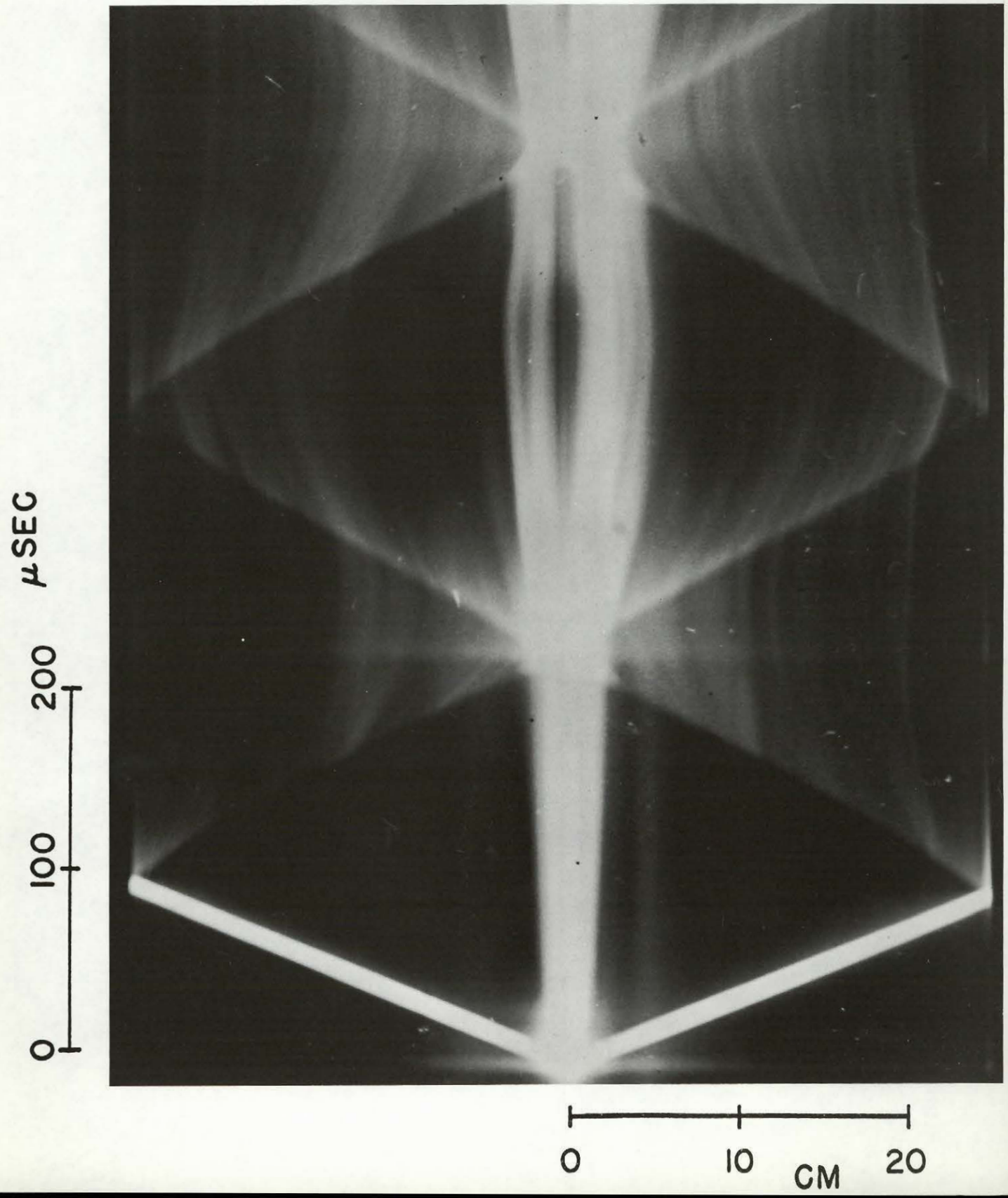

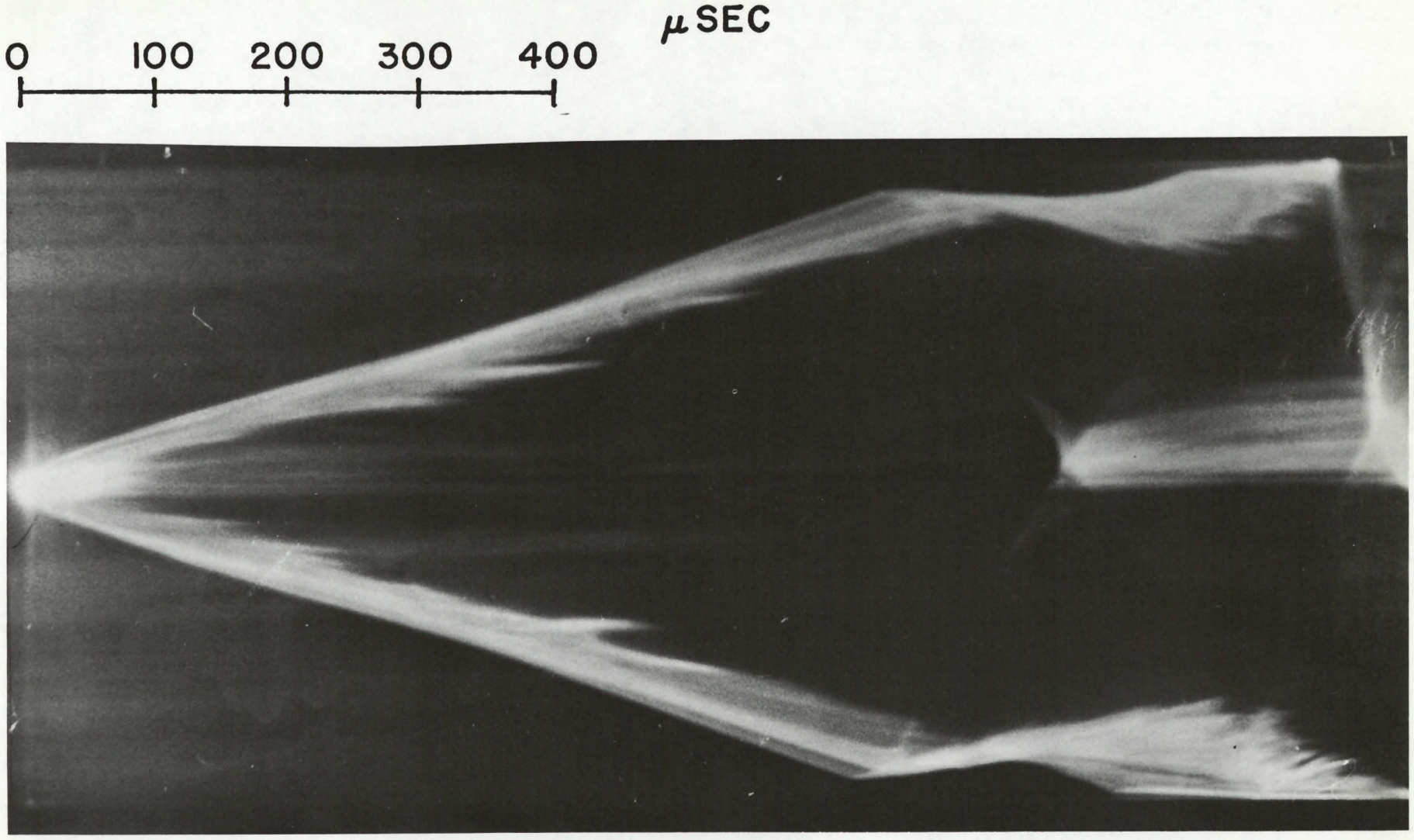

Fig. 25 Streak photograph of a cylindrical deflagration wave in equimolar acetylene-oxygen mixture at 100 mm Hg initial pressure. Ignition energy is 4.83 joules/cm, using exploding wire of .006 inch diameter.

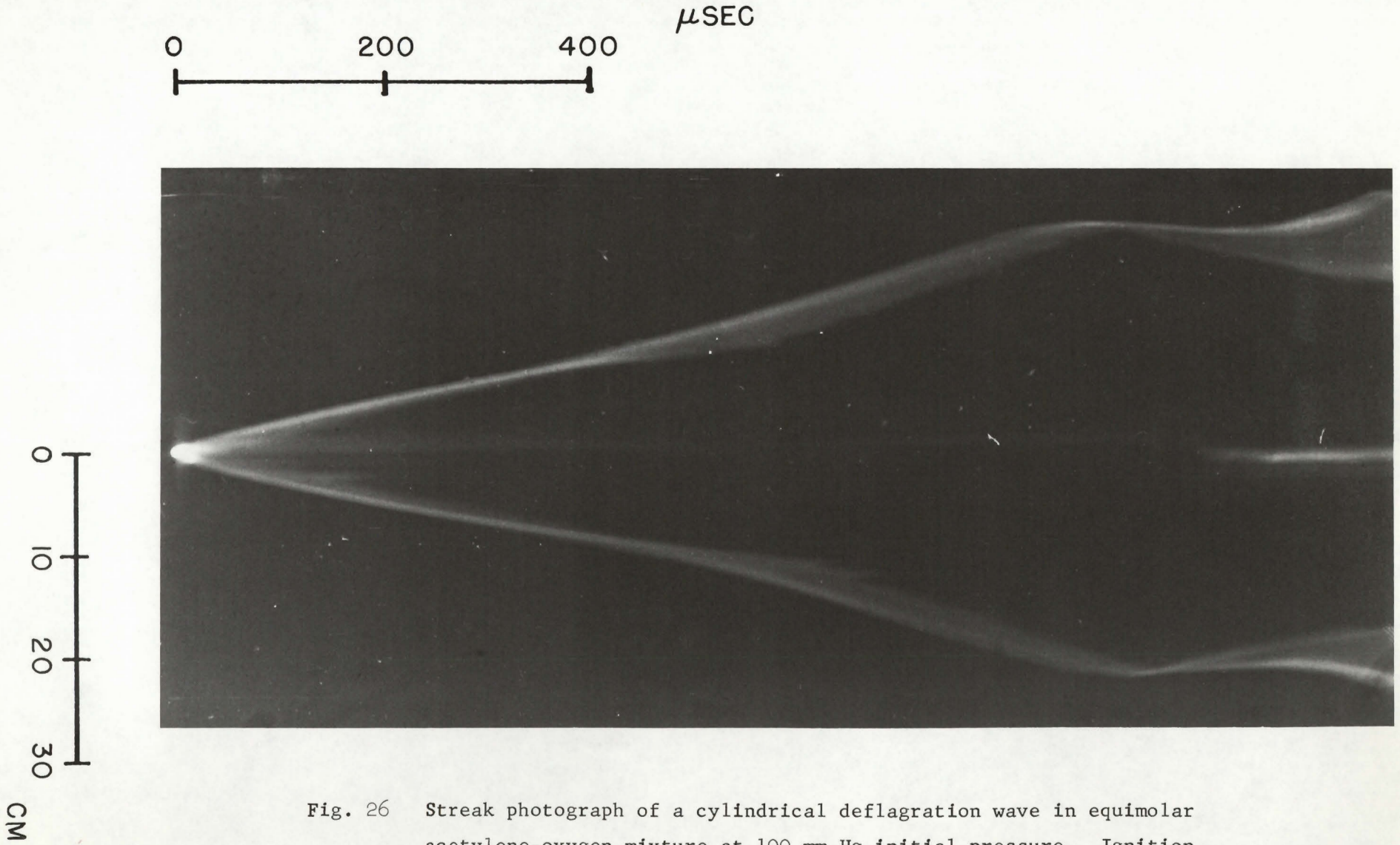

Fig. 26 Streak photograph of a cylindrical deflagration wave in equimolar acetylene-oxygen mixture at 100 mm Hg initial pressure. Ignition energy was 0.9 joules/cm, using exploding wire of .003 inch diameter.

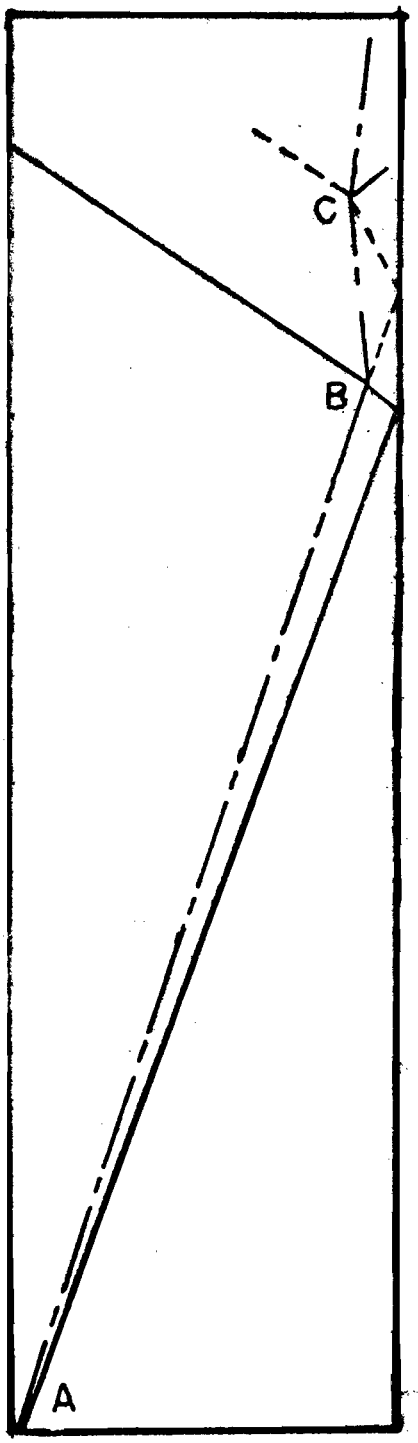

Fig. 27 Calculated flame-pressure wave interaction in equimolar acetylene-oxygen mixture.

Fig. 28 Streak photograph of a plane deflagration wave in equimolar acetylene-oxygen mixture at 100 mm Hg initial pressure. Ignition by exploding wire of .003 inch diameter at centre of closed-end tube, using an ignition energy of 4.36 joules.

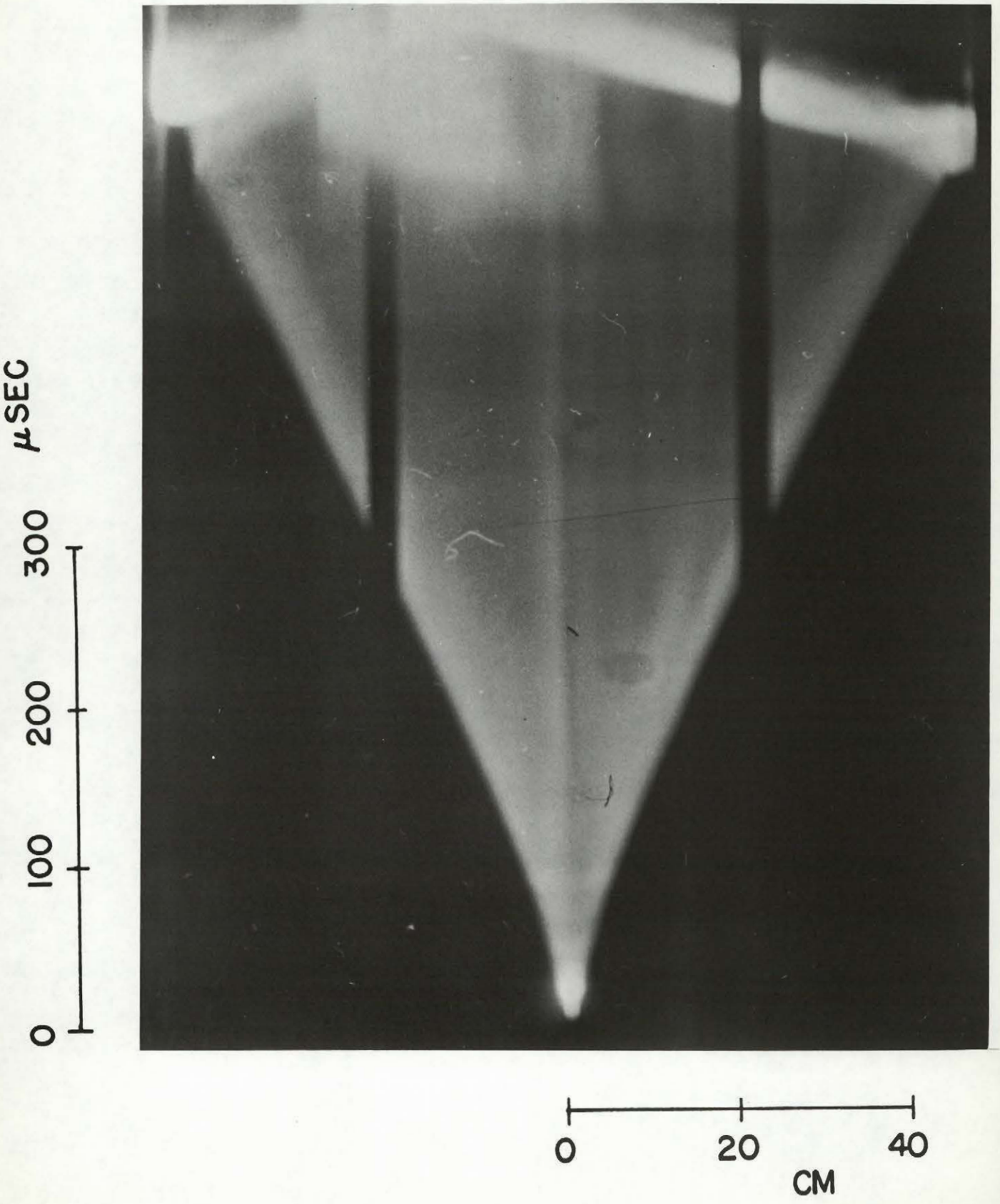

Fig. 29 Streak photograph of a cylindrical deflagration wave (with transition to detonation) in equimolar acetylene-oxygen mixture at 100 mm Hg initial pressure. Ignition energy is 0.9 joules/cm. Spiral coil is placed on one sidewall of vessel of 1 inch width.

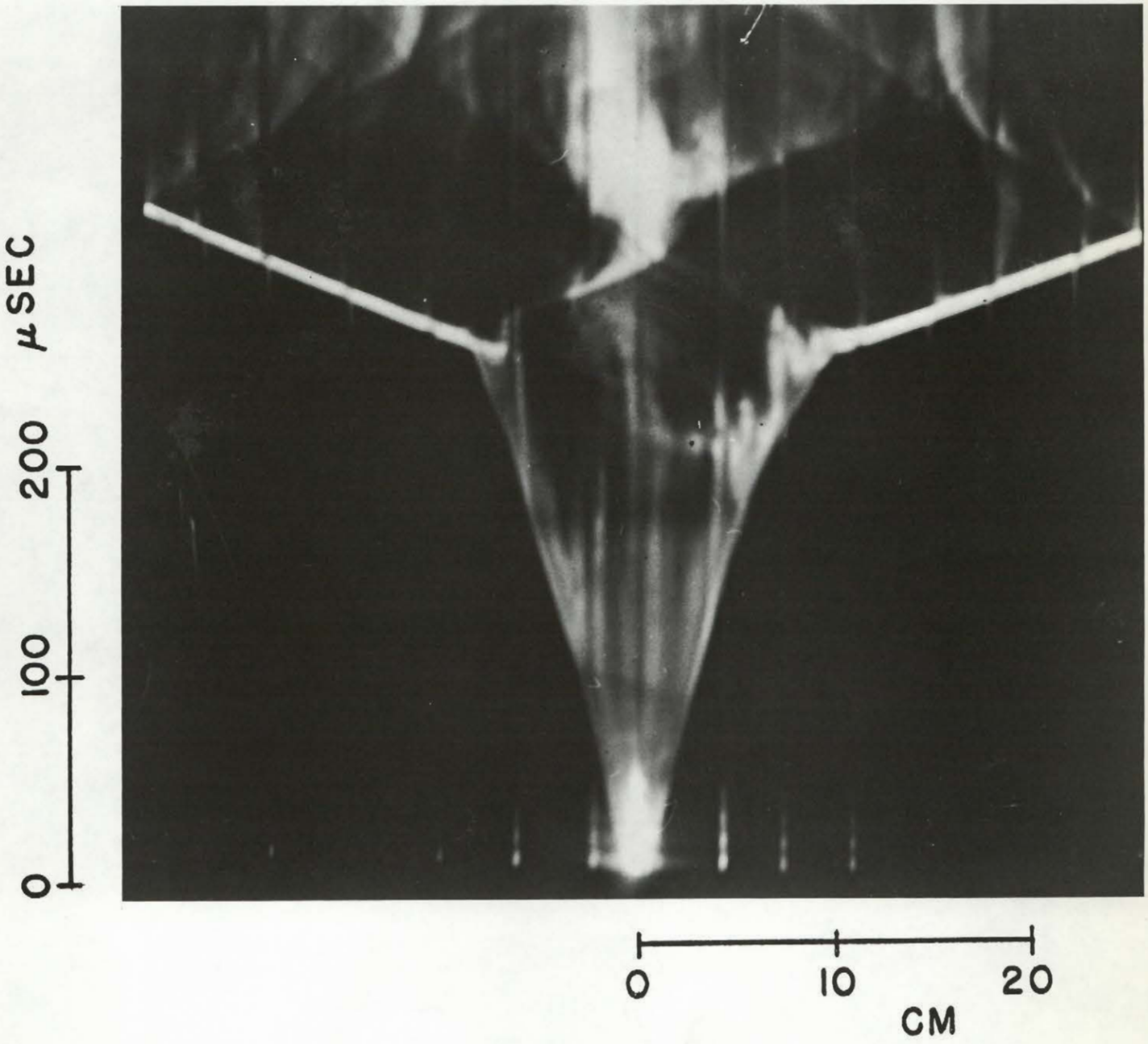

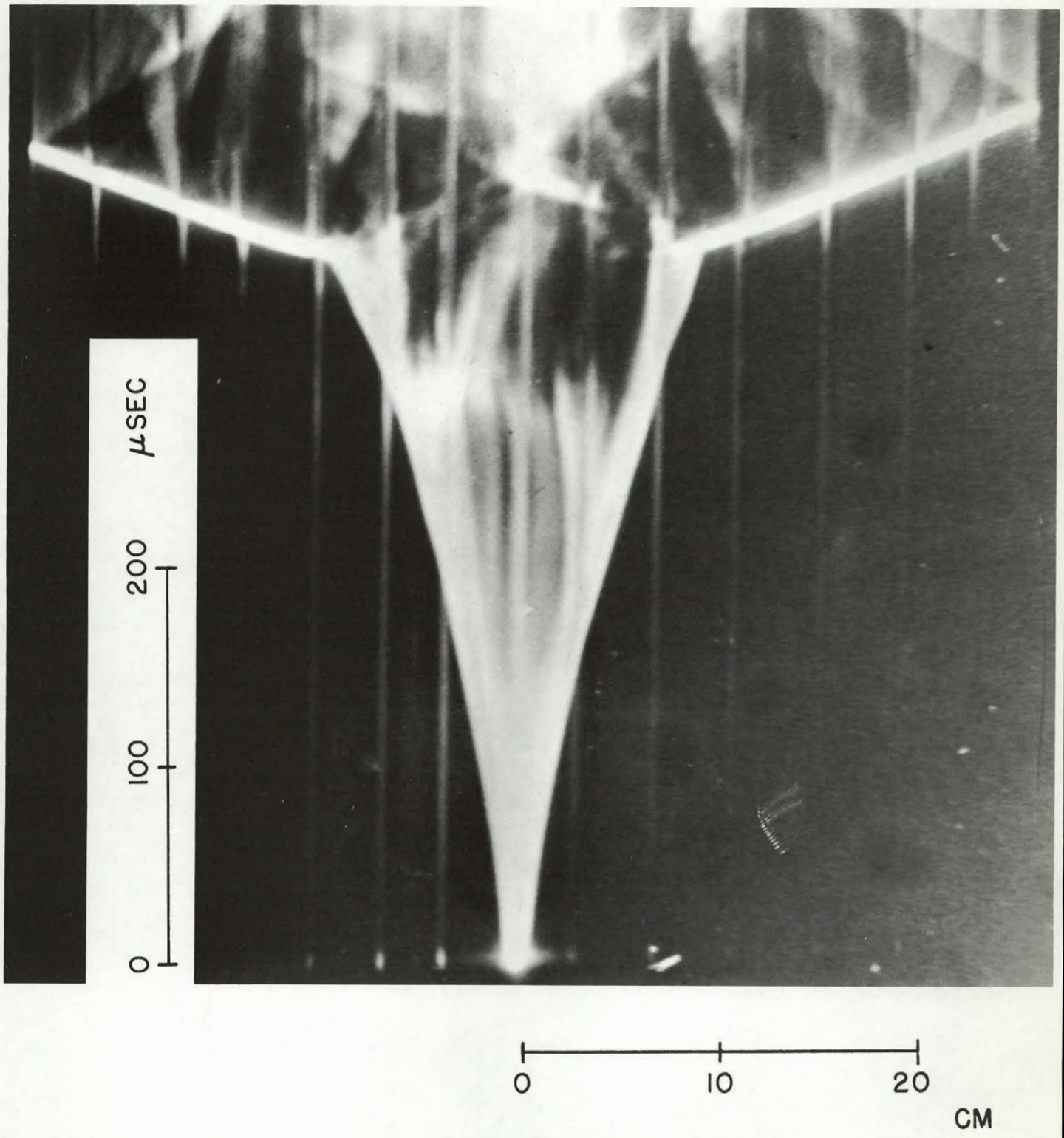

Fig. 30 Streak photograph of a cylindrical deflagration wave (with transition to detonation) in equimolar acetylene-oxygen mixture at 100 mm Hg initial pressure. Ignition energy is 0.5 joules/cm. Spiral coil is placed on one sidewall of vessel of 1 inch width.

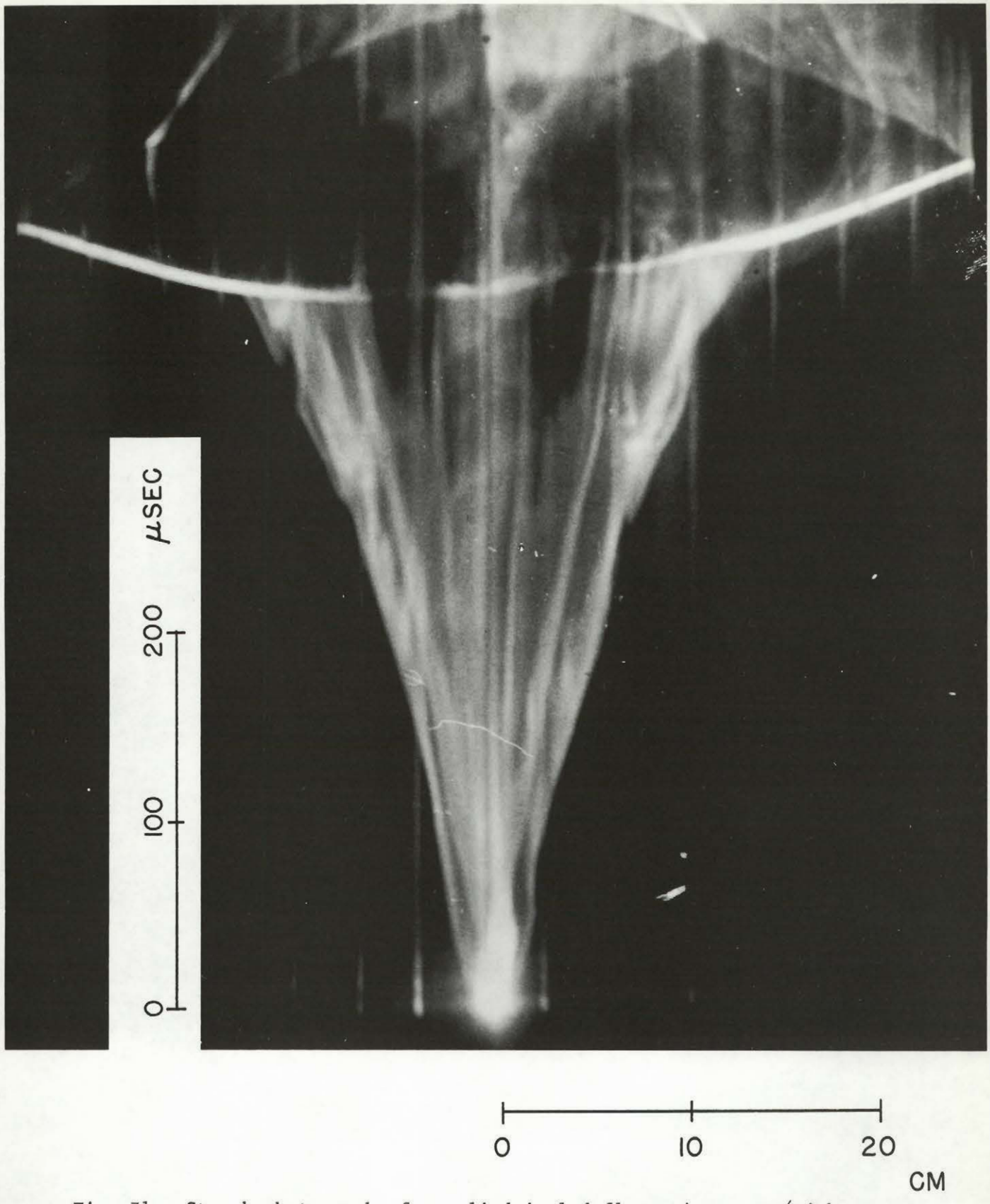

Fig. 31 Streak photograph of a cylindrical deflagration wave (with transition to detonation) in equimolar acetylene-oxygen mixture at 100 mm Hg initial pressure. Ignition energy is 0.9 joules/cm. Spiral coil is placed on one sidewall of vessel of 2 inch width.

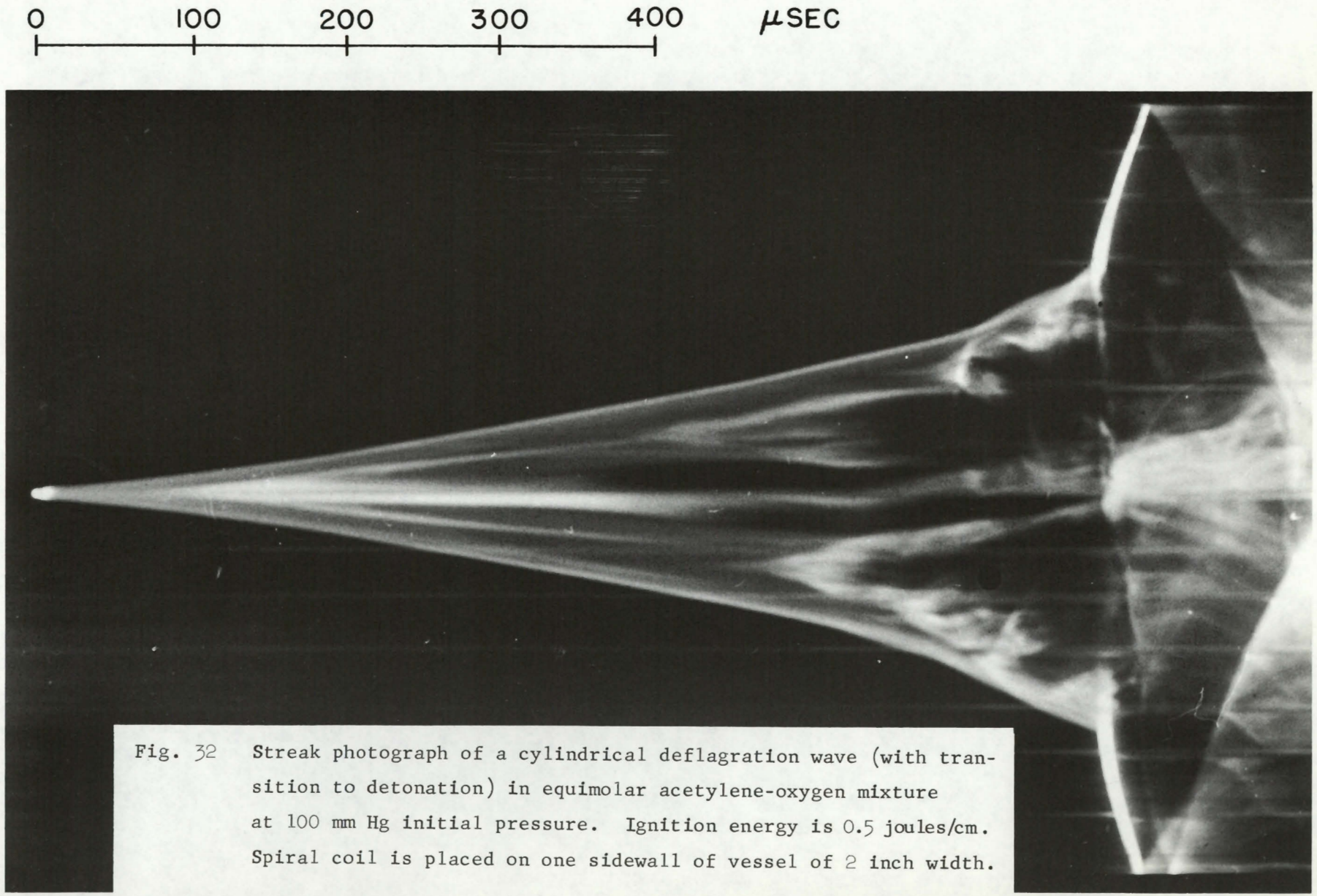

Fig. 32 Streak photograph of a cylindrical deflagration wave (with transition to detonation) in equimolar acetylene-oxygen mixture at 100 mm Hg initial pressure. Ignition energy is 0.5 joules/cm. Spiral coil is placed on one sidewall of vessel of 2 inch width.

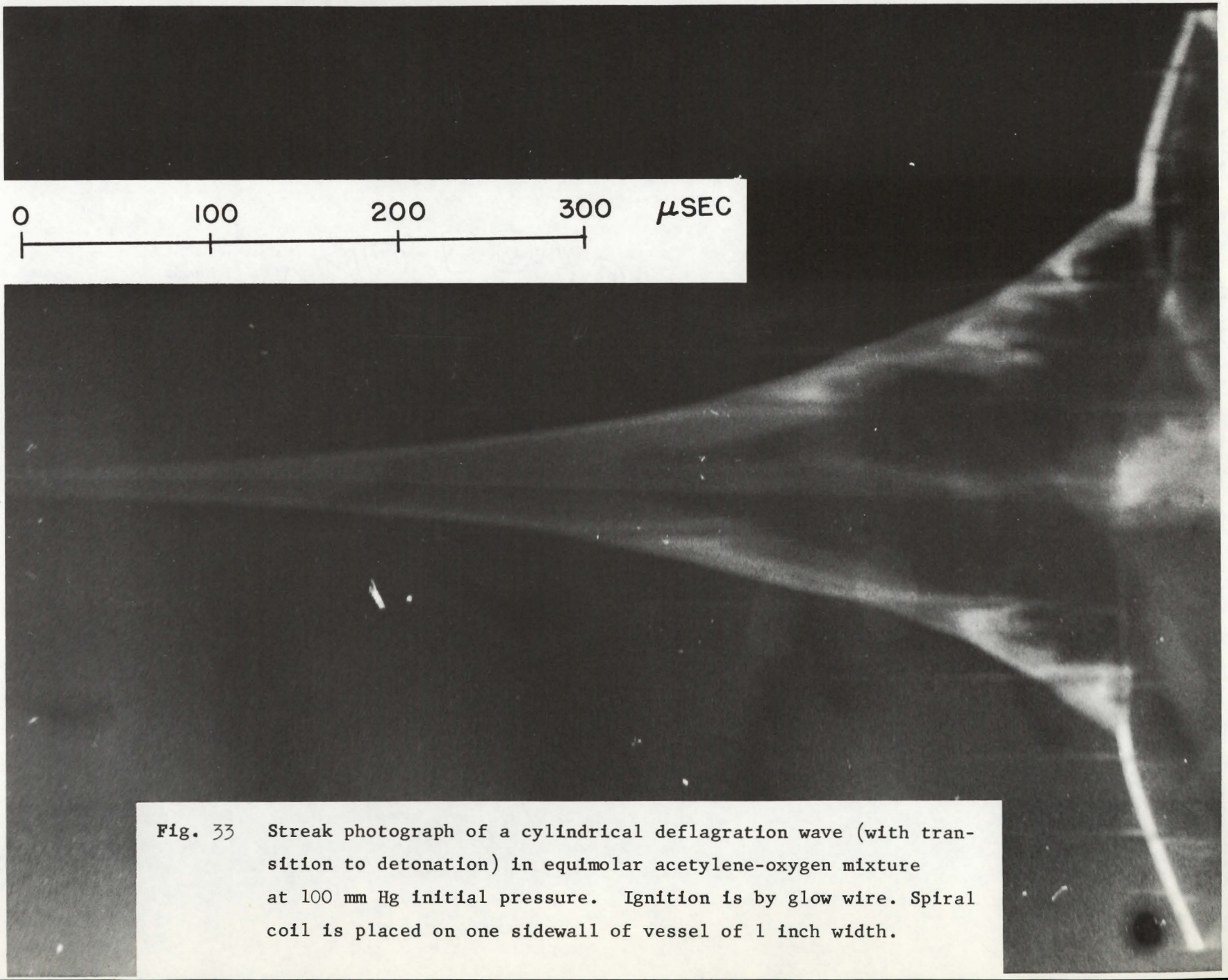

Fig. 33 Streak photograph of a cylindrical deflagration wave (with transition to detonation) in equimolar acetylene-oxygen mixture at 100 mm Hg initial pressure. Ignition is by glow wire. Spiral coil is placed on one sidewall of vessel of 1 inch width.

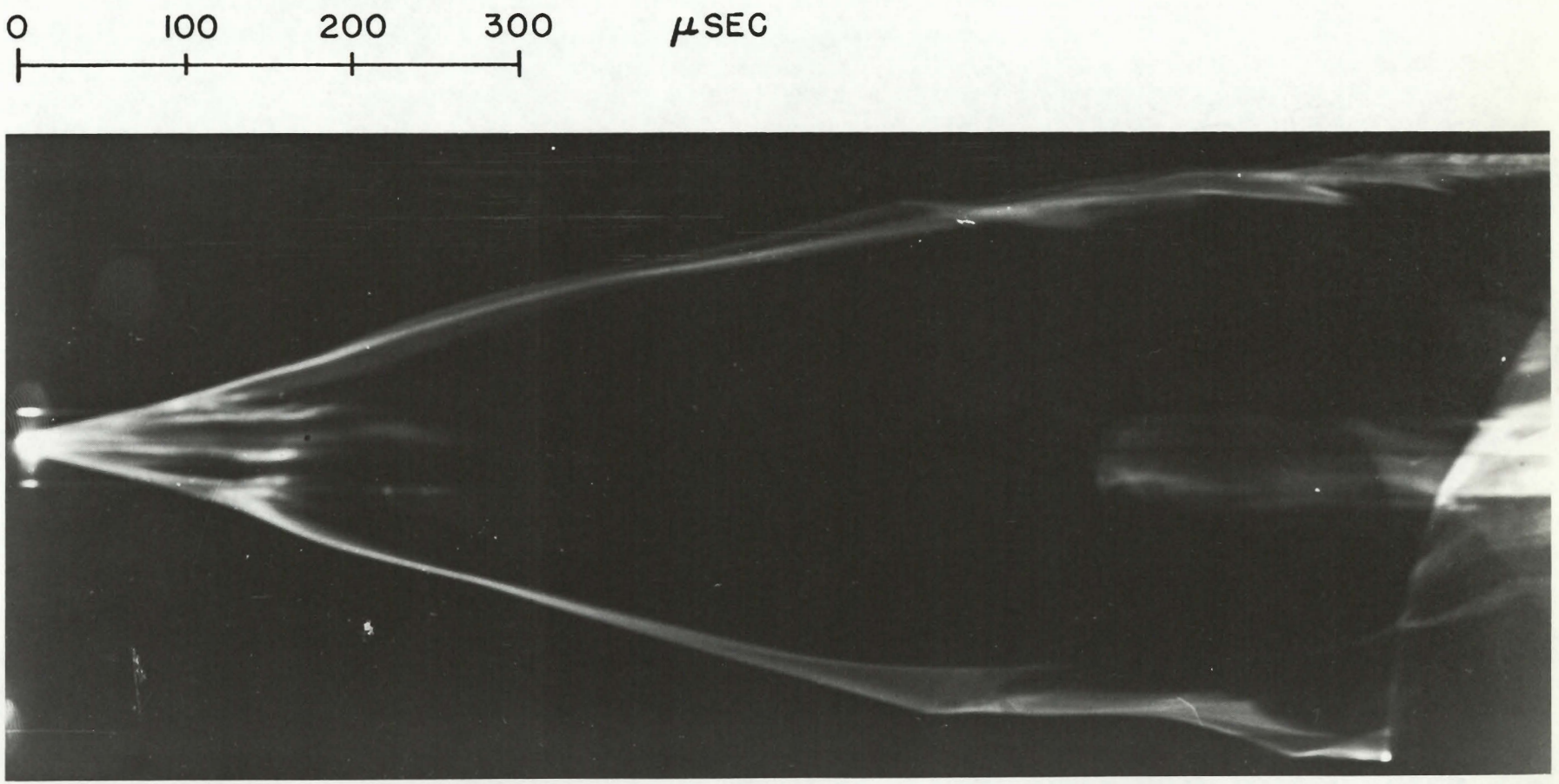

Fig. 34 Streak photograph of cylindrical deflagration in equimolar acetylene-oxygen mixture at 100 mm Hg initial pressure. Ignition energy is 0.9 joules/cm. Circular coil of 6 cm ID is placed on one sidewall of vessel of 1 inch width.

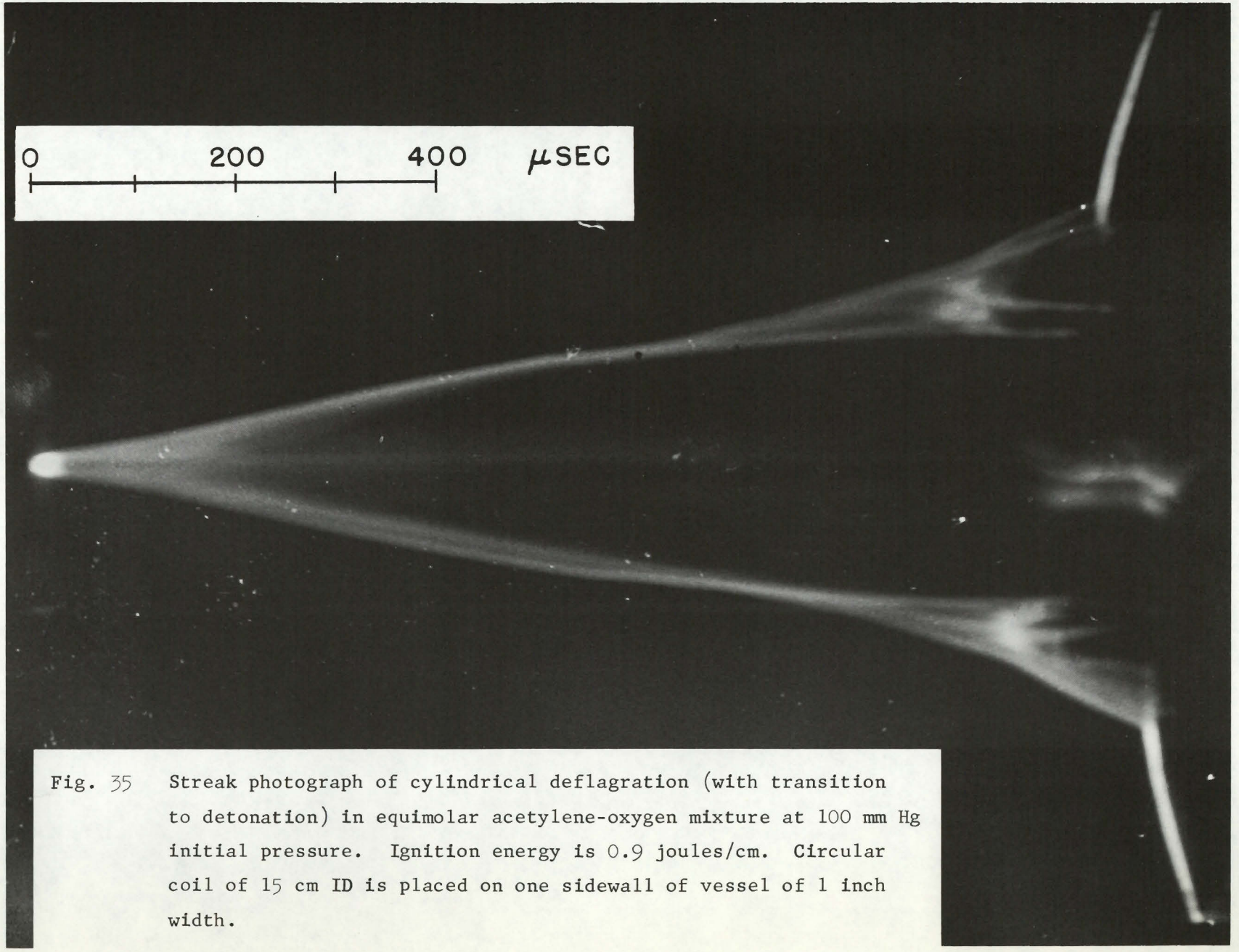

Fig. 35 Streak photograph of cylindrical deflagration (with transition to detonation) in equimolar acetylene-oxygen mixture at 100 mm Hg initial pressure. Ignition energy is 0.9 joules/cm. Circular coil of 15 cm ID is placed on one sidewall of vessel of 1 inch width.

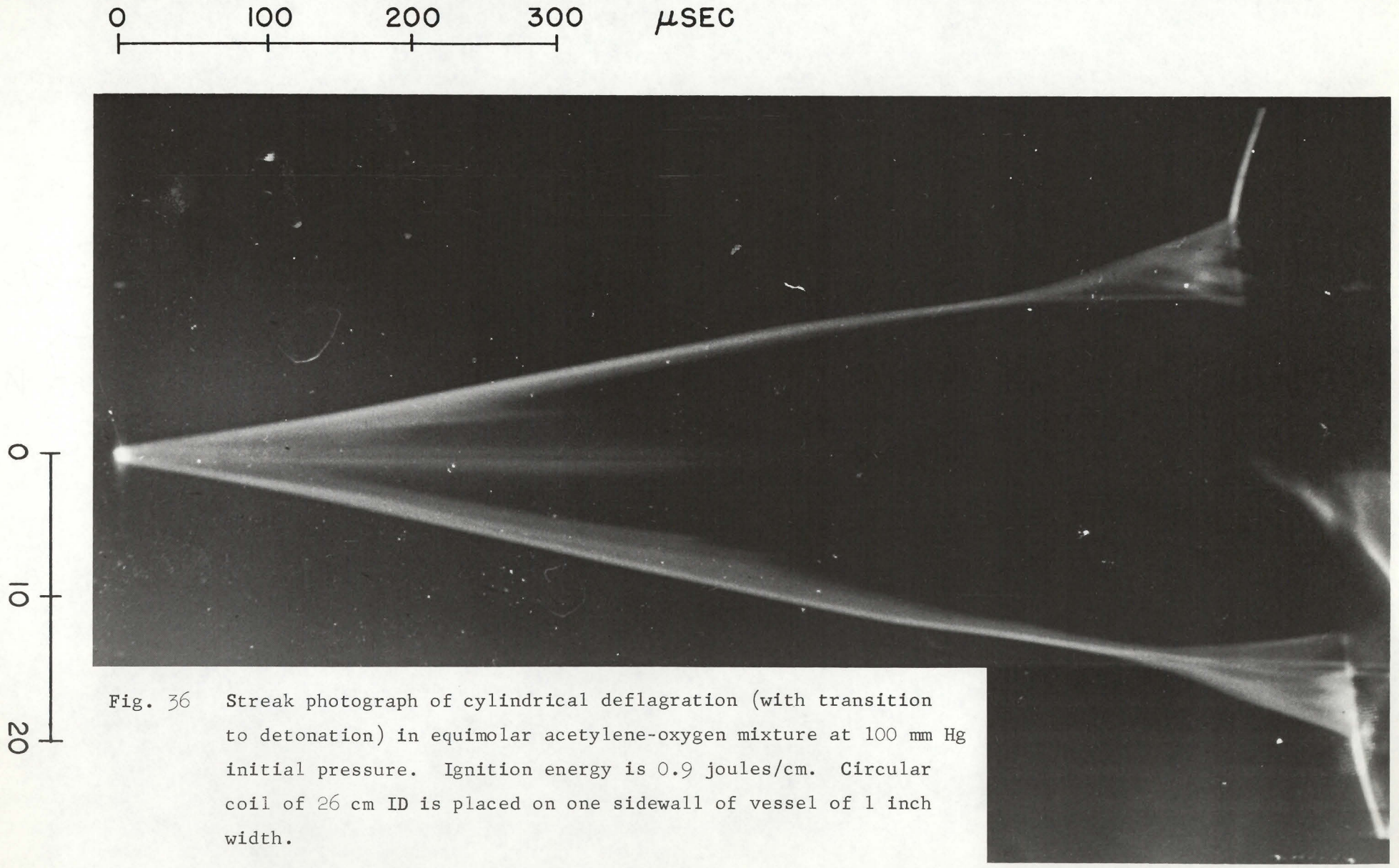

Fig. 36 Streak photograph of cylindrical deflagration (with transition to detonation) in equimolar acetylene-oxygen mixture at 100 mm Hg initial pressure. Ignition energy is 0.9 joules/cm. Circular coil of 26 cm ID is placed on one sidewall of vessel of 1 inch width.

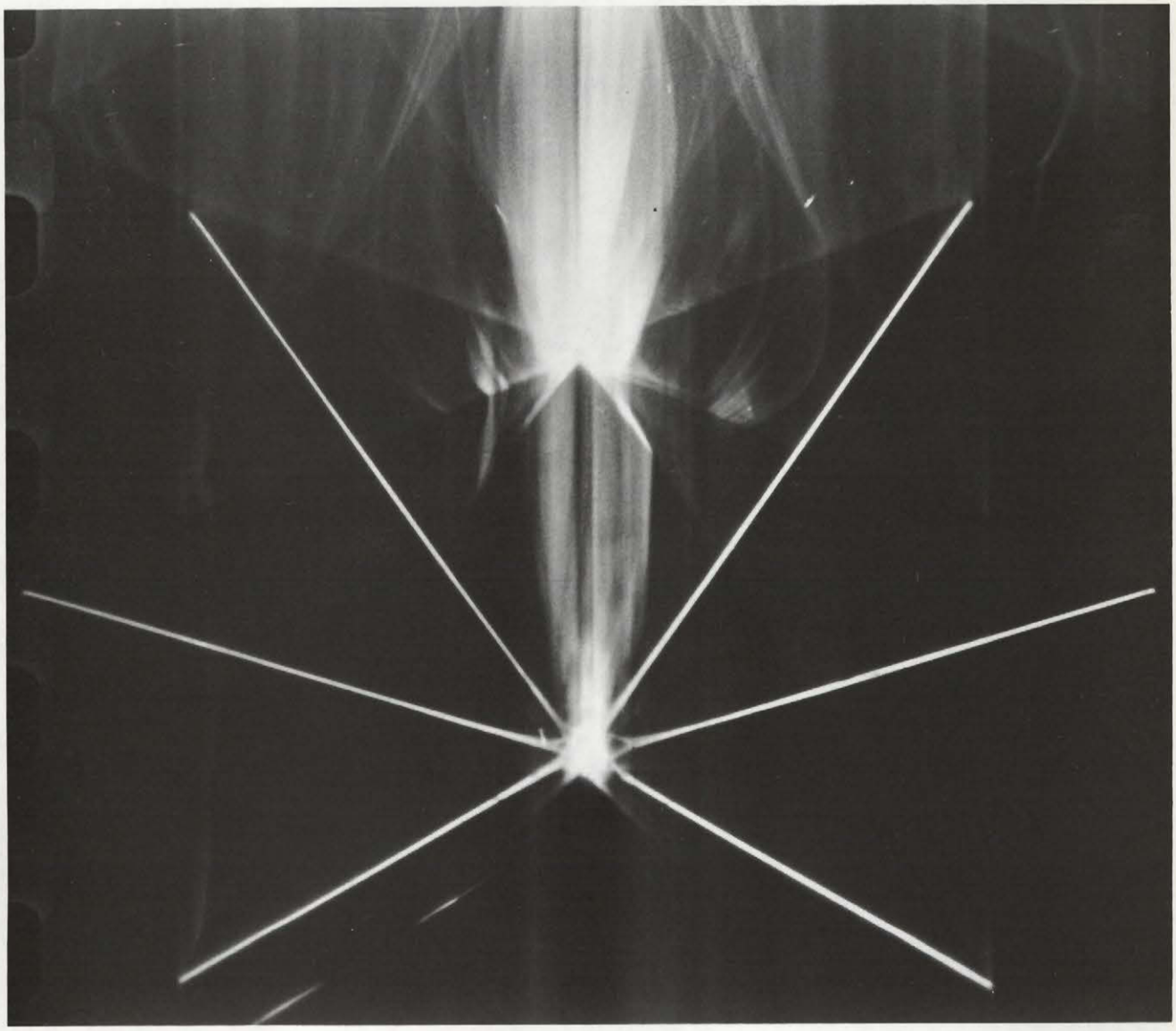

Fig. 37 Six-slit streak photograph of a cylindrical detonation wave.

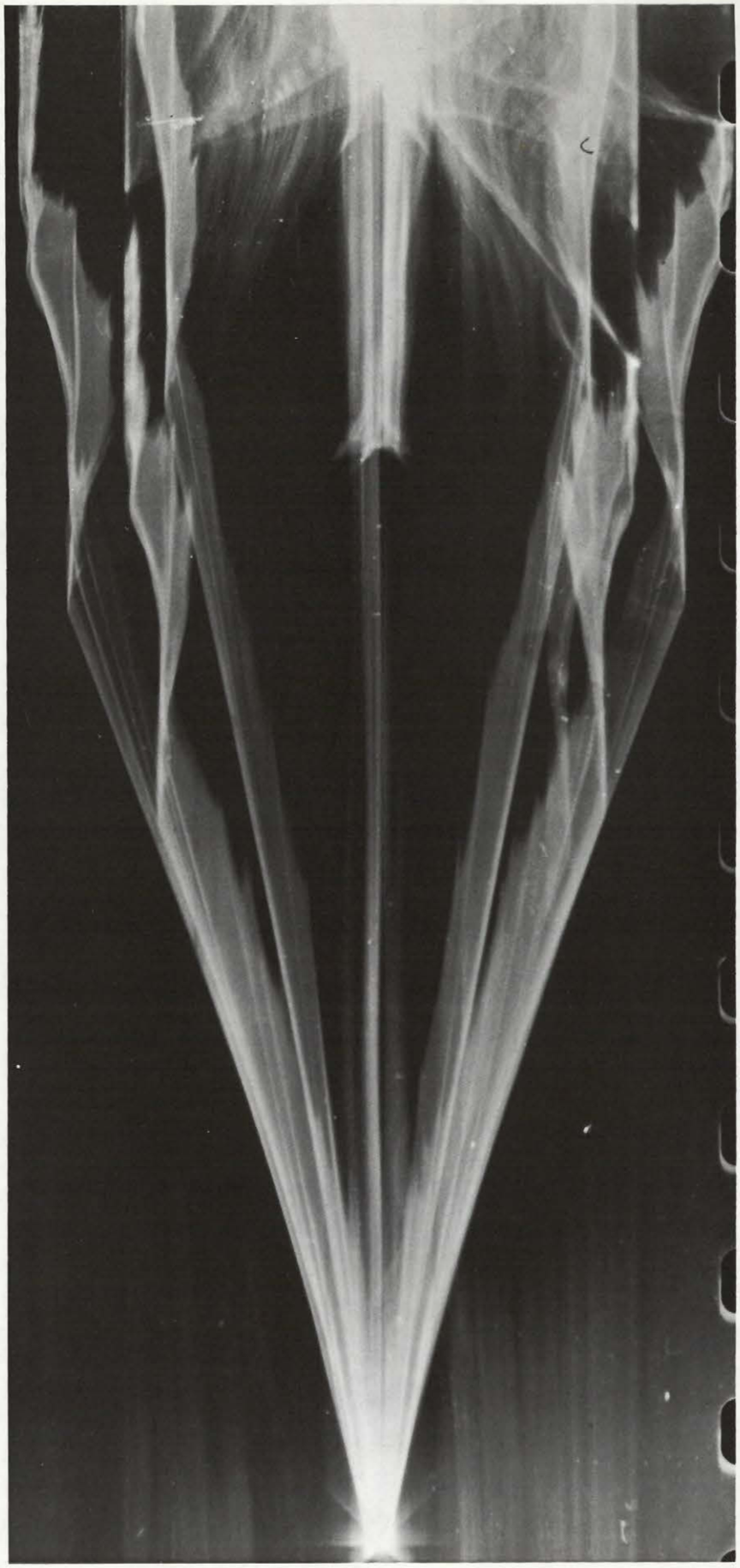

Fig. 38 Six-slit streak photograph of a cylindrical deflagration wave.

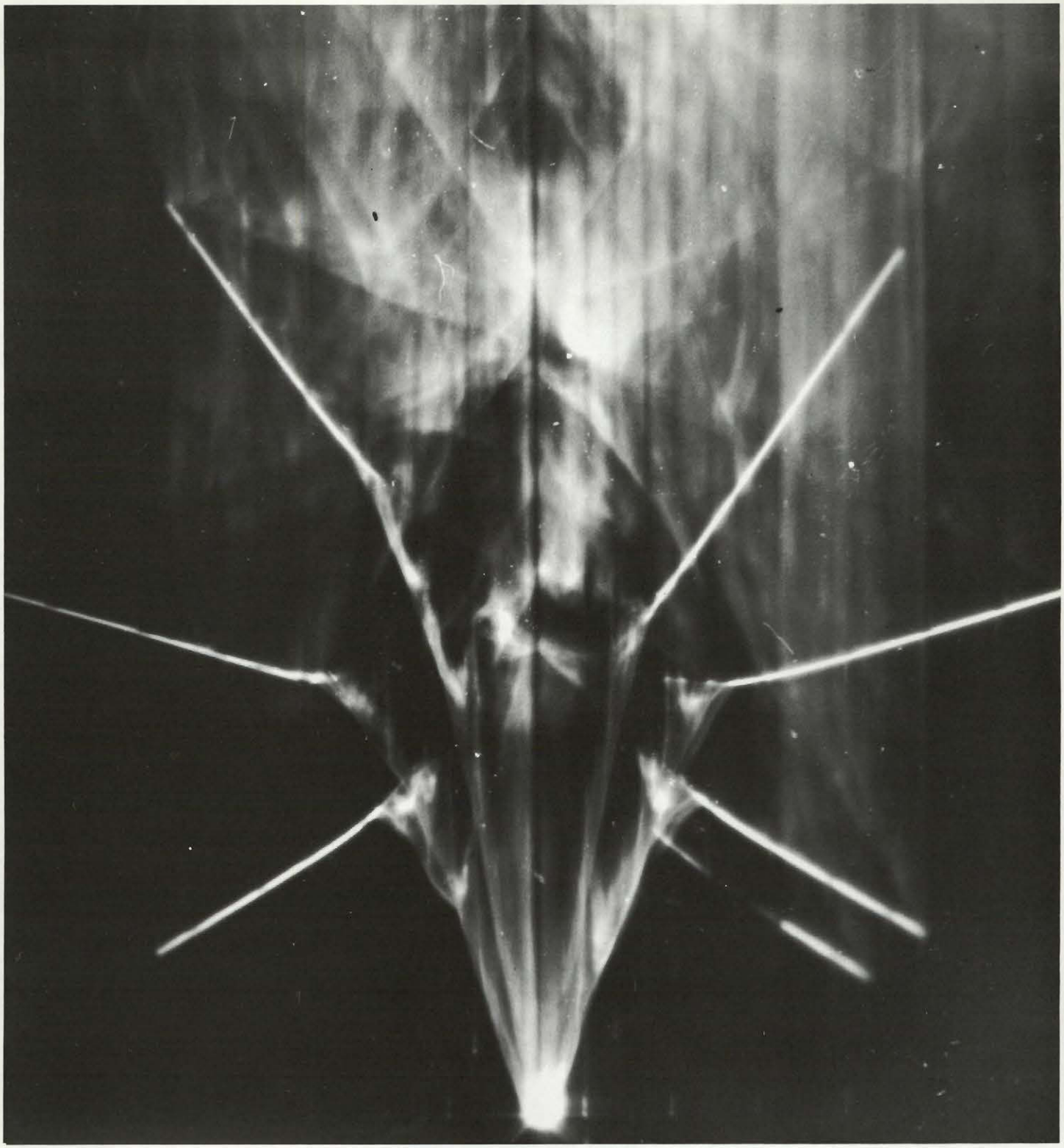

Fig. 39 Six-slit streak photograph of a cylindrical deflagration wave, with transition to detonation.